

Blue Energy: electricity production from salinity gradients by reverse electrodialysis

Jan Willem Post

Thesis committee

Thesis supervisor

Prof. dr. ir. C.J.N. Buisman

Professor of Biological Recycling Technology

Sub-department of Environmental Technology

Thesis co-supervisor

Dr. ir. H.V.M. Hamelers

Assistant professor

Sub-department of Environmental Technology

Other members

Prof. Dr. A.A. Broekhuis, University of Groningen

Prof. Dr. M.A. Cohen Stuart, Wageningen University

Prof. Dr. L. Diels, University of Antwerp / VITO

Prof. Dr. C. Kroese, Open University / Wageningen University

This research was conducted under the auspices of the Graduate School SENSE (Socio-Economic and Natural Sciences of the Environment).

Blue Energy: electricity production from salinity gradients by reverse electrodialysis

Jan Willem Post

Thesis

submitted in partial fulfilment of the requirements for the degree of doctor
at Wageningen University
by the authority of the Rector Magnificus
Prof. dr. M.J. Kropff,
in the presence of the
Thesis Committee appointed by the Doctorate Board
to be defended in public
on Tuesday 3 November 2009
at 4 PM in the Aula.

Jan W. Post

Blue Energy: electricity production from salinity gradients by reverse
electrodialysis, 224 pages.

Thesis, Wageningen University, Wageningen, NL (2009)

With references, with summaries in Dutch and English

ISBN 978-90-8585-510-1

Abstract

Salinity-gradient energy or Blue Energy is a promising renewable energy source for the future. Estimates from literature predicted coverage of over 80% of the current global electricity demand when applied in all river mouths. From thermodynamic calculations it can be derived that each m³ of river water can yield 1.4 MJ when mixed with the same amount of sea water. Two techniques are available to convert Blue Energy into electricity: pressure-retarded osmosis and reverse electrodialysis. For further research in this thesis, the latter was selected. From a review we concluded it has better prospects for river mouths regarding power density, energy recovery, fouling behavior and process economy. Until now, it has been investigated generally with a focus on obtained power, without taking care of the energy recovery. In this thesis, we emphasized the aspect of energy recovery. In our opinion, this is the most critical factor to success. We were the first to obtain a significant energy recovery of over 80%. Another important issue of this thesis is how the system will behave in practice, i.e., when it is applied to feed waters with different chemical compositions and biological activity. We investigated different operations and designs in relation to biofouling. Regarding the operations, a periodically applied feed water reversal hampers the biofouling significantly (extending the operational period with a factor 4). Regarding the design, a proof of principle was given of a newly designed spacer-free stack. This design leads to better performances (power density and energy recovery) and is less sensitive to biofouling. Based on this work, we defined requirements for membrane development and stack design (in relation to pre-treatment and friction losses). We also re-examined the economic feasibility and the global and national prospects of Blue Energy.

Keywords: Salinity-gradient energy, Blue Energy, reverse electrodialysis, pressure-retarded osmosis, power density, energy recovery, biofouling

Voor onze zonen: Richard, Jonathan en Marnix

Table of contents

1	Introduction to this thesis	9
2	Evaluation of pressure-retarded osmosis and reverse electrodialysis	31
3	Energy recovery from controlled mixing of salt and fresh water with reverse electrodialysis	71
4	Influence of multivalent ions on power production with reverse electrodialysis	93
5	Prevention of biofouling by flow reversal in reverse electrodialysis stacks	117
6	Proof-of-principle of a reverse electrodialysis stack without spacers	147
7	Technical and economic prospects of reverse electrodialysis	161
8	Global and national prospects of salinity-gradient energy	187
	Summary and discussion / Samenvatting en discussie	205
	Post Scriptum	219

1 Introduction to this thesis

Salinity-gradient energy or Blue Energy is a promising renewable energy source for the future. In densely populated delta areas, where rivers with a low salinity flows in to the saline sea, the potential is enormous. Estimates from literature predicted coverage of over 80% of the current global electricity demand. This means a potential reduction of 40% of global energy-related greenhouse gas emissions. In this introduction to the thesis, we provide a short overview of the thermodynamic base of salinity-gradient energy (Gibbs' free energy of mixing) and the investigated conversion technology (reverse electrodialysis). We present the aspects that primarily influence the technical and economic potential of Blue Energy, resulting in the aim and outline of the thesis.

1.1 Blue Energy or salinity-gradient energy

The current energy production is largely based on fossil fuels and is not only characterized by (i) vulnerability and (ii) imminent scarcity, but also by (iii) the emission of greenhouse gasses as a consequence of the combustion of fuels. It is very probable that this human fossil-fuel burning is the biggest contributor to climate change. Each of these three concerns should provide enough motivation for drastically reducing the burning of fossil fuels. This should be done by reducing the energy demand (consumption) and by changing the energy supply (sources and production). In order to meet the respective concerns, the energy supply should be based on (i) a locally available alternative energy source, (ii) a renewable energy source, and (iii) an environmental-friendly non-combustion energy conversion. In this thesis an interesting, but hardly known, alternative renewable and environment-friendly energy source is investigated: salinity-gradient energy, or according to the research and development program in The Netherlands: "Blue Energy".

Salinity-gradient energy is a renewable energy source that was recognized already in the 1950s [1]. It was mentioned that besides the gravitational potential, the natural runoff in coastal areas has a huge physical-chemical potential. This potential is the result of the salinity-gradient between the mainly-fresh runoff (river mouths) and the receiving mainly-saline reservoirs (seas and oceans). When a river runs into a sea, spontaneous mixing of fresh and salt water occurs. This natural process is irreversible; no work is attained from it. However, if the mixing is done (partly) reversibly, work can be obtained from the mixing process. In literature [2, 3] it was assumed that from each cubic meter of river water 2.3 MJ of work could be extracted. According to Norman [2]: *The tremendous energy flux available in the natural salination of fresh water is graphically illustrated if one imagines that every stream and river in the world is terminated at its*

mouth by a waterfall 225 m high... For the Netherlands, a geographically low-lying flat country with about 27% of its area and 60% of its population located below sea level [4], this provides an extremely interesting opportunity to harvest energy from the estuary of two important European rivers, which together with their distributaries form the Rhine-Meuse-Scheldt delta. As an example, keeping in mind the words of Norman, the 30-km long Afsluitdijk that dams up the river mouth of the river IJssel (a distributary of river Rhine) becomes comparable to a huge power dam of over 200 m high, see Figure 1. The 1,100-km² Lake IJssel (the artificial estuarine reservoir of river IJssel) becomes comparable to an enormous energy reservoir with over a billion m³ storage capacity (assuming a level difference of only 1 m).

The globally available power in form of salinity gradients has been estimated in the 1970s (on the basis of average ocean salinity and annual global river discharges) to be between 1.4 and 2.6 TW [5, 6]. Compared to other forms of marine energy, salinity gradient resources are in the same



Figure 1: The salinity-gradient energy potential makes the 30-km long Afsluitdijk in The Netherlands comparable to the 221 m high Hoover Dam in Nevada and Arizona (USA).

order as wave energy or thermal gradients and are 100 times higher than those of tidal energy [7]. Or, 1.4 TW (12,279 TWh/y) should be able to satisfy over 80% of the current global electricity demand (15,746 TWh/y [8]).

In 2006, coal-fired generation accounted for 41% of world electricity supply [8]. Due to expected high prices for oil and natural gas, the coming decades the coal-fired generation capacity will expand, particularly in nations that are rich in coal resources, which include China, India, and the United States. Annual coal-fired generation is projected to double from 7,400 TWh in 2006 to 9,500 TWh in 2015 and 13,600 TWh in 2030 [8]. Replacing current and planned coal-fired power plants with salinity power plants (Figure 2) could reduce global greenhouse gas emissions by 10 Pg CO₂-eq/year ($\sim 10^{10}$ tonnes/year), when calculated with standard emission factors [9, 10] and an efficiency for coal-fired power plants of 40%. This means a potential reduction of 40% of current global energy-related greenhouse gas emissions (40% of 28.9 Pg CO₂-eq/year [11]).

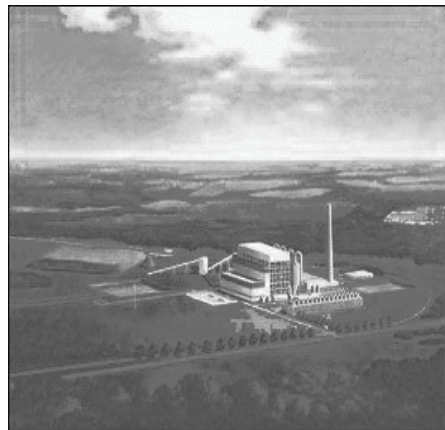
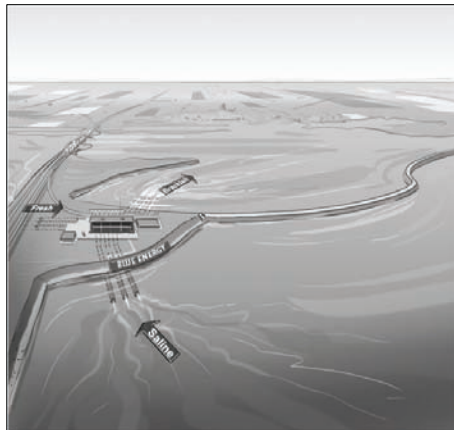


Figure 2: Replacing current and planned coal-fired power plants with salinity power plants has the promise to reduce greenhouse gas emissions.

These substantial numbers for the theoretical potential justify the research efforts in the field of salinity-gradient energy or Blue Energy in general, and the topics addressed in this thesis in particular. In this introduction to the thesis, we provide a short overview of the thermodynamic base in section 1.2 and the investigated conversion technology, called reverse electrodialysis, in section 1.3. In section 1.4 the aim and outline of the thesis are presented. We present the aspects that primarily influence the technical and economic potential of Blue Energy.

1.2 Gibbs free energy of mixing

The theoretical non-expansion work that can be produced from mixing is defined by the Gibbs energy of mixing $\Delta_{\text{mix}}G$. For ideal-dilute solutions (i.e., $\Delta_{\text{mix}}H = 0$), it can be shown that the Gibbs energy of mixing is determined by:

$$\Delta_{\text{mix}}G \equiv \Delta G_b - (\Delta G_c + \Delta G_d) \quad [1]$$

$$\Delta_{\text{mix}}G = -(n_c + n_d)T\Delta_{\text{mix}}s_b - (-n_c T\Delta_{\text{mix}}s_c - n_d T\Delta_{\text{mix}}s_d) \quad [2]$$

with subscript c for the concentrated salt solution (e.g. sea water), subscript d for the dilute salt solution (e.g. river water) and subscript b for the resulting brackish salt solution, n the amount (moles), and T the temperature; $\Delta_{\text{mix}}s$ represents the contribution of the molar entropy of mixing (J/mol.K) to the total molar entropy of the corresponding electrolyte solution, according to:

$$\Delta_{\text{mix}}s = -R \sum_i x_i \ln x_i \quad [3]$$

where R is the universal gas constant (8.314 J/mol·K), and x the mole fraction of component i ($i = \text{Na}, \text{Cl}, \text{H}_2\text{O}$). The theoretically available amount of energy from mixing 1 m³ of a diluted sodium chloride solution with an

equal amount of a concentrated sodium chloride solution is presented in *Figure 3*. The sodium chloride concentration of the diluted solution ranges from 0 to 0.5 mol/L, i.e., from pure water to sea water with a salinity of about 30 g/L. The sodium chloride concentration of the concentrated solution ranges from 0 to 5 mol/L, i.e., from pure water to saturated brine with a salinity of about 300 g/L.

The theoretically available amount of energy from mixing 1 m³ sea water (comparable to 0.5 mol/L NaCl) and 1 m³ river water (comparable to 0.01 mol/L NaCl) both at a temperature of 293 K is 1.4 MJ. An example mentioned in literature [12, 13], is the Mississippi delta with an average discharge of over 17,000 m³/s. According to Norman [12] the theoretical energy potential of this river is 40 GW [12], assuming an energy density of 2.3 MJ per m³ of river water instead of the here calculated 1.4 MJ. It was assumed that the river water is mixed with ‘infinite’ cubic meters of sea water. For a first estimation of the potential this assumption could be justified: the available discharge of river water is indeed the limiting source, whereas the sea water source could be regarded as infinitely available. However, it is clear that this value is highly theoretical as it neither takes into account that locally the salinity of the receiving sea is undeniably affected, nor the influence of intrusion causing salinity-gradients in river mouths themselves. Moreover, although the sea water might be infinitely available, in practice it represents a certain economic value as it needs also to be pretreated and transported. Our approach - a mixing of equal amounts of river water with sea water in a salinity-gradient power plant - is more realistic. For the Mississippi delta, the energy potential can than be calculated as 24 GW. According to Loeb [13], it would be technically possible to convert 9.8 GW of this to electrical power (using pressure-retarded osmosis, see next section).

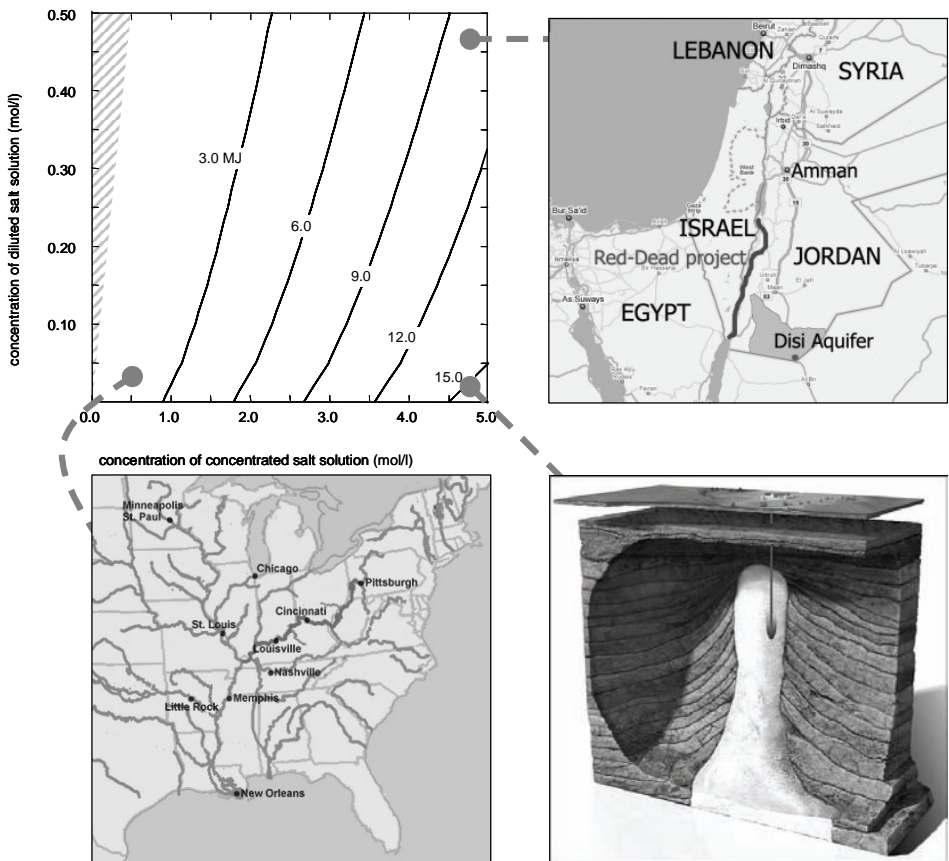


Figure 3: Theoretically available amount of energy (MJ) from mixing 1 m³ of a diluted and 1 m³ of a concentrated sodium chloride solution ($T = 293$ K, published in Post et al. [14]). Examples: mixing fresh river water from the Mississippi with sea water from the Gulf of Mexico would gain 1.4 MJ; mixing fresh sea water from the Red Sea with hypersaline water from the Dead Sea would gain 10 MJ; mixing fresh injection water from a vacuum salt mining industry with hypersaline brine from a salt cavern would gain 15 MJ.

The theoretically available amount of energy from mixing 1 m³ saturated brine (5 mol/L NaCl) and 1 m³ sea water (0.5 mol/L NaCl) at 293 K is 10 MJ. An example mentioned in literature [15] is the planned replenishment of the Dead Sea with sea water either from the Mediterranean Sea or the Red Sea in order to compensate for the evaporation of 3 million m³/d (although the mineral content of the Dead Sea is very different from that of

Chapter 1

common ocean water). The level difference of 400 m could be used to produce hydropower from the falling sea water. Moreover, the salinity-gradient could be used. With the assumption of an energy density of 10 MJ per m³ of sea water, the energy potential of this salinity-gradient energy case could count for 350 MW. According to Loeb [15], it would be technically possible to convert 130 MW to electrical power (using pressure-retarded osmosis, see next section).

The theoretically available amount of energy from mixing 1 m³ saturated brine (5 mol/L NaCl) and 1 m³ river water (0.01 mol/L NaCl) at 293 K is more than 15 MJ. An example mentioned in literature [16] is the use of salt domes, subterranean formations of solid salts that may be solution-mined. Solution-mining consists of drilling wells into an underground salt deposit, injecting fresh or recycled water to dissolve the salt, and leaving a residence time long enough for the brine solution to reach saturation with sodium chloride. The brine is then processed with evaporators and converted in pure vacuum salt and pure water (condensate). This condensate is recycled to the injection wells to dissolve the salt. A pre-mixing of the recycled condensate with brine before it is injected, would give the opportunity to harvest salinity-gradient energy. For a salt refinery plant with an annual production of 1 million tons of vacuum salt, like Frisia Zout B.V. in The Netherlands (part of Esco, European Salt Company), this would result in a 2 MW energy recovery potential.

From these examples, the focus of this thesis on the river and sea water case can be justified. Although the energy density is the lowest (in MJ per m³), the huge flows – often expressed in m³/s instead of m³/h – provide the promise of a huge impact of this renewable energy source.

1.3 Energy recovery with reverse electrodialysis

The energy can be made available from controlled mixing of two solutions with different salt concentrations. The mixing process can be controlled by means of selective membranes. The use of selective membranes means that the mixing is limited to one of the components, either the solvent (i.e., water) or solutes (i.e., dissolved salts). In the literature, several techniques for energy conversion of the salinity gradient have been proposed, either based on the use of water-permeable membranes as in pressure-retarded osmosis [17-22], or based on the use of ion-selective membranes as in reverse electrodialysis [3, 23, 24].

It is tempting to compare these technologies with their ‘mirror image’, the respective well-known reversed operated desalination technologies: reverse osmosis and electrodialysis (Figure 4). To get a grasp on the principles and the process technology this would help, even for imagination, but it is impetuous to translate the design rules and economic figures of a desalination plant to a salinity-gradient power plant (as will be discussed in chapter 7).

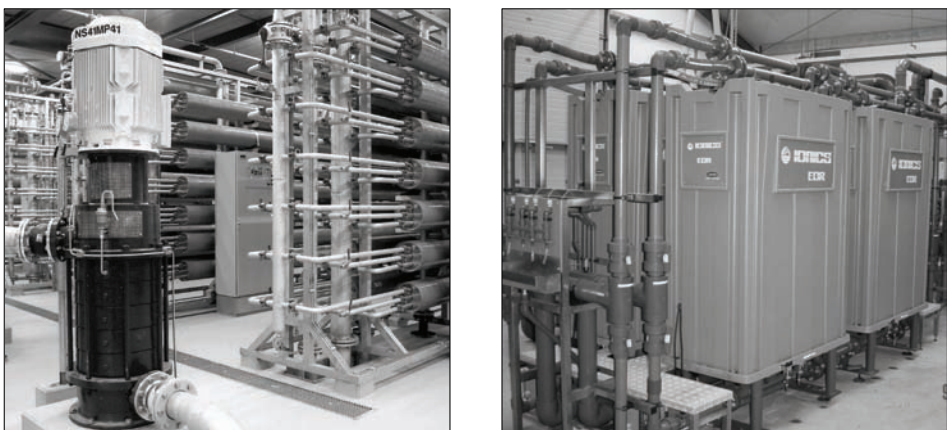


Figure 4: Reverse osmosis plant with spiral-wound membranes in pressure vessels, and electrodialysis with flat-sheet membranes in a stack.

Chapter 1

Reverse electrodialysis was selected for further investigation in this thesis, after an extensive evaluation of both techniques [14], as presented in chapter 2. Therefore, we now proceed with a brief description of a conventional electrodialysis system in order to introduce the commonly used terminology. Electrodialysis is used to transport salt ions from one solution through ion-exchange membranes to another solution under the influence of an applied electric potential difference. This is often done in an electrodialysis cell configuration, see Figure 5. The cell consists of a feed (diluate) compartment and a brine (concentrate) compartment formed by gaskets (D) and spacers (E) between a cation-exchange membrane (C) and an anion-exchange membrane (A). In almost all practical electrodialysis processes, multiple electrodialysis cells are arranged into a configuration called an electrodialysis stack, with alternating cation-exchange and anion-exchange membranes between two endplates (F) with a cathode (B) and an anode (B), respectively. The alternating distribution of diluate and concentrate through the stack is obtained via manifolds that are formed by subsequent holes in the membranes and gaskets. The position of the gasket determines whether a solution is fed to (and collected from) that specific compartment or not. The spacers – often woven fabrics - are used to keep distance between the membranes and to enhance turbulence of the feed flows.

In electrodialysis (Figure 5, schematic representation of principle), an electric potential is established between the cathode and the anode. When electrolyte solutions are pumped through the compartments, positively charged cations are forced to migrate in the direction of the cathode and negatively charged anions are forced to migrate in the direction of the anode. The cations are transported from the one compartment to the other through the negatively charged cation-exchange membrane, but are blocked for further transport by the positively charged anion-exchange membrane. Likewise, anions are transported from the one compartment

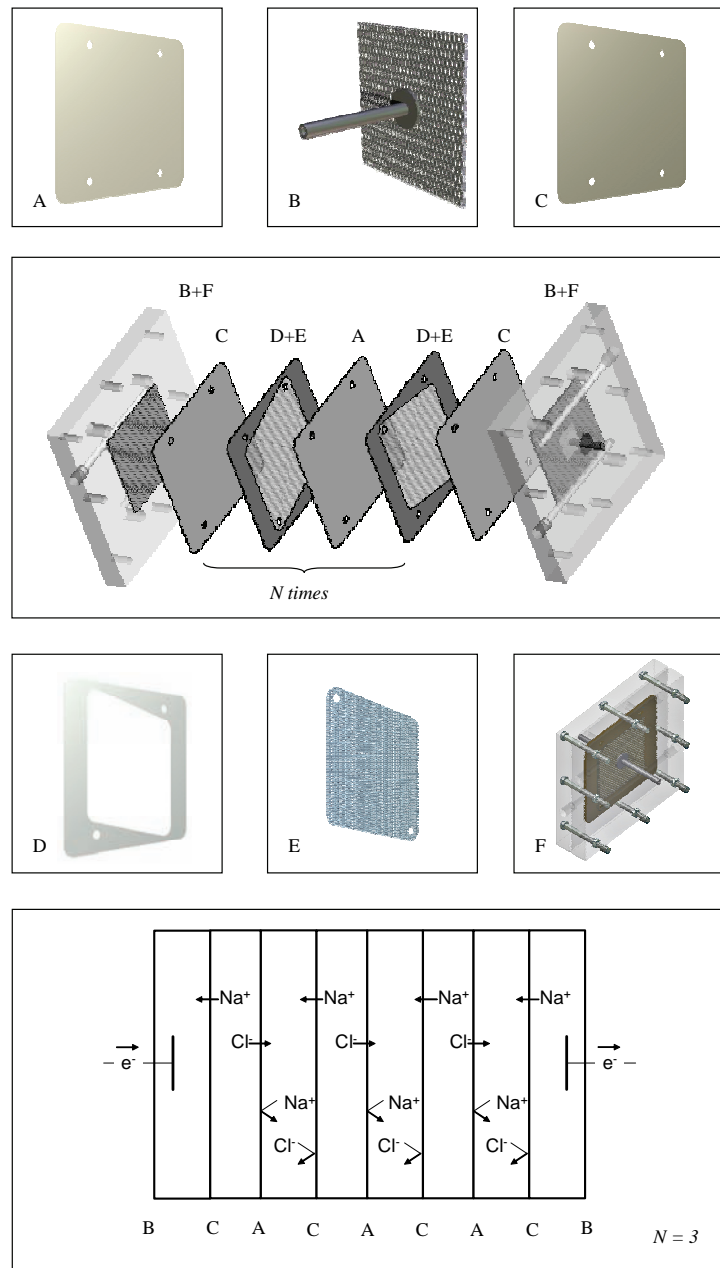


Figure 5: an electrodialysis stack, comprising of a number of cells (N) of cation-exchange membranes (C) and anion-exchange membranes (A) that are stacked in an alternating pattern between two endplates (F) with electrodes (B). Feed flow distribution between membranes are formed by gaskets (D) and screen spacers (E).

Chapter 1

to the other through the anion-exchange membrane, but are blocked for further transport by the cation-exchange membrane. The overall result is that alternating compartments become more concentrated with electrolytes, while the others become depleted. The depleted solution is often referred to as the diluate, the concentrated solution as the concentrate or brine. Depending on the application, the diluate (desalination) or the brine (table salt production, mineral recovery) is the product.

In a reverse electrodialysis system for power generation from salinity-gradients (Figure 6), like in electrodialysis, a number of cells are stacked between a cathode and an anode. The compartments between the membranes are alternately filled with a concentrated salt solution and a dilute salt solution. The salinity gradient results in a potential difference (e.g. 80-100 mV for sea water and river water) over each membrane, the so-called membrane potential. The electric potential difference between the outer compartments of the membrane stack is the sum of the potential differences over each membrane. The chemical potential difference causes the transport of ions through the membranes from the concentrated solution to the diluted solution. For a sodium chloride solution, sodium ions permeate through the cation-exchange membrane in the direction of the cathode, and chloride ions permeate through the anion-exchange membrane in the direction of the anode. Electro-neutrality of the solutions in both the anode compartment and cathode compartment is maintained through redox reactions at the electrodes. As a result, electrons can be transferred from anode to cathode via an external electric circuit. This electrical current and the potential difference over the electrodes can be used to generate electrical power, when an external load or energy consumer (e.g., a light bulb) is included in the circuit.

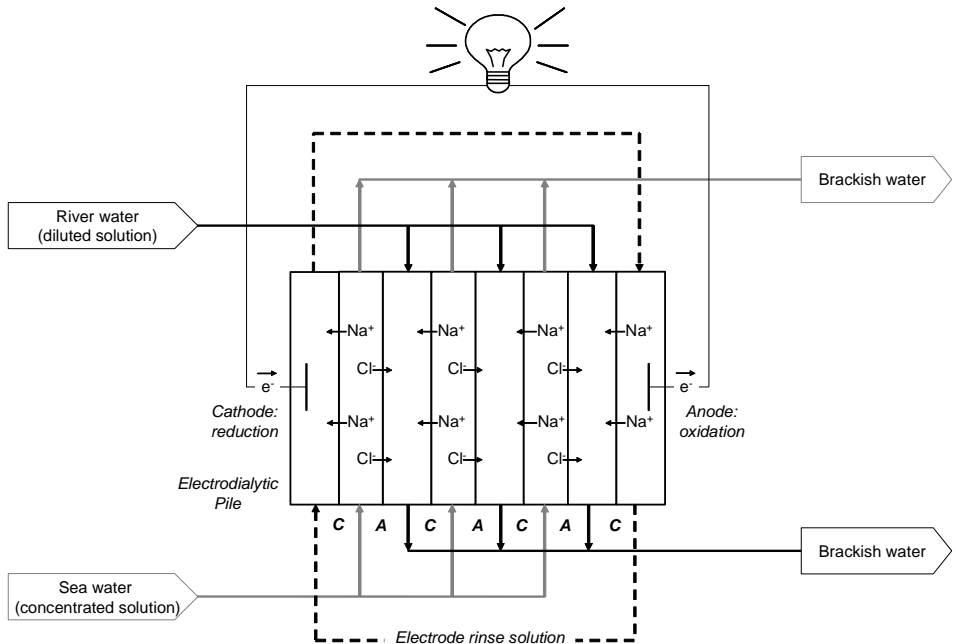


Figure 6: Conceptual presentation of salinity-gradient energy produced by reverse electrodialysis. C is cation-exchange membrane and A is anion-exchange membrane.

The driving force for transport of an ion is a gradient in free energy. The molar free energy (μ) of a component of an ideal solution can be written as follows (e.g. [25]):

$$\mu_i = \mu_i^0 + RT \ln x_i + |z_i|F\Delta\varphi \quad [4]$$

where μ^0 is the molar free energy under standard conditions (J/mol), z the valence of an ion (eq/mol), F the Faraday constant (96,485 C(eq)), and $\Delta\varphi$ the electrical potential difference (V).

For reverse electrodialysis, a potential difference across each membrane is generated that is composed of two contributions, the chemical potential difference $\Delta\mu$ (second term, J/mol) and the electrical potential difference across the membranes of a cell pair (third term, J/mol). These two

potentials may be combined to the electrochemical potential $\tilde{\mu}$ (J/mol). For a hypothetical reverse electrodialysis system operated close to equilibrium, i.e., without irreversible losses, $dG = \tilde{\mu} dn = 0$, the reversible cell-pair potential $\Delta\phi$ (V) can be derived when applied to sodium chloride solutions [14]:

$$\Delta\phi = \frac{2RT}{F} \ln\left(\frac{x_c}{x_d}\right) \quad [5]$$

As mentioned, a stack consists of a pile of cell-pairs between a cathode and an anode. When one cell-pair is represented as a voltage source, a number of cell-pairs N would result in an N times higher output voltage, or stack voltage. For a well-designed reverse electrodialysis stack, the reversible stack voltage E (V) is [26]:

$$E = N \cdot \Delta\phi \quad [6]$$

With ideal membranes (i.e., a coulombic efficiency of 100%), the reversible stack voltage can be measured under open-circuit conditions [27]. The open-circuit voltage can be used to generate an electrical flow through the electrical circuit and at the same time charge transport by cations and anions through the stack. Under current-producing conditions, the stack voltage V is lowered due to the internal resistance of the electrodialytic pile (membranes and solution compartments). We assume for now the stack voltage under current-producing conditions proportional with the current I , i.e.:

$$V = E - I \cdot R \quad [7]$$

where R is the stack resistance (Ω). This means that the stack voltage and thus the obtainable electrical energy (Joules per Coulomb) decrease with 22

an increasing current (Coulombs per second), see Figure 7. The obtainable electrical power W (Joules per second) forms a parabolic correlation with the current:

$$W = I \cdot V = I \cdot (E - I \cdot R) \quad [8]$$

The thermodynamic efficiency, defined as the ratio of the actual work (electrical potential) to the potential work (electrochemical potential), can also be related to the current:

$$\eta = \frac{V}{E} = 1 - \frac{I \cdot R}{E} \quad [9]$$

The reverse electrodialysis can be operated between two extremes (Figure 7). The first extreme is an operation under almost short-circuit conditions, i.e., when $V \downarrow 0$ and thus $I \uparrow E/R$. This is a useless extreme as both the power and the thermodynamic efficiency are zero. The other extreme is an operation under almost open-circuit conditions, i.e., when $I \downarrow 0$ and thus $V \uparrow E$. In this case the system would indeed be operated with a thermodynamic efficiency of close to 100% but without producing functional power.

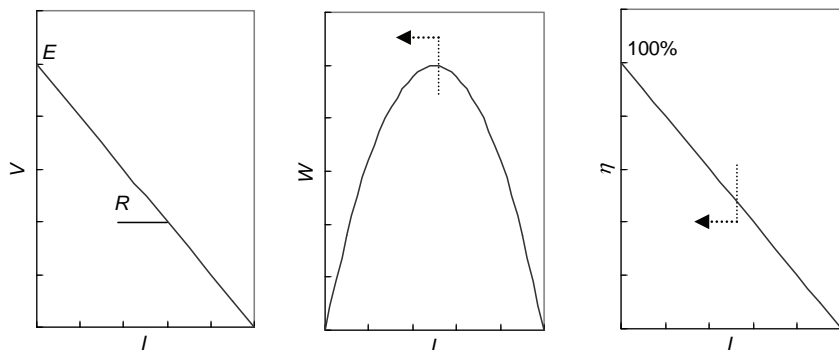


Figure 7: Curves to show the operational window of reverse electrodialysis: somewhere between maximum power output and maximum thermodynamic efficiency.

As a first estimate of a practical operation often the power is maximized, i.e., with $I = \frac{1}{2}E/R$ and $V = \frac{1}{2}E$, and consequently a thermodynamic efficiency of 50%. For a first estimation this assumption could be justified: the power obtained per m^2 of membrane (the power density) is than at maximum. It is, however, questionable if this is the real optimal operation when also the transport and pre-treatment efforts are taken into account. Keeping the entire process in mind, one can argue that 50% of these efforts are wasted just to get a maximum power density for the membranes. From this broader perspective, it is worthwhile to operate the system at a sub-optimal power density and current density but at a higher thermodynamic efficiency.

It should be noted that the discussion becomes more complicated when the process dynamics are taken into account. The reversible stack voltage (and thus the available work) decreases with increasing extent of transported charge Q , as the concentration of the concentrated solution is decreasing ($x_c \downarrow$) and the concentration of the diluted solution is increasing ($x_d \uparrow$). On the other hand, as the stack resistance is largely determined by the low-conductive diluted solution, the stack resistance also decreases with increasing extent of transported, as the conductivity of the diluted solution is increasing with an increasing salt concentration ($x_d \uparrow$). Taking this process dynamics into account, instead of the thermodynamic efficiency as defined here, the term energy recovery can better be used. The amount of recovered energy w can be calculated with:

$$w = \int V \, dQ \quad [10]$$

With this in mind, we started this thesis with evaluating the process with respect to energy recovery, and also with identifying and investigating the most critical process losses (i.e., the stack resistance).

1.4 Aim and outline of thesis

The scope of this thesis is to investigate the identified technical constraints which may be crucial for the technical and economic potential of salinity-gradient energy. As the technology is in its early phase of research and development, the focus of this thesis is on the process technology and not on the infrastructural and ecological aspects. The topics covered in this thesis are summarized in Table 1. In next paragraphs, we address the associated research gaps in order to define the topics for each chapter.

As mentioned previously, pressure-retarded osmosis and reverse electrodialysis are the most frequently studied membrane-based processes for energy conversion of salinity-gradient energy. To the best of our knowledge, there is no study which compares both techniques. Such an evaluation is not only necessary for system selection, but even a prerequisite to get a clear sight on the important parameters and challenges for further development. Therefore, in **chapter 2** both techniques are described based on what is known from scientific literature containing experimental data. Last addition is important as the amount of literature with speculations - ranging from optimistic to illusive expectations - is enormous, where the amount of references with reproducible experiments is limited.

A main question is how much of this salinity-gradient energy can be converted into sustainable electricity. From the review in chapter 2 we found that actually hardly attention was paid to the energetic efficiency. Described experiments focused on power output or power density whereas the energy recovery was never directly measured. As discussed, energy recovery is a very important aspect considering the feasibility of the entire process. Therefore, in **chapter 3** our aim was to investigate the energy recovery that can be obtained.

Chapter 1

Table 1: Topics and outline of thesis

Chapter	Research question	Topic
2	What is the status of the technologies at the start of our research program?	Critical review and evaluation of status of technologies, justification of the choice of reverse electrodialysis.
3	What is the obtainable energy recovery from these technologies?	Experimental work to prove whether the technology is able to obtain a considerable energy recovery, a prerequisite for success.
4	How do other salts than sodium chloride influence the process?	Experimental work to investigate the influence of the chemical composition of feed water on the performance.
5	How can the process be operated in biological active surface waters?	Experimental work to investigate the influence of biofilm formation on the performance and to test preventive measures.
6	What is a most practical design for the process concerning biofouling?	Experimental work to investigate the influence of the design on the robustness of the process concerning biofilm formation.
7	Which technical and economic challenges should be met?	Outlook envisioning technical and economic challenges, discussion of field tests with pre-treatment and system engineering.
8	Knowing all above, what are the prospects of Blue Energy on global and national level?	Outlook envisioning the prospects of Blue Energy for policy makers.

In the research on reverse electrodialysis, so far, the presence of other ions than sodium and chloride was hardly taken into account. However, in most practical cases also other ions are present in both feed solutions. Concerns mentioned in literature are possible fouling effects [23] and high resistivity of membranes against transport of multivalent ions [24, 28]. We think, however, that there is a more fundamental effect. The presence of multivalent ions may also have a lowering effect on stack voltage and consequently on the power density. The objective of our study was to investigate the effect of the presence of multivalent ions in the feed solutions on the power density of a reverse electrodialysis system. In **chapter 4**, we investigated the influence of multivalent ions on stack voltage and ion transport in the stack. We also investigated whether monovalent-selective ion-exchange membranes can be used to improve the performance of reverse electrodialysis.

Applying the system on feed waters with different chemical compositions as in chapter 4 may be the first step to practice, a second step is to investigate how reverse electrodialysis behaves when applied to biologically active feed waters. Fouling of ion-exchange membranes is considered to be one of the most important limitations for practical use of electrodialysis processes. Little is known, however, about the effects of fouling on the reverse electrodialysis process. There is only one preliminary study on the effect of biofilm formation [29] that concluded that the economy of reverse electrodialysis will depend largely on if and how the effects of biofilm formation can be controlled. In **chapter 5**, we focused on biofouling. As biofilm formation can not be prevented by any pretreatment process [30] and the use of supplied chemicals or reagents for fouling prevention or cleaning of the stacks should be limited for reasons of sustainability, our challenge was to find operational biofouling control methods.

Chapter 1

In chapter 3, we addressed that the screen spacers between the membranes are of major importance regarding the internal losses of reverse electrodialysis [27]. The spacers are not only identified as undesired isolators, but from chapter 5 it became clear that they also form a place for biofilm accumulation causing pressure-drop increases [31] and a subsequent decline of the electrical performances. The objective of **chapter 6** was to give a proof of principle of a spacer-free reverse electrodialysis system, firstly on performance and secondly on biofouling behavior.

Wetsus - centre for sustainable water technology in the Netherlands - started in 2005 with the project 'Blue Energy' with a focus on reverse electrodialysis. The achievements of previous chapters, but also from relating academic research within Wetsus, formed the starting point of **chapter 7**. In this chapter, we discussed the challenges we are facing concerning the economic and technological feasibility. The following issues were discussed: (i) the development of low-cost membranes, (ii) the pre-treatment in relation to stack design and operation, and (iii) an economic evaluation. Also the further steps on the developing path of reverse electrodialysis were presented.

As an outlook of this thesis, the aim of **chapter 8** was to estimate the prospects of the new technology more accurately on global and national level. The available estimates of the global potentials must be considered as first order estimates, as these were based neither on a regionally specific assessment of river discharge and salinity gradients nor on accurate assumptions for the state-of-the-art technology. The promising prospects, especially for Netherlands where salinity gradients could be a significant source of energy, leads to a strong recommendation to policy makers, captains of industry, and principal scientists to proceed with research and development of reverse electrodialysis.

1.5 References

1. Pattle, R.E., Production of electric power by mixing fresh and salt water in the hydroelectric pile, *Nature* 174(4431) (1954), p. 660-660.
2. Norman, R.S., Water salination: A source of energy, *Science* 186 (1974), p. 350-352.
3. Weinstein, J.N. and F.B. Leitz, Electric-power from difference in salinity - dialytic battery, *Science* 191(4227) (1976), p. 557-559.
4. Rosenberg, M., Polders and dykes of the Netherlands, the reclamation of land in the Netherlands. 2009, About.com: New York.
5. Wick, G.L. and W.R. Schmitt, Prospects for renewable energy from sea, *Marine Technology Society Journal* 11(5-6) (1977), p. 16-21.
6. Isaacs, J.D. and R.J. Seymour, The ocean as a power resource, *International Journal of Environmental Studies* 4(1) (1973), p. 201-205.
7. Isaacs, J.D. and W.R. Schmitt, Ocean energy: Forms and prospects, *Science* 207(4428) (1980), p. 265-273.
8. EIA, International energy outlook 2009. Office of integrated analysis and forecasting. 2009, Washington D.C.: U.S. Department of energy.
9. IPCC, Guidelines for national greenhouse gas inventories. Vol. 2. 2006.
10. Boudri, J.C., L. Hordijk, C. Kroese, M. Amann, J. Cofala, I. Bertok, L. Junfeng, D. Lin, Z. Shuang, H. Runqing, T.S. Panwar, S. Gupta, S. Singh, A. Kumar, M.C. Vipradas, P. Dadhich, N.S. Prasad, and L. Srivastava, The potential contribution of renewable energy in air pollution abatement in China and India, *Energy Policy* 30 (2002), p. 409-424.
11. Olivier, J.G.J., J.A. Van Aardenne, F. Dentener, V. Pagliari, L.N. Ganzeveld and J.A.H.W. Peters, Recent trends in global greenhouse gas emissions: Regional trends 1970-2000 and spatial distribution of key sources in 2000, *Env. Sc.*, 2(2-3) (2005), p. 81-99.
12. Norman, R.S., Water salination: A source of energy, *Science* 4161 (1974), p. 350-352.
13. Loeb, S., Large-scale power production by pressure-retarded osmosis, using river water and sea water passing through spiral modules, *Desalination* 143 (2002), p. 115-122.
14. Post, J.W., J. Veerman, H.V.M. Hamelers, G.J.W. Euverink, S.J. Metz, D.C. Nijmeijer and C.J.N. Buisman, Salinity-gradient power: Evaluation of pressure-retarded osmosis and reverse electrodialysis, *Journal of Membrane Science* 288 (2007), p. 218-230.
15. Loeb, S., Energy production at the Dead Sea by pressure-retarded osmosis: Challenge or chimera? *Desalination* 120 (1998), p. 247-262.
16. Wick, G.L. and J.D. Isaacs, Salt domes: Is there more energy available from their salt than from their oil? *Science* 199(4336) (1978), p. 1436-1437.
17. Jellinek, H.H.G. and H. Masuda, Osmo-power. Theory and performance of an osmo-power pilot plant, *Ocean Engineering* 8(2) (1981), p. 103-128.
18. Loeb, S., Osmotic power plants, *Science* 189(4203) (1975), p. 654-655.
19. Loeb, S., Production of energy from concentrated brines by pressure-retarded osmosis: I. Preliminary technical and economic correlations, *Journal of Membrane Science* 1 (1976), p. 49-63.
20. Loeb, S., One hundred and thirty benign and renewable megawatts from Great Salt Lake? The possibilities of hydroelectric power by pressure-retarded osmosis, *Desalination* 141(1) (2001), p. 85-91.

Chapter 1

21. Loeb, S., F. Van Hessen and D. Shahaf, Production of energy from concentrated brines by pressure retarded osmosis. ii. Experimental results and projected energy costs, *Journal of Membrane Science* 1(3) (1976), p. 249-269.
22. Panyor, L., Renewable energy from dilution of salt water with fresh water: Pressure retarded osmosis, *Desalination* 199(1-3) (2006), p. 408-410.
23. Lacey, R.E., Energy by reverse electrodialysis, *Ocean Engineering* 7(1) (1980), p. 1-47.
24. Jagur-Grodzinski, J. and R. Kramer, Novel process for direct conversion of free-energy of mixing into electric-power, *Industrial & Engineering Chemistry Process Design And Development* 25(2) (1986), p. 443-449.
25. Strathmann, H., *Ion-exchange membrane separation processes*, 1st ed. 2004: Elsevier.
26. Veerman, J., J.W. Post, S.J. Metz, M. Saakes and G.J. Harmsen, Reducing power losses caused by ionic shortcut currents in reverse electrodialysis stacks by a validated model, *Journal of Membrane Science* (310) (2008), p. 418-430.
27. Post, J.W., H.V.M. Hamelers and C.J.N. Buisman, Energy recovery from controlled mixing salt and fresh water with a reverse electrodialysis system, *Environ Science Technology* 42 (2008), p. 5785-5790.
28. Audinos, R., Electric-power produced from 2 solutions of unequal salinity by reverse electrodialysis, *Indian Journal Of Chemistry* 31(6) (1992), p. 348-354.
29. Ratkje, S.K., T. Holt and L. Fiksdal. Effect of biofilm formation on salinity power plant output on laboratory scale, in *Industrial Membrane Processes (Aiche Symposium Series)*. 1986.
30. Flemming, H.C., G. Schäule, T. Griebel, J. Schmitt and A. Tamachkiarowa, Biofouling - the achilles heel of membrane processes, *Desalination* 113 (1997), p. 215-225.
31. Vrouwenvelder, J.S., S.A. Manolarakis, J.P. van der Hoek, J.A.M. van Paassen, W.G.J. van der Meer, J.M.C. van Agmaal, H.D.M. Prummel, J.C. Kruithof, and M.C.M. van Loosdrecht, Quantitative biofouling diagnosis in full scale nanofiltration and reverse osmosis installations, *Water Research* (42) (2008), p. 4856-4868.

2 Evaluation of pressure-retarded osmosis and reverse electrodialysis

A huge potential to obtain clean energy exists from mixing water streams with different salt concentrations. Two membrane-based energy conversion techniques are evaluated: pressure-retarded osmosis and reverse electrodialysis. From the literature, a comparison is not possible since the reported performances are not comparable. A method was developed which allows for a comparison of both techniques at equal conditions, with respect to power density and energy recovery. Based on the results from the model calculations, each technique has its own field of application. Pressure-retarded osmosis seems to be more attractive for power generation using concentrated saline brines because of the higher power density combined with higher energy recovery. Reverse electrodialysis seems to be more attractive for power generation using sea water and river water. These conclusions are valid for present and latent performances of both techniques. According to the model, the potential performances of both techniques are much better than the current performances. In order to achieve these potential performances, the development of pressure-retarded osmosis must focus on membrane characteristics, i.e., increasing the water permeability of the membrane skin and optimization of the porous support. The development of reverse electrodialysis, however, must focus on system characteristics, i.e., optimization of the internal resistance, which is mainly determined by the width of the spacers.

This chapter has been published as:

Post, J.W., J. Veerman, H.V.M. Hamelers, G.J.W. Euverink, S.J. Metz, D.C. Nijmeijer and C.J.N. Buisman, Salinity-gradient power: Evaluation of pressure-retarded osmosis and reverse electrodialysis, *Journal of Membrane Science* 288 (2007), p. 218-230.

2.1 Introduction

The need for clean and sustainable energy sources is quite evident, since fossil fuels have a number of drawbacks: such as emissions of greenhouse gases, depletion of finite sources, and dependence on a few oil-exporting regions in the world. Current energy conversion techniques that are considered to be sustainable include solar, wind, biomass, and hydro energy. There are other sources of sustainable energy including, but not limited to tidal power, ocean wave power, ocean thermal energy conversion which are discussed by Wick et al [1]. A significant potential to obtain clean energy exists from mixing water streams with different salt concentrations. This salinity-gradient energy, in the research programs of our institutes also called blue energy, is available worldwide where fresh water streams flow into the sea. The global energy output from estuaries is estimated at 2.6 TW [1], which represents approximately 20% of the present worldwide energy demand. Large amounts of blue energy can also be made available from natural or industrial salt brines.

In general, techniques currently available for desalination could be used to generate power from salinity gradients when operated in the reversed mode [2]. In the literature, several techniques for energy conversion of the salinity gradient have been proposed: pressure-retarded osmosis [3], reverse electrodialysis [4], and vapor-pressure difference utilization [5]. Although the potential for salinity-gradient energy was recognized more than half a century ago [4], until now utilization has been considered to be neither economically feasible nor technically attractive when compared to fossil fuel systems. The main drawback of these membrane-based conversion techniques was the high price of membranes. However, the decreasing prices of membranes for desalination and water reuse applications as well as the increasing prices of fossil fuels make salinity-gradient power attractive in near future. Therefore, reconsideration of the

available membrane-based processes for the production of sustainable power from salinity-gradient energy is worthwhile.

Pressure-retarded osmosis and reverse electrodialysis are the most frequently studied membrane-based processes for energy conversion of salinity-gradient energy. To the best of our knowledge, there is no study which compares both techniques. Such an evaluation is a prerequisite to highlight the potential and challenges for further development of both techniques. Our objective is to evaluate and compare the potential of pressure-retarded osmosis and reverse electrodialysis.

2.2 Theory

2.2.1 Principles

Principle of pressure-retarded osmosis. In a pressure-retarded osmosis system, two solutions of different salinity are brought into contact by a semi-permeable membrane (*Figure 1*). This membrane allows the solvent (i.e., water) to permeate and retains the solute (i.e., dissolved salts). The chemical potential difference between the solutions causes transport of water from the diluted salt solution to the more concentrated salt solution. If hydrostatic pressure is applied to the concentrated solution, the water transport will be partly retarded. The transport of water from the low-pressure diluted solution to the high-pressure concentrated solution results in a pressurization of the volume of transported water. This pressurized volume of transported water can be used to generate electrical power in a turbine.

Principle of reverse electrodialysis. In a reverse electrodialysis system, a number of cation and anion-exchange membranes are stacked in an alternating pattern between a cathode and an anode (*Figure 2*).

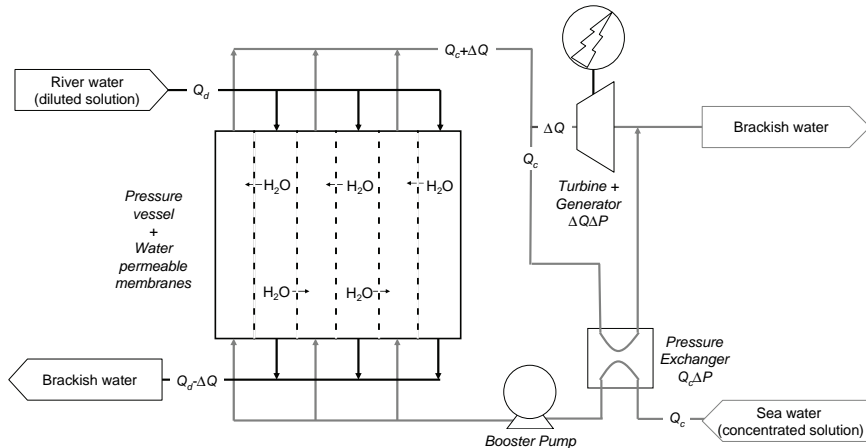


Figure 1: Conceptual representation of an energy conversion scheme using pressure-retarded osmosis; Q is the volumetric solution flow (m^3/s), ΔQ the transported amount of water in time through the membranes (m^3/s), ΔP the applied hydrostatic pressure difference between both solutions (Pa), whereas the power generated by means of a turbine and generator is $\Delta Q \cdot \Delta P$ (W).

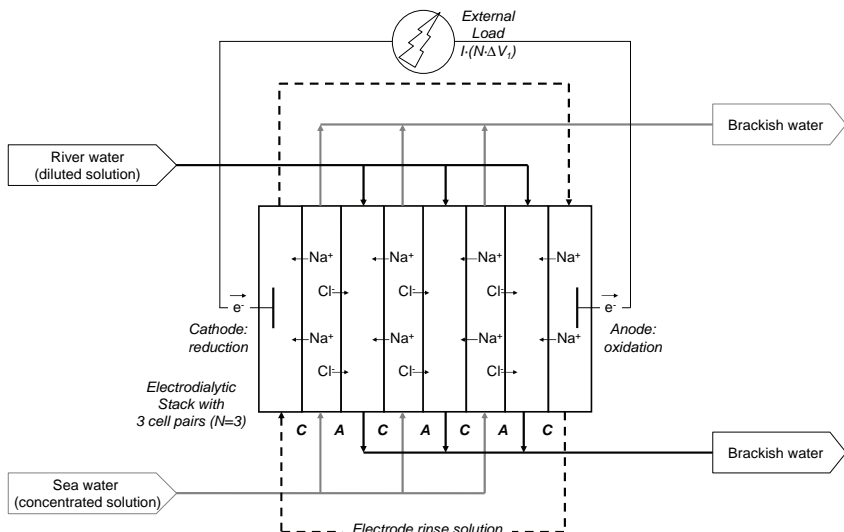


Figure 2: Conceptual representation of an energy conversion scheme using reverse electrodialysis; A is an anion-exchange membrane, C a cation-exchange membrane, I the electrical current or transported charge (A), N the number of cell pairs (in this case $N=3$), $N \cdot \Delta V_i$ the potential difference over the applied external load (V), whereas the power generated is $I(N \cdot \Delta V)$ (W).

Chapter 2

The compartments between the membranes are alternately filled with a concentrated salt solution and a diluted salt solution. The salinity gradient results in a potential difference (e.g. 80 mV for sea water and river water) over each membrane, the so-called membrane potential. The electric potential difference between the outer compartments of the membrane stack is the sum of the potential differences over each membrane.

The chemical potential difference causes the transport of ions through the membranes from the concentrated solution to the diluted solution. For a sodium chloride solution, sodium ions permeate through the cation-exchange membrane in the direction of the cathode, and chloride ions permeate through the anion-exchange membrane in the direction of the anode. Electro-neutrality of the solution in the anode compartment is maintained via oxidation at the anode surface. Electro-neutrality of the solution in the cathode compartment is maintained via reduction at the cathode surface. As a result, an electron can be transferred from the anode to the cathode via an external electric circuit. This electrical current and the potential difference over the electrodes can be used to generate electrical power, when an external load or energy consumer is connected to the circuit.

2.2.2 Comparison of techniques based on data from the literature

An evaluation and comparison of pressure-retarded osmosis and reverse electrodialysis is made by reviewing the literature. The literature that reported experimental data was culled.

Experimental data for pressure-retarded osmosis. Pressure-retarded osmosis is the most studied membrane-based technique for energy production from salinity gradients. The amount of experimental data, however, is limited and difficult to compare with each other. In general, the obtained power is not reported separately, but can be derived from the

available data (e.g. water flux, applied hydrostatic pressure). Obtained power densities are presented in *Figure 3*. Currently available reverse osmosis membranes in a pressure-retarded osmosis application on sea water and fresh water (osmotic pressure difference $\Delta\pi = 20\text{-}25$ bar) could yield a power density between 0.11 and 1.22 W/m² (*Figure 3*).

The higher value is obtained for mixing two solutions with $\Delta\pi = 39$ bar using cellulose acetate membranes [9]. According to Lee [10], cellulose acetate membranes should have favorable characteristics for pressure-retarded osmosis: high permeability, high salt rejection and low transport resistance of the support layer. A power density of 1.54 W/m² was predicted [10].

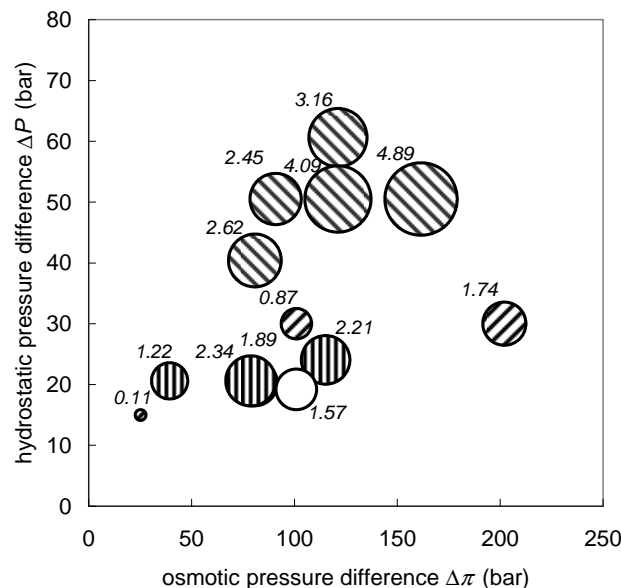


Figure 3: Power densities (W/m²) obtained with pressure-retarded osmosis; $\Delta\pi$ is the osmotic pressure difference between the two salt solutions and ΔP the applied hydrostatic pressure difference over the membrane. Diameter of the bullets represents the power density as derived from reported osmotic pressure, hydrostatic pressure, and from water fluxes (▨ Loeb et al., 1976 [6]); or from permeation coefficients (▨ Mehta et al., 1979 [7]; □ Loeb et al., 1979 [8]; Mehta et al., 1982 [9]). Applied membrane materials: poly amide [6, 7], cellulose acetate [9], furan skin [8].

Currently available reverse osmosis membranes in a pressure-retarded osmosis application on more concentrated brines and fresh water ($\Delta\pi > 75$ bar) could yield a power density of 2 to 5 W/m² (Figure 3). Hollow-fiber aromatic polyamide membranes provide the most promising power densities [7]. Later experiments with spiral-wound cellulose acetate membranes were limited by the applied hydrostatic pressure difference ($\Delta P < 24$ bar) [9]. For this reason, it is not possible to draw conclusions on which membrane material (e.g. aromatic polyamide or cellulose acetate) or which configuration (e.g. hollow-fiber or flat-sheet) is favorable for application on more concentrated brines.

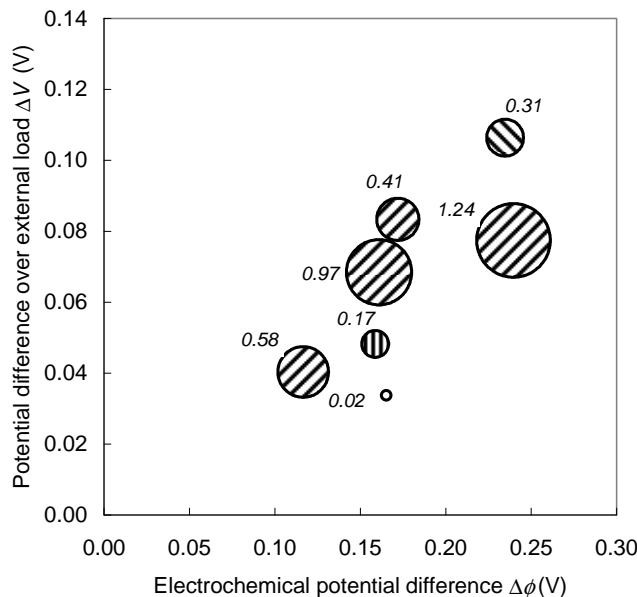


Figure 4: Power densities (W/m²) obtained with reverse electrodialysis (power density for total membrane area, i.e. both anion and cation-exchange membranes); $\Delta\phi$ is the electrochemical potential difference, and ΔV the potential difference over the external load. Diameter of the bullets represents the power densities either reported (▨ Jagur-Grodzinski et al., 1986 [11]), or derived from reported potential, resistances and current (□ Pattle, 1954 [4]; Weinstein et al., 1976 [13]; ▲ Audinos, 1992 [14]).

Experimental data for reverse electrodialysis. For reverse electrodialysis, the published experimental data is scarcer than for pressure-retarded osmosis. Obtained power densities are presented in *Figure 4*. Currently available electrodialysis membranes in a reverse electrodialysis application on sea water and fresh water (electrochemical potential difference $\Delta\phi = 0.17$ V) could yield a power density of 0.41 W/m^2 (*Figure 4*). This power density was obtained with heterogeneous modified polyethylene membranes and shaped, chemically modified spacers. According to Jagur-Grodzinski et al. [11], the spacer characteristics, i.e. the control of flow patterns, seemed to be more important than the membrane characteristics, since all tested membranes were comparable with respect to perm selectivity and resistance.

Currently available electrodialysis membranes in a reverse electrodialysis application on more concentrated brines and fresh water could yield a power density of 1.2 W/m^2 (*Figure 4*). Most promising power outputs were obtained with the same membranes and spacers as was the case for the sea water application [11]. A limit on applicable salt concentrations in the concentrated brines was suggested [12], which is in accordance with the observation that the power density has a non-linear response to increasing electrochemical potential (which is the result of a decreasing permselectivity with increasing salt concentrations, as explained later in the chapter).

Comparison of techniques. From the literature, one may suggest that the two techniques have their own field of application. Pressure-retarded osmosis may be preferable to convert salinity-gradient energy from mixing more concentrated brines with diluted solutions, whereas reverse electrodialysis may be preferable to convert salinity-gradient energy from mixing sea water with diluted solutions. However, such a conclusion is not well-founded for more than one reason:

Chapter 2

- For pressure-retarded osmosis, the efficiency losses due to conversion of hydrostatic potential energy to electrical energy by a turbine and generator were not taken into account, whereas for reverse electrodialysis the efficiency losses due to electrode reactions were taken into account.
- Different mixtures of sodium chloride solutions were used. For pressure-retarded osmosis, generally, the salt concentrations of the diluted solutions were kept considerably low (pure water) whereas for reverse electrodialysis the salt concentrations of the diluted solutions were higher.
- The only reported measure of performance for each technique is the obtained power or the power density (W/m^2) as shown in *Figure 3* and *Figure 4*. However, the obtained power can not be seen separately from the energy recovery. This energy recovery represents the amount of energy converted per volume of feed solutions (J/m^3).

A comparison of pressure-retarded osmosis and reverse electrodialysis using experimental data available from the literature is not sufficient as the conditions were not equal and the reported performances were incomplete. Therefore, we developed a method which allows for a better comparison under equal conditions, namely, on power density and energy recovery.

2.3 Methods

2.3.1 Assumptions

In order to compare pressure-retarded osmosis and reverse electrodialysis under equal conditions we developed a model in which each equation valid for pressure-retarded osmosis was compared to its equivalent for reverse electrodialysis. The following assumptions were made:

- Feed solutions were assumed to consist of pure sodium chloride solutions. No distinction was made between concentrations and activities (i.e. ideal behavior). Mole fractions were used, which were defined as:

$$x_i = c_i \cdot \bar{V} \quad [1]$$

- Where subscript i refers to the component under consideration, x is the mole fraction (-), c the concentration (mol/m^3), and \bar{V} the molar volume of the solution (m^3/mol). The molar volumes were derived from data on volumetric properties of aqueous sodium chloride [15]. Mole fractions which were mentioned without subscript should be read as mole fractions of the dissolved sodium and chloride ions.
- Sodium chloride solutions of different molarities were annotated as 'river', 'sea' and 'brine'. They correspond to following sodium chloride concentrations: river 0.05 mol/L, sea 0.5 mol/L, and brine 5.0 mol/L.
- The temperature of the solutions was 293 K.
- The volumetric mixing rate of the concentrated solution to the diluted solution was 1:1.
- Membranes were considered to behave ideal; pressure-retarded-osmosis membranes were only permeable to water and reverse-

electrodialysis membranes were only permeable to salt ions (mainly for counter-ions, but to a limited extent also to co-ions).

- We used the *gross* power density instead of the *net* power density, which means that internal efficiency losses (e.g. friction losses, pump and turbine efficiencies, electrochemical (over-)potentials) were not taken into account. For comparison of pressure-retarded osmosis and reverse electrodialysis, configuration specific efficiency losses were neglected, assuming that these did not account for a distinction between both techniques. For instance, external concentration polarization in both systems could be minimized by an appropriate cross-flow velocity.

2.3.2 Model

Several models are available, which are using many of the assumptions described in the previous section (for pressure-retarded osmosis e.g. [3, 10]; for reverse electrodialysis e.g. [13]). In the present work we translated each equation valid for pressure-retarded osmosis into its equivalent for reverse electrodialysis in order to get a usable model for comparison at same conditions.

Energy from mixing salt and fresh water. The driving force for transport of a component is a gradient in free energy. The molar free energy (μ) of a component of an ideal solution can be written as follows (e.g. [16]):

$$\mu_i = \mu_i^0 + \bar{v}_i \Delta p + RT \ln x_i + |z_i|F\Delta\varphi \quad [2]$$

where μ^0 is the molar free energy under standard conditions (J/mol), \bar{v} the partial molar volume, Δp the pressure change compared to atmospheric conditions (Pa), R the gas constant (8.314 J/mol·K), T the absolute temperature (K), z the valence of an ion (eq/mol), F the Faraday constant

(96,485 C/eq), and $\Delta\varphi$ the electrical potential difference (V). The theoretical amount of free energy which can be obtained from mixing two solutions of different salinity can be calculated by using Equation 2. Since there is no pressure change or charge transport, the total amount of energy can be determined from the chemical potential difference before mixing subtracted by the chemical potential after mixing. The free energy difference from mixing a concentrated and a diluted solution becomes:

$$\begin{aligned}\Delta G &= \sum_i (G_{i,c} + G_{i,d} - G_{i,b}) \\ &= \sum_i (c_{i,c} V_c RT \ln(x_{i,c}) + c_{i,d} V_d RT \ln(x_{i,d}) - c_{i,b} V_b RT \ln(x_{i,b}))\end{aligned}\quad [3]$$

where G is the free energy (J) and V the volume (m^3), subscript c refers to the concentrated salt solution, subscript d to the diluted salt solution, subscript b to the brackish salt solution which remains after mixing. Often the free energy difference of the water is not taken into account (e.g. [17]), which results in an under-estimation of <10%.

The theoretically available amount of energy from mixing 1 m^3 sea water (comparable to 0.5 mol/L NaCl) and 1 m^3 river water (comparable to 0.01 mol/L NaCl) both at a temperature of 293 K is 1.5 MJ; the theoretically available amount of energy from mixing 1 m^3 brine (5 mol/L NaCl) and 1 m^3 river water (0.01 mol/L NaCl) at 293 K is more than 16.9 MJ. The theoretically available amount of energy for an extensive range of sodium chloride concentrations is presented in *Figure 5*.

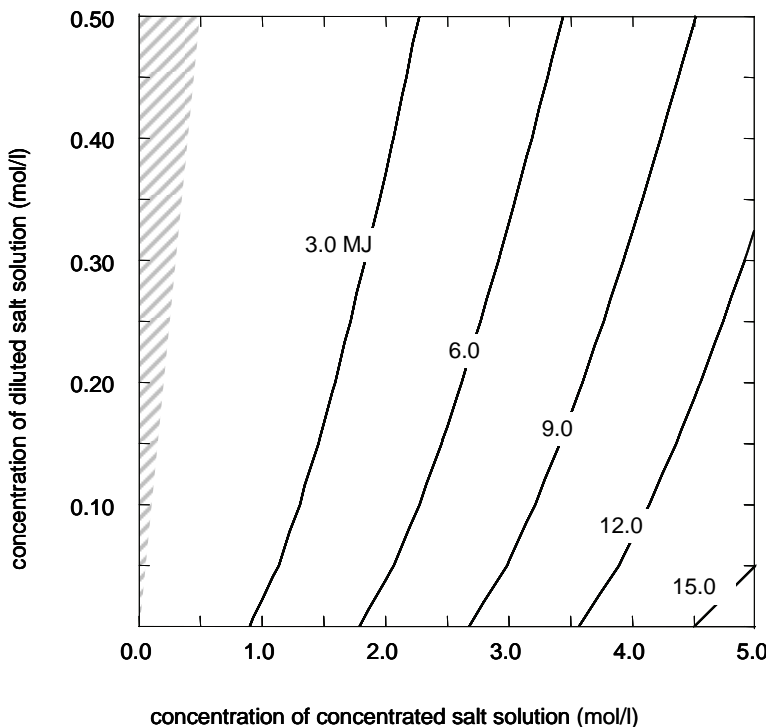


Figure 5: Theoretically available amount of energy (MJ) from mixing 1 m³ of a diluted and 1 m³ of a concentrated sodium chloride solution ($T = 293\text{ K}$). Shaded area: is kept out of consideration since here the salt concentration of the concentrated solutions is lower than that of the diluted solution.

Driving force for pressure-retarded osmosis. Osmosis can only occur due to the presence of a semi-permeable membrane, which separates a concentrated solution (salt water) from a diluted solution (fresh water). This membrane allows the passage of water and retains the transport of ions. The driving force for the permeation of water is a difference in free energy between the salt and the fresh water side. This water transport is opposed by a higher hydrostatic pressure at the concentrated salt solution compartment. Water transport will continue until equilibrium is reached. Since there is no transport of ions ($|z_i|F\Delta\varphi=0$) and to the diluted solution a

hydrostatic pressure $\Delta p = 0$ is applied, Equation 2 reduces at equilibrium conditions ($\mu_{H_2O,c} = \mu_{H_2O,d}$) to:

$$\bar{v}_{H_2O,c}\Delta\pi + RT \ln(x_{H_2O,c}) = RT \ln(x_{H_2O,d}) \quad [4]$$

where $\Delta\pi$ is the osmotic pressure difference between both solutions (Pa). Since for sodium chloride solutions $\ln(x_{H_2O}) = \ln(1 - 2x) \approx 2\ln(1 - x)$ and $\bar{v}_{H_2O,c} = \bar{v}$, Equation 4 can be reduced to:

$$\Delta\pi = \frac{2RT}{\bar{v}} \ln \frac{(1 - x_d)}{(1 - x_c)} \quad [5]$$

The osmotic pressure difference between both solutions is the driving force for osmotic water transport. In pressure-retarded osmosis a hydrostatic pressure is applied at the salt water side (ΔP , Pa), which reduces the driving force for water transport to $\Delta\pi - \Delta P$. The applied hydrostatic pressure difference should be less than the osmotic pressure ($\Delta P < \Delta\pi$) but can also be limited by the configuration of the system and the mechanical strength of the membrane ($\Delta P < \Delta P_{max}$, where ΔP_{max} is the maximum allowable hydrostatic pressure difference over the membrane). The transport of water through the membrane (Q , m³/s) and the hydrostatic pressure difference (ΔP) can be used for power production by a turbine and generator (see *Figure 1*).

Driving force for reverse electrodialysis. Ion transport in reverse electrodialysis can only occur due to the presence of perm-selective ion-exchange membranes (i.e. cation-exchange membranes and anion-exchange membranes), which separate a concentrated solution from the diluted solution. These membranes allow the selective passage of ions and retain the transport of water. The driving force for the migration of ion is a

difference in free energy between the concentrated and the diluted solution side. This ion transport will continue until equilibrium is reached. Since there is no transport of water and there is no pressure difference between both solutions (for both solution Δp is equal), Equation 2 reduces at equilibrium conditions ($\mu_{NaCl,c} = \mu_{NaCl,d}$ and to both solutions an electrical potential $\Delta\phi$ is applied which equals their electrochemical potential ϕ) to:

$$\begin{aligned} \frac{RT}{|z_{Na}|F} \ln(x_{Na,c}) + \frac{RT}{|z_{Cl}|F} \ln(x_{Cl,c}) &= \\ \frac{RT}{|z_{Na}|F} \ln(x_{Na,d}) + \frac{RT}{|z_{Cl}|F} \ln(x_{Cl,d}) + \Delta\phi & \end{aligned} \quad [6]$$

where $\Delta\phi$ is the electrochemical potential difference between both solutions (V). Since for sodium chloride solutions $|z_{Na}| = |z_{Cl}| = 1$ and $x_{Na} = x_{Cl} = x$, Equation 6 can be reduced to a Nernst-equation for an aqueous monovalent electrolyte:

$$\Delta\phi = \frac{2RT}{F} \ln\left(\frac{x_c}{x_d}\right) \quad [7]$$

The electrochemical potential difference between both solutions is the driving force for ion transport. Notice that, in practice, cell pairs are stacked and the electrochemical potential difference should be multiplied by the number of cell pairs. In reverse electrodialysis an electrical potential difference is applied over an external load ($N \cdot \Delta V_1$, V), which in case of one cell pair ($N = 1$, and thus $\Delta V = \Delta V_1$), reduces the driving force for ion transport to $\Delta\phi - \Delta V$. The charge transport through the membranes (I , C/s) and the applied potential difference (ΔV) result in a power production (see Figure 2).

Molar flux of pressure-retarded osmosis. In practice, the apparent driving force for water transport in pressure-retarded osmosis deviates from $\Delta\pi - \Delta P$. The driving force seems not to be determined by the osmotic pressure difference of the bulk solutions, but by the osmotic pressure difference over the semi-permeable skin (see *Figure 6*). In other words, the driving force needs to be corrected for the internal concentration polarization occurring in the porous support layer at the fresh water side [3, 10, 18]. This corrected osmotic pressure difference is given by:

$$\Delta\pi_{eff} = \pi_c - \pi_d \exp(J_w k) \quad [8]$$

where $\Delta\pi_{eff}$ is the corrected or effective osmotic pressure difference over the semi-permeable skin (Pa), J_w the volumetric water flux (m/s), and k the transport resistance to a salt in the porous support layer (s/m). In practice, the internal concentration polarization is also determined by salt diffusion through the skin from the concentrated salt solution to the diluted salt solution. However, this salt diffusion is excluded from the model assuming ideal behavior of the membranes.

The molar flux J_{H_2O} (mol/m²·s) can be calculated from the volumetric water flux J_w , as measured on the membrane side facing the concentrated salt solution, according to the relationship:

$$J_{H_2O} = \frac{J_w}{V_c} = \frac{A_w (\Delta\pi_{eff} - \Delta P)}{\bar{V}_c} \quad [9]$$

where A_w is the water permeation coefficient of the membrane (m/Pa·s) at actual $\Delta\pi$ and hydrostatic pressure difference over the membrane ΔP . This permeation coefficient does not have a constant value (see discussion section 2.4.3), but it can be related to the absolute average of the mole

fractions on both sides of the membrane and the hydrostatic pressure [19]. In order to define such correlations for the water permeation coefficient an appropriate number of data points should be used. For this reason the data for a hollow-fiber TFC PA membrane of Mehta et al. [7] was used. For this type of membrane a correlation was found for the water permeation coefficient A_w with only the osmotic pressure difference of both (bulk) solutions, according to:

$$A_w = i(\Delta\pi \cdot 10^{-5})^j \quad [10]$$

where i and j are correlation coefficients which can be derived from pressure-retarded osmosis experiments and direct osmosis experiments.

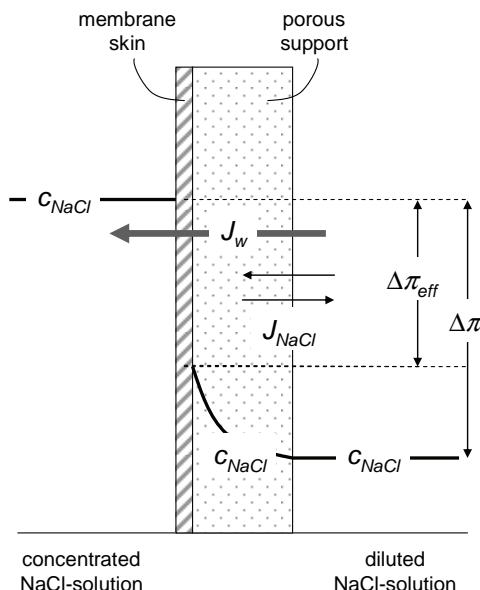


Figure 6: Schematic representation of apparent driving force of pressure-retarded osmosis ($\Delta\pi_{eff}$), which deviates from the osmotic pressure difference of the bulk solutions ($\Delta\pi$) due to concentration polarization in the porous support. J_w and J_{NaCl} are fluxes of water and salt, c the salt concentration. Salt diffusion through the membrane skin is excluded by the assumption of ideal membrane behavior.

Molar flux of reverse electrodialysis. In practice, the apparent driving force for charge transport in reverse electrodialysis deviates from $\Delta\phi - \Delta V$. The driving force seems not to be determined by the electrochemical potential difference between the bulk solutions, but by the sum of the Donnan-potentials of the membrane solution interfaces. In other words, the driving force needs to be corrected for the mole fraction of the free counter-ions within the membrane matrix at both interfaces ($x_{m,c}$ and $x_{m,d}$). This corrected electrochemical potential difference can be calculated with:

$$\begin{aligned}\Delta\phi_{eff} &= \alpha\Delta\phi = \frac{2RT}{F} \left(\ln\left(\frac{x_c}{x_{m,c}}\right) + \ln\left(\frac{x_{m,d}}{x_d}\right) \right) \\ &= \frac{2RT}{F} \ln\left(\frac{x_c \left(\bar{x} + \sqrt{4x_d^2 + \bar{x}^2} \right)}{x_d \left(\bar{x} + \sqrt{4x_c^2 + \bar{x}^2} \right)} \right)\end{aligned}\quad [11]$$

where $\Delta\phi_{eff}$ is the so-called membrane potential (V), which is in fact the corrected or mean effective electrochemical potential difference over the anion *and* cation-exchange membrane, \bar{x} the mean mole fraction of the active groups of the ion-exchange membranes (-), α the perm selectivity coefficient (-). This perm selectivity coefficient reflects the discrimination between counter-ions and co-ions by the ion-exchange membrane in given solutions [13]. Equation 11 generally is expressed in molarities (c) instead of mole fractions (x), e.g. [20].

The molar flux of sodium chloride J_{NaCl} (mol/m²·s) can be calculated from the charge flux J_i (i.e. the current density, A/m²) divided by the Faraday constant, according to the relationship:

$$J_{NaCl} = \frac{J_i}{F} = \frac{1}{Fr} (\Delta\phi_{eff} - \Delta V) \quad [12]$$

where r is the internal area resistance ($\Omega \cdot m^2$) of a cell pair consisting of a cation-exchange membrane, a compartment filled with a concentrated salt solution, an anion-exchange membrane, and a compartment filled with a diluted salt solution (Figure 2). The internal area resistance of a cell pair can be calculated from the sum of the area resistance of the membranes and that of both solutions:

$$r = r_c + \frac{h_c \bar{V}_c}{\lambda_c x_c} + r_A + \frac{h_d \bar{V}_d}{\lambda_d x_d} \quad [13]$$

where r_c is the area resistance of the cation-exchange membrane ($\Omega \cdot m^2$), h is the compartment or spacer width (m), λ the equivalent conductance ($m^2/\Omega \cdot mol$), and r_A is the area resistance of the anion-exchange membrane ($\Omega \cdot m^2$).

Power density of pressure-retarded osmosis. For pressure-retarded osmosis, the power density W (W/m^2) is equal to the product of the volumetric water flux and the hydrostatic pressure difference over the membrane:

$$W^{PRO} = J_w \Delta P = A_w (\Delta\pi_{eff} - \Delta P) \Delta P \quad [14]$$

The *optimal* power density can be derived from differentiating Equation 14 with respect to the hydrostatic pressure difference over the membrane (ΔP). Neglecting internal concentration polarization (i.e. $k = 0$ s/m), the optimal power output is obtained when ΔP equals $\Delta\pi_{eff}/2$. Substitution of this value for ΔP and the effective osmotic pressure difference results in the

following equation for the optimal power density obtainable in pressure-retarded osmosis:

$$W_{opt}^{PRO} = A_w \frac{\Delta\pi_{eff}^2}{4} \quad [15]$$

This *optimal* power density, however, is not always achievable in practice. The applied hydrostatic pressure difference can be limited by the configuration of the system and the mechanical strength of the membrane. In case $\Delta\pi_{eff}/2 > \Delta P_{max}$, the (sub)optimal power density is given by Equation 14 with $\Delta P = \Delta P_{max}$ (instead of by Equation 15).

Power density of reverse electrodialysis. For reverse electrodialysis, the power density W (W/m^2) is defined as the power generated per unit of total membrane area. This power density is equal to the product of half the current density (i.e. current passing area contains *both* cation *and* anion-exchange membrane) and the potential difference over an external load:

$$W^{RED} = \frac{J_i}{2} \Delta V = \frac{1}{2r} (\Delta\phi_{eff} - \Delta V) \Delta V \quad [16]$$

The *optimal* power density can be derived from differentiating Equation 16 with respect to the potential difference over the external load (ΔV). As a result the optimal power output is obtained when ΔV equals $\Delta\phi_{eff}/2$. This is the case when the resistance of the external load or power consumer equals the internal resistance of the reverse electrodialysis cell pair. Substitution of this ΔV and the membrane potential results in the following equation for the optimal power density obtainable in reverse electrodialysis:

$$W_{opt}^{RED} = \frac{1}{2r} \frac{\Delta\phi_{eff}^2}{4} \quad [17]$$

Maximum and average power density of both techniques. Like in literature, the model calculated up to this point the optimized power density at a given concentrations of the diluted and concentrated salt solutions. Systems in literature are continuously fed and are optimized with respect to power density in a steady state.

These systems are operated with a short residence time such that no appreciable changes in the concentrations take place. A small change in concentration means that only a very small part of the available mixing energy is used. In practice, however, one wants to use a considerable fraction of the available energy. Consequently, the concentrations will change appreciably and thus the driving force and power density. Therefore, a proper evaluation of the power density must take these changing concentrations into account.

To illustrate this, we will analyze a co-current operation and investigate the effect of the residence time on the power density. It is expected that with increasing residence time the power density decreases and the energy recovery increases. Hence, if the optimal power density is evaluated over a time period ($t - t_0$) a *maximum* power density exists:

$$W_{\max} = \max(W_{opt,t_0} : W_{opt,t}) \quad [18]$$

Over the same time period also a (time) *average* power density can be defined:

$$W_{\text{average}} = \frac{\int_{t_0}^t W_{opt} dt}{t - t_0} \quad [19]$$

Energy recovery of both techniques. The residence time also determines the exhaustion of the available energy. Therefore, also the energy recovery can be evaluated over time. The energy recovery η (%) is calculated as the
52

ratio of power produced over the time interval ($t - t_0$) to the amount of free energy ΔG at initial conditions (at time t_0 ; see Equation 3):

$$\eta = \frac{\int_{t_0}^t (W_{opt} \cdot A_m) dt}{\Delta G} \cdot 100\% \quad [20]$$

Where A_m is the applied membrane surface. If the time period is infinite small, the energy recovery will be close to 0%. In accordance with the above, the energy recovery will be close to 0% when the system is operating at the maximum power density.

2.3.3 Performance indicators

For evaluation, two measures of performance can be calculated with the present model: power density (W/m^2) and energy recovery (%). However, as power density and energy recovery are both determined by the residence time, we define the performance indicators for comparison of the techniques more strictly. Two performance indicators are distinguished:

- the *maximum* power density as calculated with Equation 18. This measure was also reported in the literature (or can be derived from presented data). In general, the maximum power density is achieved under initial process conditions, i.e. from mixing the original feed solutions (energy recovery $\eta \approx 0\%$). Consequently, the maximum power density can be evaluated separately from the energy recovery.
- the *average* power density (Equation 19) at a specified energy recovery (Equation 20). For a given design and operation, the residence relates the energy recovery and the average power density. In the results section, therefore, the average density is expressed as a function of the energy recovery. The average power density generally decreases with an increase of energy recovery. The average power density can not be seen separately from the energy recovery.

2.4 Results and discussion

2.4.1 Comparison based on published system characteristics

The input values for the model calculations consist of system characteristics for both pressure-retarded osmosis and reverse electrodialysis. These characteristics can be obtained from the literature referred to in the theoretical section. In this way the model calculations can be considered as an approximation of the state-of-the-art of both techniques.

System characteristics. For pressure-retarded osmosis, membrane characteristics are derived from Mehta et al. [7] using a fit of Equation 10 through the data points. The water permeation coefficient of the polyamide membranes used in this reference can be correlated to $\Delta\pi$ according to $i = 4.8 \cdot 10^{-12}$ and $j = -0.8$ (i.e. $A_w = 4.8 \cdot 10^{-12} \cdot (\Delta\pi \cdot 10^{-5})^{-0.8}$). The transport resistance for sodium chloride in the porous support layer is estimated to be equal to the transport resistance for a thin film composite membrane, $k = 10 \text{ d/m} = 9 \cdot 10^5 \text{ s/m}$ [21], which seems to be an optimistic but reasonable value. The maximum allowable hydrostatic pressure difference is chosen to be $\Delta P_{\max} = 60 \text{ bar} = 60 \cdot 10^5 \text{ Pa}$ since this value does not exceed all values in the experiments presented in *Figure 3*.

For reverse electrodialysis, membrane characteristics are obtained from Jagur-Grodzinski et al. [11]. From their measurements of membrane perm selectivity (α), the charge density of the membranes (\bar{c}) is estimated to be $3 \cdot 10^3 \text{ eq/m}^3$ by using Equation 11. A typical value reported for the membrane resistance (r_m) is $3 \Omega \cdot \text{cm}^2 = 3 \cdot 10^{-4} \Omega \cdot \text{m}^2$ (in a 0.5 mol/L NaCl solution). The minimum compartment or spacer width which is applied in reverse electrodialysis is $6.5 \cdot 10^{-4} \text{ m}$ [11].

Maximum power density. By using the model equations and the membrane characteristics reported in the literature, the maximum power density can be calculated (Equation 18). For both techniques the results are presented in *Figure 7*. For applications on sea water and river water, current reverse electrodialysis seems to have a higher maximum power density than pressure-retarded osmosis. For applications on brines, maximum power densities obtained with pressure retarded osmosis are higher than for reverse electrodialysis.

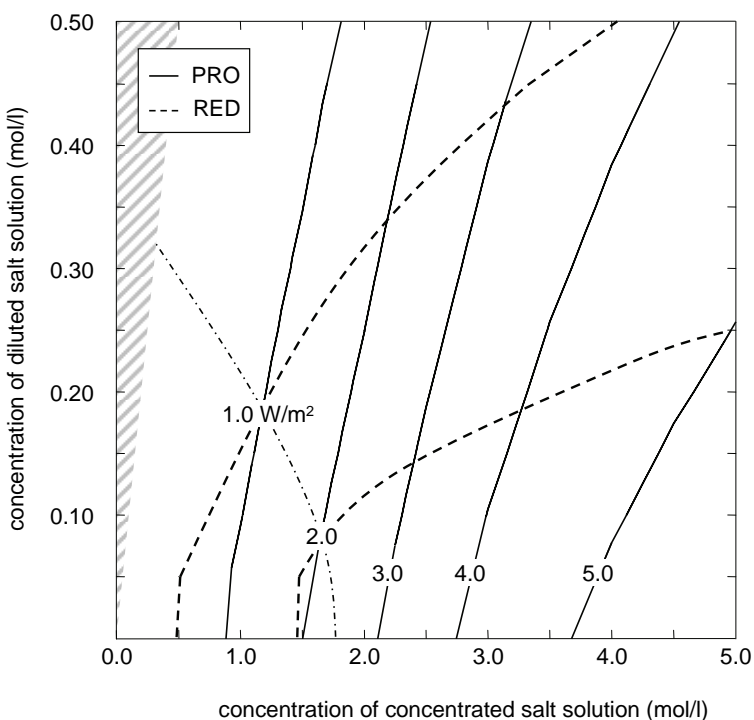


Figure 7: Calculated maximum power density (W/m^2) for pressure-retarded osmosis (PRO) and reverse electrodialysis (RED) using published membrane characteristics. Below the break-even-line (dash-dot-line) reverse electrodialysis has a higher maximum power density than pressure-retarded osmosis; above the break-even-line the opposite is true. Shaded area: is kept out of consideration since here the salt concentration of the concentrated solutions is lower than that of the diluted solution.

Chapter 2

The contour lines in *Figure 7* show that the maximum power density of reverse electrodialysis is more sensitive to the concentration of the diluted solution and less sensitive to the concentration of the concentrated solution (i.e. more horizontal orientated isohyps), when compared to pressure-retarded osmosis which is more sensitive to the concentration of the concentrated solution. For both techniques, however, the same trends can be observed, that is a non-linear response of the maximum power density to an increase in concentration of the concentrated salt solution. From a sensitivity analysis we found that for pressure-retarded osmosis this non-linear response at higher concentrations of the concentrated solutions is mainly determined by the limitation of the applied hydrostatic pressure difference ($\Delta P_{\max} < \Delta\pi_{eff}/2$). For reverse electrodialysis, the response of the maximum power density to the concentration of the concentrated salt solution is mainly determined by the negative effect of the decrease in perm selectivity on the membrane potential ($\Delta\phi_{eff} \ll \Delta\phi$, Equation 11) and thus on optimal power density (Equation 17), more than by a positive effect of the decrease in internal resistance (Equation 13) on optimal power density.

Average power density at variable energy recovery. In general, the maximum power density is achieved at (almost) initial concentrations for both feed solutions. If mixing continues, the optimal power density will decrease. The decrease of the optimal power density with residence time for mixing sea water with river water is presented in *Figure 8*. The area below the curve of the optimal power density represents the amount of energy converted as explained by Equation 20. The amount of energy converted (and thus the energy recovery) increases with time.

From *Figure 8* it can be seen that although the maximum power density of reverse electrodialysis is twice the maximum power density of pressure-retarded osmosis, at the end the average power density (Equation 19) is

almost the same after conversion of the same amount of energy (i.e. almost the same area under the curve of the optimal power densities for both techniques). In other words, this confirms that the power density should be considered in combination with energy recovery as in *Figure 9*.

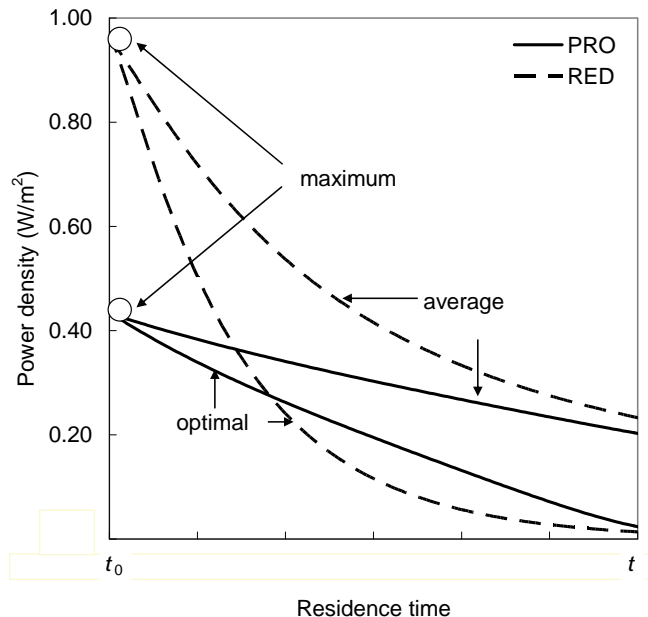


Figure 8: Calculated maximum and average power density for pressure-retarded osmosis (PRO) and reverse electrodialysis (RED) based on published membrane characteristics, for mixing sea water (0.5 mol/L NaCl) with river water (0.05 mol/L NaCl).

Figure 9 shows that the maximum energy recovery seems to be 50%. This can be explained by the fact that both techniques operate at optimal power density when the spontaneous mixing is retarded by a back-force which is half the effective driving force (Equations 15 and 17, where $\Delta P = \Delta\pi_{eff}/2$ and $\Delta V = \Delta\phi_{eff}/2$). In theory the energy recovery could come close to 100% once the mixing is retarded by a back-force which almost equals the effective driving force ($\Delta P \uparrow \Delta\pi_{eff}$ and $\Delta V \uparrow \Delta\phi_{eff}$). In this case, however, the achieved

Chapter 2

power density will be close to zero, according to Equations 14 and 16. In the same way the energy recovery theoretically could be lower than 50% when the mixing is less retarded by a back-force ($\Delta P < \Delta\pi_{eff}/2$ and $\Delta V < \Delta\phi_{eff}/2$). The achieved power density will then also be lower than the optimal power density (Equations 14 and 16).

For mixing sea water and river water, the techniques come close to a energy recovery of 50%; the maximum energy recovery of pressure-retarded osmosis is 43% and the maximum energy recovery of reverse electrodialysis is 49%. These somewhat lower fuel efficiencies are caused by irreversible mixing due to internal concentration polarization (pressure-retarded osmosis, $\Delta\pi_{eff} < \Delta\pi$) or a perm selectivity being less than unity caused by transport of co-ions (reverse electrodialysis, $\Delta\phi_{eff} < \Delta\phi$). Both average power density and energy recovery are higher for reverse electrodialysis than for pressure-retarded osmosis.

For application on brine, the obtained results are more complex. It is clear that both the average power density and the energy recovery are higher for pressure-retarded osmosis than for reverse electrodialysis. Especially for reverse electrodialysis, the energy recovery is considerably lower than 50%; the maximum energy recovery of pressure-retarded osmosis is 36% and the maximum energy recovery of reverse electrodialysis is even lower. These lower fuel efficiencies are mainly caused by limitations in the applied hydrostatic pressure difference (pressure-retarded osmosis, $\Delta P_{max} < \Delta\pi_{eff}/2$) or by irreversible mixing due to a significant perm selectivity loss (reverse electrodialysis, $\Delta\phi_{eff} < \Delta\phi$).

Both techniques have different profiles of the average power density-energy recovery curve. The sharp profile of the curve of pressure-retarded osmosis shows that at maximum energy recovery still a relative high average power density is obtained.

So, for power generation from mixing sea water and river water with currently available membranes, results show a better performance for reverse electrodialysis than for pressure-retarded osmosis, both on power density (maximum and average) and energy recovery. For power generation from mixing a brine and less concentrated water, the opposite is true. These conclusions are in accordance to what already was suggested from the literature review.

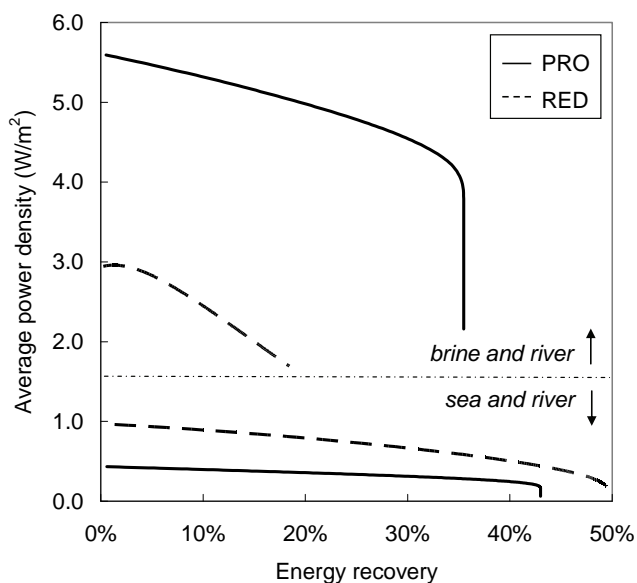


Figure 9: Calculated average power density and energy recovery for pressure-retarded osmosis (PRO) and reverse electrodialysis (RED) using currently available membrane characteristics, for mixing sea water (0.5 mol/L NaCl) with river water (0.05 mol/L NaCl) and for mixing brine (5 mol/L NaCl) with river water.

2.4.2 Potential of both techniques

The derived model calculations can also be used to show the potential of these techniques by using favorable but realistic estimates for the system characteristics.

System characteristics. For pressure-retarded osmosis, according to predictions of Lee et al. [10] membrane characteristics of cellulose acetate membranes would be the most promising. They have predicted a power density of 1.54 W/m^2 for applications on sea and river water. The characteristics of a cellulose acetate membrane can be estimated using the data of Mehta et al. [9] from which one may derive that the water flux is almost independent of the osmotic pressure difference, i.e $j = -1$. Assuming $j = -1$, from the predicted power density of 1.54 W/m^2 it can be estimated that $i = 2.2 \cdot 10^{-11}$ (i.e. $A_w = 2.2 \cdot 10^{-11} \cdot (\Delta\pi \cdot 10^{-5})^{-1}$). The maximum allowable hydrostatic pressure difference can be obtained from common sea water desalination applications where ΔP_{\max} is $80 \cdot 10^5 \text{ Pa}$. Loeb [22] suggested that the transport resistance of the support can be limited to $k = 1 \cdot 10^5 \text{ s/m}$.

For reverse electrodialysis, a membrane charge density of 3 eq/m^3 and a membrane resistance r_m of $0.5 \Omega \cdot \text{cm}^2 = 5 \cdot 10^{-5} \Omega \cdot \text{m}^2$ is realistic. The minimum compartment or spacer width which can be applied without excessive friction losses, can be $0.25 \cdot 10^{-3} \text{ m}$ (or even lower) since the cross flow velocity can be 100 times lower than for normal electrodialysis [11].

Maximum power density. By using the model equations and favorable membrane characteristics, the potential maximum power density can be calculated (Equation 18). The results are presented in Figure 10. The calculated maximum power densities for both systems are now comparable over the whole range of concentrations, varying from $2-10 \text{ W/m}^2$. For applications on sea water and river water, reverse electrodialysis has a

higher potential maximum power density than pressure-retarded osmosis ($2\text{-}4 \text{ W/m}^2$ versus $<2 \text{ W/m}^2$). For pressure-retarded osmosis, the maximum power density from the model is 1.2 W/m^2 , which is less than the expected 1.54 W/m^2 for a cellulose acetate membrane predicted by Lee et al. [10]. This difference, however, is due to the use of a lower sea water concentration in the model compared to the literature (0.5 instead of 0.6 mol/L NaCl).

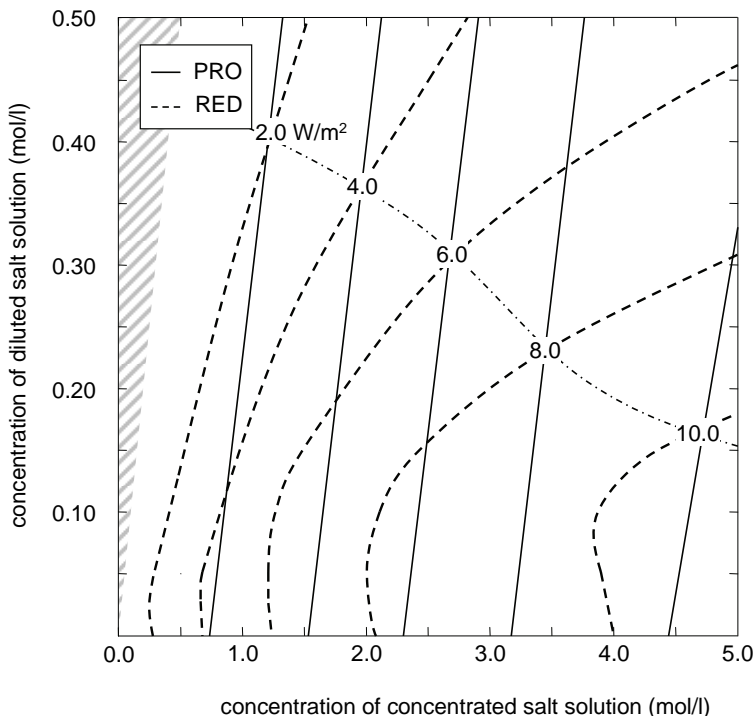


Figure 10: Calculated potential maximum power density (W/m^2) for pressure-retarded osmosis (PRO) and reverse electrodialysis (RED) using best membrane characteristics. Below the break-even-line (dash-dot-line) reverse electrodialysis has a higher maximum power density than pressure-retarded osmosis; above the break-even-line the opposite is true. Shaded area: is kept out of consideration since here the salt concentration of the concentrated solutions is lower than that of the diluted solution.

For applications on brines, maximum power densities are comparable for both techniques ($>10 \text{ W/m}^2$). Pressure-retarded osmosis seems to be less sensitive to the concentration of the diluted solution than reverse electrodialysis which is a benefit of pressure-retarded osmosis when the energy recovery is taken into account.

Average power density at variable energy recovery. The average power density and energy recovery are presented in *Figure 11*. For mixing sea water and river water, the average power density at certain energy recovery is higher for reverse electrodialysis than for pressure-retarded osmosis. Both techniques come close to a energy recovery of 50%, which is explained earlier. Irreversible mixing can now be neglected since internal concentration polarization hardly exists (pressure-retarded osmosis) or perm selectivity is close to unity (reverse electrodialysis).

For application on brine, the average power density at certain energy recovery generally is higher for pressure-retarded osmosis than for reverse electrodialysis. For pressure-retarded osmosis, the energy recovery is hardly limited by internal concentration polarization or the applied hydrostatic pressure difference (energy recovery close to 50%). For reverse electrodialysis, the energy recovery is relatively low ($<30\%$) and the average power density is rapidly decreasing with increasing energy recovery. Both techniques have different profiles of the average power density-energy recovery curve. The curve of reverse electrodialysis shows a maximum value which indicates that the initial conditions that after some mixing the decrease in internal resistance (Equation 13) is higher than the decrease in potential (Equation 11), which results in an increase of the optimal power density (Equation 17).

So, for power generation from mixing sea water and river water the potential of reverse electrodialysis is higher than for pressure-retarded

osmosis, both on power density (maximum and average) and energy recovery. For power generation from mixing a brine and less concentrated water, the opposite is true. The potential performances of both techniques are much higher than current performances (see 2.4.1). In order to achieve these potential performances, the development of pressure-retarded osmosis must focus on membrane characteristics, i.e. increasing the water permeability of the membrane skin and optimization of the porous support. The development of reverse electrodialysis, however, must focus on system characteristics, i.e. optimization of the internal resistance, which is mainly determined by the width of the spacers.

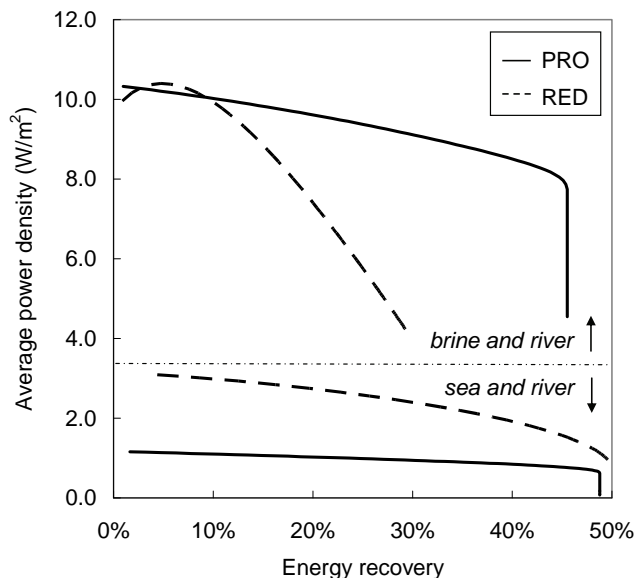


Figure 11: Calculated average power density and energy recovery for pressure-retarded osmosis (PRO) and reverse electrodialysis (RED) using best-available system characteristics, for mixing sea water (0.5 mol/L NaCl) with river water (0.05 mol/L NaCl) and for mixing brine (5 mol/L NaCl) with river water.

2.4.3 Discussion

Behavior of pressure-retarded osmosis membranes. In our model the fit function for the permeation coefficient A_w (Equation 10) seems to have a key-role in the model calculations for pressure-retarded osmosis. This can be seen as unsatisfactory, but it represents in our view the best practical approach. Also in literature, there is still a discussion on the not-well-understood behavior of osmosis membranes under pressure-retarded osmosis conditions with respect to permeability. From the beginning in 1976 [6], a major topic of research was to define an appropriate correlation between the osmotic pressure difference and the hydrostatic pressure difference on the one hand, and the water flux on the other, because this correlation defines the power output of the system. The correlation factor was defined as the permeation coefficient A_w . This permeation coefficient, however, seemed to be not a constant, and therefore was still subject of recent studies [19, 23]. A number of mechanisms which could be responsible for the non-linear behavior was mentioned in the literature: ‘osmotic deswelling’ or ‘osmotic dehydration’ of the membranes at high osmotic pressures [7], cavitation and partial clogging [24]. Although the mechanisms are not yet well understood, it was concluded that this permeation coefficient itself could be related to the absolute average of the mol fractions of the solutes in the feed solutions and to the hydrostatic pressure [19]. However, from the limited amount of data available, we were not able to define an appropriate correlation factor between the permeation coefficient and the hydrostatic pressure. Therefore, in the present work the permeation coefficient is only correlated to the osmotic pressure difference according to Equation 10.

Evaluation of practical behavior (fouling). Besides the power density and the energy recovery, the practical behavior of both systems when applied to real surface waters also is a key-indicator. A good measure for

this could be the sensitivity towards fouling. For pressure-retarded osmosis, there is no literature which deals with this aspect. However, it should be noticed that several references reported a permanent damage of the membranes in contact with high concentrated saline brines [6, 7]. From desalination experiences with reverse osmosis one could expect a serious impact of (bio)fouling when pressure-retarded osmosis is applied to real sea water and real river water. For reverse electrodialysis, we found only one reference in which a fouling experiment was carried out. It was suggested that bio-film growth might have a significant negative effect on power density [25]. However, one could expect less impact of (bio)fouling on performances of reverse electrodialysis when compared to pressure-retarded osmosis since from comparable desalination experiences it is claimed that electrodialysis membranes are generally less sensitive to fouling than reverse osmosis membranes (e.g. electrodialysis has lower pre-treatment requirements and membranes are more chemical-resistant [26]).

Comparison of engineered and well-operated systems. The assumption that differences in specific efficiency losses can be neglected for the comparison between pressure-retarded osmosis and reverse electrodialysis may be subject to discussion. The different forms of loss can have considerably different kinds of effect to pressure-retarded osmosis than to reverse electrodialysis. For example, each system has a different optimal flow velocity which is a result of the balance between pressure losses and external concentration polarisation. These differences in turn should in a real system result in differences in the optimal configuration of the membrane module (length, channel width (or diameter), packing density etc.) and the optimal operating conditions (e.g. mixing rate). For the sake of simplicity, in our model we assumed a co-current system which is not necessarily applied in practical operation. Therefore, in future work

it would be worthwhile to compare the performances of two well-engineered and optimal operated systems.

Capital costs and costs of operation and maintenance are probably the most important for evaluation of both techniques. However, since both techniques are still in the development stage, we were not able to perform realistic cost calculations. In order to make an estimation of the economic aspects, again we could make a comparison with the equivalent desalination techniques. The membrane area costs for currently available membranes for electrodialysis are 2-3 times higher than for reverse osmosis. The *installed* area costs (including membranes, pumps, pressure vessels, turbines etc.), however, are in the same order of magnitude. From this one could expect that costs of reverse electrodialysis and pressure-retarded osmosis will not make distinction. Nevertheless, we assume that once the new membrane market for power production is emerging, membrane prizes for especially (reverse) electrodialysis will be reduced tremendously since electrodialysis has never had a real breakthrough in the desalination market [27].

2.5 Conclusions

There is a huge potential to obtain clean energy from mixing water streams with different salt concentrations. All techniques currently available for desalination can be used to generate power from salinity gradients. Our objective was to evaluate and to compare the technical performance of the two membrane-based energy conversion techniques: pressure-retarded osmosis and reverse electrodialysis. A comparison based on the literature was not sufficient since the reported performances were incomplete (the power output was not related to energy recovery) and the measurement conditions were not comparable. A method was developed which allows a

comparison of both techniques at equal conditions, both with respect to power density and energy recovery.

Based on the results from the model calculations, it can be concluded that each technique has its own field of application. Pressure-retarded osmosis seems to be more attractive for power generation using concentrated saline brines because of the higher power density combined with higher energy recovery. For the same reason reverse electrodialysis seems to be more attractive for power generation using sea water and river water. These conclusions are valid for both present and latent performances of both techniques.

According to the model, the potential performances of both techniques are much better than the current performances. In order to achieve these potential performances, the development of pressure-retarded osmosis must focus on membrane characteristics, i.e. increasing the water permeability of the membrane skin and optimization of the porous support. The development of reverse electrodialysis, however, must focus on system characteristics, i.e. optimization of the internal resistance, which is mainly determined by the width of the spacers.

Besides the power density and energy recovery, the practical behavior or the sensitivity for fouling is a key-indicator which should be investigated. Furthermore, the feasibility of these techniques will mainly depend on reduced membrane prices. It is believed that the membrane prices, especially for reverse electrodialysis, will decrease significantly once a new membrane market for power generation emerges. Therefore, it is worthwhile to further investigate and develop both membrane techniques in order to make sustainable conversion of salinity-gradient energy available for the future.

2.6 List of Symbols

Symbols

A_m	membrane area (m^2)
A_w	water permeation coefficient ($\text{m}/(\text{s}\cdot\text{Pa})$)
c	concentration (mol/m^3)
\bar{c}	charge density of (monovalent) functional groups ($\text{eq}/\text{m}^3 = \text{mol}/\text{m}^3$)
F	Faraday constant (96,485 C/mol)
G	free energy (J)
J_w	volumetric water flux ($\text{m}^3/\text{m}^2\cdot\text{s} = \text{m}/\text{s}$)
J_{H2O}	molar water flux ($\text{mol}/\text{m}^2\cdot\text{s}$)
J_i	charge flux or current density ($\text{C}/\text{m}^2\cdot\text{s} = \text{A}/\text{m}^2$)
J_{NaCl}	molar salt flux ($\text{mol}/\text{m}^2\cdot\text{s}$)
h	width (height) of spacer (m)
i, j	correlation coefficients (dependent)
k	resistance to salt diffusion through porous substrate (s/m)
N	number of cell pairs (-)
Δp	static pressure difference compared to standard static pressure (Pa)
ΔP	hydrostatic pressure difference between solutions (Pa, in Figures: bar)
Q	volumetric water flow (m^3/s)
r	area resistance ($\Omega\cdot\text{m}^2$)
R	universal gas constant (8.314 J/mol·K)
t	time (s)
T	temperature (K)
V	volume (m^3)
\bar{V}	molar or specific volume of solution (m^3/mol)
\bar{v}	partial molar volume (m^3/mol)
ΔV	potential difference over external load (V)
W	power density (W/m^2)
x	mole fraction (-)
\bar{x}	mole fraction of (monovalent) functional groups (-)
Z	valence of ions (eq/mol)
α	perm selectivity (-)
η	energy recovery (%)
$\Delta\varphi$	electrical potential difference (V)
$\Delta\phi$	electrochemical potential difference between solutions (V)

λ	equivalent conductance ($\text{m}^2/\Omega\cdot\text{mol}$)
μ	molar free energy (J/mol)
$\Delta\pi$	osmotic pressure difference (Pa, in Figures: bar)

Subscripts and superscripts

b	brackish solution
c	concentrated solution
d	diluted solution
eff	effective
i	current (in J_i)
i	component i (all other cases)
m	membrane
max	maximum
opt	optimal under given conditions
<i>PRO</i>	pressure-retarded osmosis
<i>RED</i>	reverse electrodialysis
w	water

2.7 References

1. Wick, G.L. and W.R. Schmitt, Prospects for renewable energy from sea, Marine Technology Society Journal 11(5-6) (1977), p. 16-21.
2. Norman, R.S., Water salination - source of energy, Science 186(4161) (1974), p. 350-352.
3. Loeb, S., Production of energy from concentrated brines by pressure-retarded osmosis.1. Preliminary technical and economic correlations, Journal Of Membrane Science 1(1) (1976), p. 49-63.
4. Pattle, R.E., Production of electric power by mixing fresh and salt water in the hydroelectric pile, Nature 174(4431) (1954), p. 660-660.
5. Olsson, M., G.L. Wick and J.D. Isaacs, Salinity gradient power - utilizing vapor-pressure differences, Science 206(4417) (1979), p. 452-454.
6. Loeb, S., F. Vanhessen and D. Shahaf, Production of energy from concentrated brines by pressure-retarded osmosis.2. Experimental results and projected energy costs, Journal Of Membrane Science 1(3) (1976), p. 249-269.
7. Mehta, G.D. and S. Loeb, Performance of permasep b-9 and b-10 membranes in various osmotic regions and at high osmotic pressures, Journal Of Membrane Science 4(3) (1979), p. 335-349.
8. Loeb, S. and G.D. Mehta, 2-coefficient water transport-equation for pressure-retarded osmosis, Journal Of Membrane Science 4(3) (1979), p. 351-362.
9. Mehta, G.D., Further results on the performance of present-day osmotic membranes in various osmotic regions, Journal Of Membrane Science 10(1) (1982), p. 3-19.
10. Lee, K.L., R.W. Baker and H.K. Lonsdale, Membranes for power-generation by pressure-retarded osmosis, Journal Of Membrane Science 8(2) (1981), p. 141-171.

Chapter 2

11. Jagur-grodzinski, J. and R. Kramer, Novel process for direct conversion of free-energy of mixing into electric-power, Industrial & Engineering Chemistry Process Design And Development 25(2) (1986), p. 443-449.
12. Lacey, R.E., Energy by reverse electrodialysis, Ocean Engineering 7(1) (1980), p. 1-47.
13. Weinstein, J.N. and F.B. Leitz, Electric-power from difference in salinity - dialytic battery, Science 191(4227) (1976), p. 557-559.
14. Audinos, R., Electric-power produced from 2 solutions of unequal salinity by reverse electrodialysis, Indian Journal Of Chemistry Section A-Inorganic Bio-Inorganic Physical Theoretical & Analytical Chemistry 31(6) (1992), p. 348-354.
15. Lide, D.R., Handbook of chemistry and physics, 85th ed. 2004: CRC Press.
16. Strathmann, H., Ion-exchange membrane separation processes, 1st ed. 2004: Elsevier.
17. Forgacs, C., Recent developments in the utilization of salinity power, Desalination 40(1-2) (1982), p. 191-195.
18. Mehta, G.D. and S. Loeb, Internal polarization in the porous substructure of a semipermeable membrane under pressure-retarded osmosis, Journal Of Membrane Science 4(2) (1978), p. 261-265.
19. Seppala, A. and M.J. Lampinen, On the non-linearity of osmotic flow, Experimental Thermal And Fluid Science 28(4) (2004), p. 283-296.
20. Sata, T., Ion exchange membranes, 1st ed. 2004: Royal Society of Chemistry.
21. Loeb, S., Large-scale power production by pressure-retarded osmosis, using river water and sea water passing through spiral modules, Desalination 143(2) (2002), p. 115-122.
22. Loeb, S., Energy production at the dead sea by pressure-retarded osmosis: Challenge or chimera? Desalination 120(3) (1998), p. 247-262.
23. Ludwig, W., A. Seppala and M.J. Lampinen, Experimental study of the osmotic behaviour of reverse osmosis membranes for different nacl solutions and hydrostatic pressure differences, Experimental Thermal And Fluid Science 26(8) (2002), p. 963-969.
24. Massaldi, H.A. and C.H. Borzi, Nonideal phenomena in osmotic flow through selective membranes, Journal Of Membrane Science 12(1) (1982), p. 87-99.
25. Ratkje, S.K., T. Holt and L. Fiksdal. Effect of biofilm formation on salinity power plant output on laboratory scale, in Industrial membrane processes. 1986: AIChE.
26. Pilat, B., Practice of water desalination by electrodialysis, Desalination 139(1-3) (2001), p. 385-392.
27. Van der Bruggen, B. and C. Vandecasteele, Distillation vs. Membrane filtration: Overview of process evolutions in seawater desalination, Desalination 143(3) (2002), p. 207-218.

3 Energy recovery from controlled mixing of salt and fresh water with reverse electrodialysis

The global potential to obtain clean energy from mixing river water with sea water is considerable. Reverse electrodialysis is a membrane-based technique for direct production of sustainable electricity from controlled mixing of river water and sea water. It has been investigated generally with a focus on obtained power, without taking care of the energy recovery. Optimizing the technology to power output only, would generally give a low energetic efficiency. In the present work, therefore, we emphasized the aspect of energy recovery. No fundamental obstacle exists to achieve an energy recovery of >80%. This number was obtained with taking into account no more than the energetic losses for ionic transport. Regarding the feasibility, it was assumed to be a necessary but not sufficient condition that these internal losses are limited. The internal losses could be minimized by reducing the inter-membrane distance, especially from the compartments filled with the low-conducting river water. It was found that a reduction from 0.5 mm to 0.2 mm indeed could be beneficial, although not to the expected extent. From an evaluation of the internal losses, it was supposed that besides the compartment thickness, also the geometry of the spacer affects the internal resistance.

This chapter has been published as:

Post, J.W., H.V.M. Hamelers and C.J.N. Buisman, Energy recovery from controlled mixing salt and fresh water with a reverse electrodialysis system, Environmental Science Technology 42 (2008), p. 5785-5790.

This chapter has been awarded as top technical paper of 2008:

Pelley, J., Top Paper in Environmental Technology: Saltwater power, Environmental Science & Technology 43 (2009), p. 2194

3.1 Introduction

3.1.1 Huge global potential of salinity-gradient energy

The dependency on limited fossil fuel sources and the threat of global warming, raised the attention to exploration of conventional and unconventional renewable energy sources. A well-known conventional renewable energy source is hydropower, the gravitational potential of natural runoff. The gross hydropower potential, defined as the theoretically available power when the average runoff of each country is harnessed down to the sea level or to the border line of the country, was estimated to be 5.1-5.9 TW (calculated from data taken from Lehner et al., [1]). Less-known is that, complementary to this gravitational potential, the natural runoff in coastal areas has a huge physical-chemical potential. This potential is the result of the salinity gradient between the mainly-fresh runoff (river mouths) and the receiving mainly-saline reservoirs (seas and oceans). When a river runs into a sea, spontaneous (irreversible) mixing of fresh and salt water occurs, i.e., the opportunity to produce work is lost. It was calculated [2, 3] that from each cubic meter of river water that flows into the sea, 2.3 MJ of work could be extracted. The gross power potential of this unconventional energy source was estimated to be 2.4-2.6 TW [3, 4] when the average discharges of all rivers were taken into account. This considerable amount justifies serious attempts to develop technologies required for electrical power generation from this salinity gradient or so-called blue energy source.

3.1.2 Unknown how much can be converted into electricity

A main question is how much of this salinity-gradient energy can be converted into sustainable electricity. Recently, we reviewed literature on two membrane-based techniques that can be used for this conversion [5], namely pressure-retarded osmosis and reverse electrodialysis, and found that actually hardly attention was paid to the energetic efficiency.

Described experiments focused on power output or power density whereas the energy recovery was never directly measured. From the papers concerning reverse electrodialysis, we obtained more-or-less founded estimates for the obtainable energy recovery. Forgacs [6] conservatively predicted a net energy yield of 0.35 MJ per m³ of river water. Audinos [7] measured a gross energy yield in this order and calculated an energy recovery of 21% (i.e., without taking into account parasitic system losses for pumping and AC/DC conversion). Jagur-Grodzinski and Kramer [8] concluded from their experiments that the obtained amount of energy (net) could be 0.25-0.6 MJ per m³ of river water, depending the chosen power density. It was supposed that the latter value would be obtained when the system is operated at a sub-optimal power density [8]. The main conclusion that could be drawn from these estimations is that the energy recovery is rather low, especially when compared to the mentioned 2.3 MJ of available work [2, 3]. From these numbers, the attractiveness of reverse electrodialysis to harness this energy source could be called into question. The energy recovery is an important issue. River water discharge is an enormous energy source indeed, yet a limited one. Moreover, both feed solutions (sea water and river water) represent a certain economic value as they are pretreated and transported. From this point of view, the absence of experimental investigations regarding the obtainable energy recovery is a peculiar gap in the field of reverse electrodialysis.

3.1.3 Objective

The aim of this study, therefore, was to investigate the energy recovery that can be obtained. The energy recovery is determined by internal and external energetic losses. This study was restricted to the internal energetic losses related to ion transport. The external energetic losses such as pumping and DC/AC conversion can only be investigated on a full-scale

and well-known system, where all design and operational aspects are optimized.

Concerning the internal losses, it was well-recognized [3, 5, 8-10] that the main contribution comes from ionic transport in the compartments filled with river water, because of the low conductivity of this diluted salt solution. Minimization of this internal loss is a necessary but not sufficient condition to obtain a considerable energy recovery in practical applications. A reduction of the thickness of these compartments would limit these losses. We, therefore, included in our study two different reverse electrodialysis stacks: one with compartment thicknesses of 0.5 mm and one with compartment thicknesses of 0.2 mm.

3.2 Experimental

3.2.1 Reverse electrodialysis stack

The principle of reverse electrodialysis is described in literature (e.g. [3]). Figure 1 shows a schematic overview of a reverse electrodialysis stacks used for this study. The square stacks consisted of five cation-exchange (Neosepta CMS; Tokuyama Co., Japan) and four anion-exchange membranes (Neosepta ACS; Tokuyama Co., Japan) that are piled in an alternating pattern between a cathode and an anode (both of stretched Titanium with a Ruthenium/Iridium Mixed Metal Oxide coating with a specific surface of 1 m²/m²; Magneto Special Anodes B.V., The Netherlands). The active area of each membrane was 104 cm², the area of the electrodes 100 cm². The repeating unit is called a cell pair, which consists of a cation-exchange membrane, a compartment filled with a spacer and a concentrated salt solution ('sea water'), an anion-exchange membrane, and a compartment filled with a spacer and a diluted salt solution ('river water'). The compartments were formed with silicone gaskets.

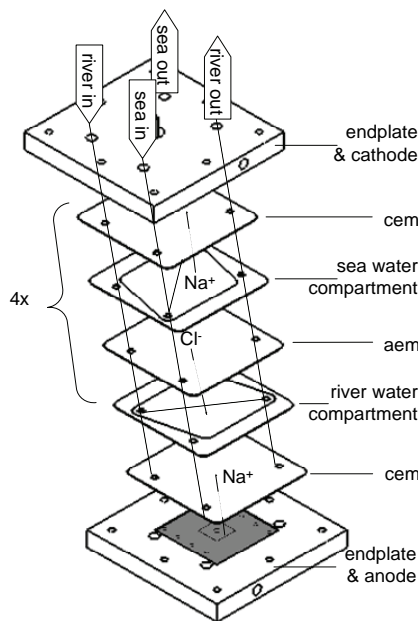


Figure 1: Conceptual representation of a reverse electrodialysis stack used in this study; cem is cation-exchange membrane, aem is anion-exchange membrane; repetitive cell pair is drawn only once; the electrode rinse solution is not indicated.

In this study, two types of reverse electrodialysis stacks were used. The difference between the stacks was the compartment width (inter-membrane distance) and thus also the applied gasket and spacer. One stack was provided with a PET fabric with a thickness of 500 μm (Nitex 06-700/53, Sefar), the other with a PA fabric with a thickness of 200 μm (Nitex 03-300/51, Sefar). Main characteristics of the spacers are summarized in Table 1. These fabrics were chosen as they have comparable characteristics for porosity and open area.

Table 1: Specifications of used spacer materials.

	unit	ref.	06-700/53	03-300/51
Spacer material			PET	PA 6.6
A spec. gravity	kg/m ³	[specs]	1380	1140
Spacer porosity				
B weight fabric	kg/m ²	[specs]	0.14	0.075
C thickness fabric	m	[specs]	0.0005	0.0002
D app. gravity	kg/m ³	D = B / C	280	375
E porosity	-	E = 1 - D / A	80%	67%
Spacer shadow				
F wire diameter	mm	[specs]	0.265	0.12
G mesh opening width	mm	[specs]	0.7	0.3
H open area	-	H = G ² / (F + G) ²	53%	51%
I max. shadow	-	I = 1 - H	47%	49%

3.2.2 Salt-solution batches

The concentrated salt solution (0.5 M NaCl, ‘sea water’), the diluted salt solution (5 mM NaCl, ‘river water’), and an electrode rinse solution (0.25 M NaCl, ‘brackish water’) were fed to the stacks with a flow rate 57.5 ml/min. The solutions were recycled over bottles stored in a thermostatic bath (with a temperature of 25±1 °C). Each bottle contained 500 mL of described solutions. Before each experiment, the stacks and tubes were flushed and filled with matching solutions. Each stack with connected tubes had an estimated system volume of 50 mL. The total batch volume of each solution was accordingly 550 mL. Before and after each experiment the solutions in the bottles were weighed. Concentrations of sodium and chloride were analyzed with inductive-coupled plasma (Optima 3000XL, Perkin Elmer) and ion chromatography (761 Compact IC, Metrohm), respectively.

3.2.3 Electrochemical measurement

The electrodes were connected to a galvanostat (IviumStat Electrochemical Interface & Impedance Analyser; Ivium Technologies, The Netherlands). With the galvanostat a block-pulse direct current was generated with cycles of a 200 s period of zero current conditions (open circuit) followed by a 1,000 s period with an adjusted current level of 50, 100...250 mA (i.e., a current density 5, 10...25 A/m²). The corresponding stack voltage was measured with an interval of 0.2 s. For the measurement of the stack voltage, Ag/AgCl reference electrodes were used, in order to leave losses associated with electrode reactions out of consideration. The reason to exclude the potential losses at the electrodes was the fact that in a stack with a limited number of cell pairs (like in the used stacks) these losses would be dominant, whereas in practice, with a high number of cell pairs these losses could be neglected. The reference electrodes were placed within reservoirs that were connected to the electrode compartments via salt bridges. The tips of the salt bridges probes were placed at a distance of 1 mm to the shielding membranes.

The potential-transients measured with the reference electrodes occurring as a result of the periodical current-steps, could be interpreted as in a conventional current-interrupt technique [11]. The potential-transients resulting from each current-pulse provides each 1,200 s the actual internal resistance of the electrodialytic pile (membranes and solution compartments only). Since each current-pulse consists of a successive current-interrupt and a current-supply which gives two opposite potential-transients, the actual internal resistance is measured twice. In view of the fact that the experiments were performed in duplo, the actual resistance was determined each 1,200 s in quadruplicate. From the potential-transients, the actual internal loss could be divided into an ohmic part and a non-ohmic part. The instantaneous potential-jump resulting from a

current-step could be related to the ohmic losses due to ionic transport through the bulk solutions and the membranes. The following time-dependent potential-change could be related to the non-ohmic losses due to concentration polarization at the membrane surfaces.

3.3 Results and discussion

3.3.1 Available work from mixing salt-solution batches

In our experimental setup, the batch volumes (550 mL) and flow rates (57.5 ml/min) of the concentrated salt solution and the diluted salt solution were equal. Before we start to present and interpret results on energy recovery, it is necessary to calculate the available work from mixing these batches.

In literature [2, 3] it was calculated that from each cubic meter of river water that flows into the sea, 2.3 MJ of work could be extracted. This calculation was based on the assumption that a cubic meter of river water is mixed with ‘infinite’ cubic meters of sea water. This assumption could be justified by the fact that the available discharge of river water is the limiting source, whereas the sea water source could be regarded as infinitely available. However, although the sea water might be infinite, in practice it represents a certain economic value as it needs also to be pretreated and transported. An optimization solely to the energy yield of river water is, therefore, not practical. A more realistic approach is to optimize the work of the total amount of water involved in the mixing process.

The theoretical non-expansion work that can be produced from mixing a relatively concentrated salt solution c (e.g. sea water) and a dilute salt solution d (e.g. river water), at constant pressure p and temperature T , to give a brackish solution b , is defined by the Gibbs energy of mixing $\Delta_{\text{mix}}G$:

Chapter 3

$$\Delta_{\text{mix}}G \equiv \Delta G_b - (\Delta G_c + \Delta G_d) \quad [1]$$

Assuming that solutions are ideal-dilute, it can be shown that the Gibbs energy of mixing can be calculated just from the change in molar entropy (i.e., $\Delta_{\text{mix}}H = 0$):

$$\Delta_{\text{mix}}G = -(n_c + n_d)T\Delta_{\text{mix}}s_b - (-n_c T\Delta_{\text{mix}}s_c - n_d T\Delta_{\text{mix}}s_d) \quad [2]$$

Where n is the amount (moles), and $\Delta_{\text{mix}}s$ represents the contribution of the molar entropy of mixing (J/mol.K) to the total molar entropy of the corresponding electrolyte solution, according to:

$$\Delta_{\text{mix}}s = -R \sum_i x_i \ln x_i \quad [3]$$

where R is the universal gas constant (8.314 J/mol·K), and x the mole fraction of component i ($i = \text{Na}, \text{Cl}, \text{H}_2\text{O}$). For a given amount of moles n , of which a fraction f consists of river water with a sodium chloride concentration of 5 mM ($x = 10^{-4}$) and another fraction ($1-f$) of sea water with a sodium chloride concentration of 0.5 M ($x = 10^{-2}$), an optimum exists for $f = 0.6$ (see Figure 2A). In this case, at $T = 298$ K, the available work is 0.84 kJ for mixing 1 L of solutions, i.e., consisting of 0.6 L of river water with 0.4 L of sea water. It should be noticed that in this case, the available work per m³ of river water amounts 1.36 MJ, which is considerably lower than the mentioned 2.3 MJ for $f \downarrow 0$ (see Figure 2B).

A mixing ratio of 1:1 ($f = 0.5$) as used in this study, gives just a small shift from the optimized case, and would also be favorable in practical applications as it allows a symmetrical hydrodynamic design for distribution of sea water and river water and the utilization of the limited river water source is then increased (Figure 2B) without a considerable loss of the available work (Figure 2A).

The available work is, after correction for non-ideal behavior of the solutions, 0.73 kJ for mixing 1 L of solutions. In case of the experiment where 550 mL of dilute is mixed with 550 mL of concentrate, the available work is 0.80 kJ.

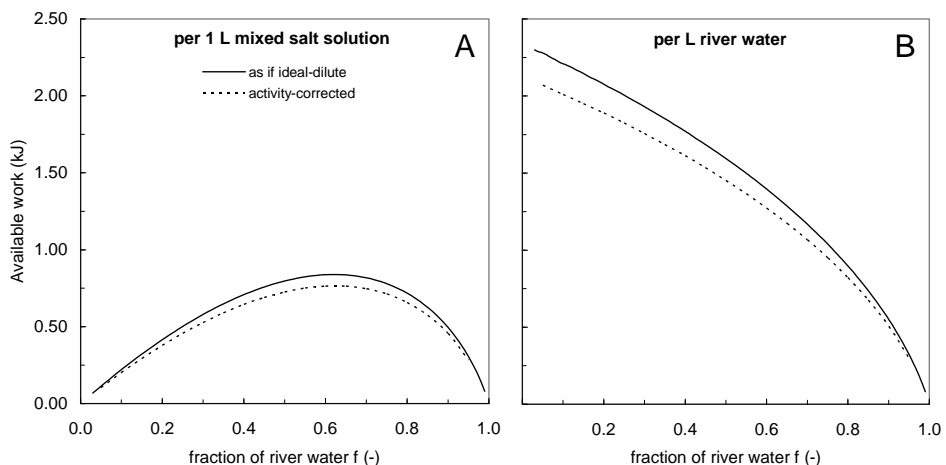


Figure 2: Theoretically available work from mixing (kJ) for a given number of moles ($n = 55.5$, equivalent to ca. 1 L of solutions), consisting of a fraction (f) of river water (5 mM NaCl) and another fraction ($1 - f$) of sea water (0.5 M NaCl), at $T = 298\text{ K}$ (A). Theoretically available work from mixing (kJ) per L of river water (B).

3.3.2 Reversible stack voltage as a measure of available work

For reverse electrodialysis, a potential difference across each membrane is generated that is composed of two contributions, the chemical potential difference $\Delta\mu$ and the electrical potential difference across the membranes of a cell pair. These two potentials may be combined to the electrochemical potential $\tilde{\mu}$. For a hypothetical reverse electrodialysis system operated close to equilibrium, i.e., without irreversible losses, $dG = \tilde{\mu} dn = 0$, the reversible cell-pair potential $\Delta\phi(V)$ can be derived when applied to sodium chloride solutions:

$$\Delta\phi = \frac{2RT}{F} \ln \left(\frac{\gamma_c^\pm \cdot x_c}{\gamma_d^\pm \cdot x_d} \right) = \frac{2RT}{F} \ln \left(\frac{a_c}{a_d} \right) \quad [4]$$

where γ^\pm is the mean mole fraction based activity coefficient of sodium chloride (-) and a the activity. For applications on sea water and river water, with given sodium chloride concentrations, the reversible cell-pair potential is 220 mV.

As mentioned, a stack consists of a pile of cell-pairs between a cathode and an anode. When one cell-pair is represented as a voltage source, a number of cell-pairs N would result in a N times higher output voltage, or stack voltage. As shown by Veerman et al. [9], this is a reasonable assumption for low N since the ionic shortcut currents through the distribution manifolds are then still small. The reversible stack voltage E (V) is:

$$E = N \cdot \Delta\phi \quad [5]$$

For a stack consisting of 4 cell-pairs, under given conditions at the start of each experiment, the reversible stack voltage is about 0.88 V. At the start of each experiment, the measured open circuit voltage was in all cases 0.86 ± 0.01 V, i.e., close to the calculated reversible stack voltage. The reversible stack voltage decreases during the experiments, as the concentration of the concentrated solution is decreasing and the concentration of the diluted solution is increasing with the amount of transferred charge per cell pair (Q , in C):

$$\begin{aligned} x_d(Q) &= x_{d,0} + \frac{N \cdot Q}{n_d \cdot F} \\ x_c(Q) &= x_{c,0} - \frac{N \cdot Q}{n_c \cdot F} \end{aligned} \quad [6]$$

For the given solutions, it can be calculated that the maximum charge transfer per cell pair is $3.3 \cdot 10^3$ C from the concentrated solution batch to the diluted solution batch. This maximum amount of transferred charge is obtained when concentrations of both solutions are equal, i.e., $x_d(Q) = x_c(Q)$. The actual reversible stack voltage reflects the available work that is left at any given amount of transported charge, i.e., at any given extent of charge transfer. Consequently, the reversible stack voltage E is decreasing with increasing transferred charge, see Figure 3.

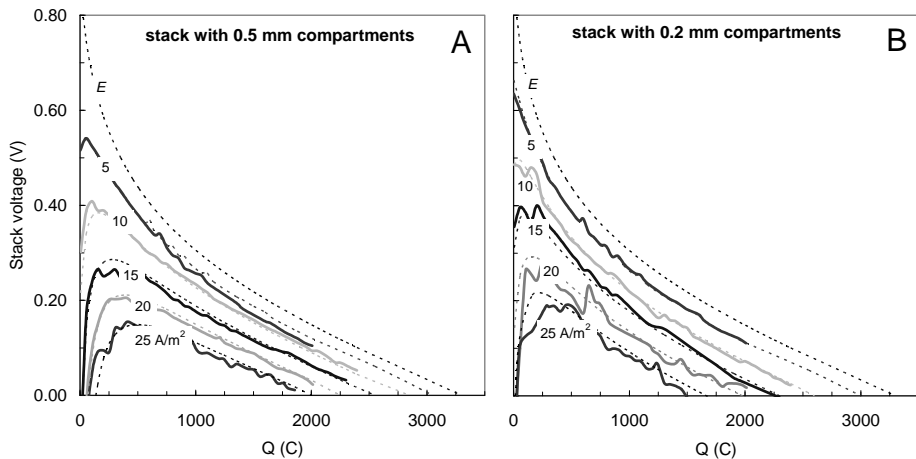


Figure 3: Stack voltage with increasing amount of transported charge Q at variable current density (5, 10...25 A/m²) for the stack with 0.5 mm spacers (A), and the stack with 0.2 mm spacers (B). Thick lines are measured values, dotted lines are projections.

3.3.3 Obtained stack voltage and energy recovery

In Figure 3 also the measured stack voltage V for each applied current density is given with proceeding charge transfer. Apparently, the charge transport in the electrodialytic pile is subject to increasing irreversible losses with increasing current density. At the start of the experiments with higher current densities, the stack voltage dropped even below zero (not

Chapter 3

shown in Figure 3), indicating the internal losses to be higher than the reversible stack voltage. With increasing charge transfer, the internal losses are decreasing as can be seen from the stack voltage coming closer to the reversible stack voltage. As will be discussed in the following paragraphs in more detail, this would be the result of increasing conductivity of the diluted solution with increasing salinity. At a certain point, the stack voltage shows an optimum, where the decrease of reversible stack voltage with increasing charge transfer is balanced with the decrease of the internal losses. For a higher current density, this optimum occurs at a higher amount of transferred charge. This can be explained by a multipliable effect of mentioned increasing irreversible losses with increasing current density and mentioned decreasing stack resistance with increasing charge transfer.

During the charge transfer, a certain amount of work w (J) is obtained from the system. The energy yield as given in Table 2 can be calculated from the stack voltage:

$$w = \int V \, dQ \quad [7]$$

For the stack with 0.5 mm spacers operated with a current density of 5 A/m², the energy yield was 0.56 kJ (energy recovery of 72%) with an uncompleted charge transfer. From projections for complete charge transfer (dotted lines in Figure 3), a maximum energy recovery of 83% could be expected. Although the stack voltages of the stack with 0.2 mm spacers were initially higher, the numbers were almost the same: an obtained energy recovery of 76% and a predicted maximum of 83%. This is a remarkable result, since a reduction of compartment thicknesses was expected to decrease the internal losses. Therefore, in the following paragraphs, the losses are analyzed in more detail: First the losses due to

non-ideality of the membranes and, second, the losses associated with charge transfer.

Table 2: Obtained and projected energy yield (kJ) and energy recovery (%).

current density A/m ²	stack with 0.5 mm compartments				stack with 0.2 mm compartments			
	obtained		projected		obtained		projected	
	kJ	%	kJ	%	kJ	%	kJ	%
5	0.56	72%	0.65	83%	0.59	76%	0.65	83%
10	0.51	65%	0.50	64%	0.50	64%	0.51	65%
15	0.35	45%	0.37	47%	0.41	52%	0.39	50%
20	0.25	31%	0.26	33%	0.26	33%	0.28	36%
25	0.16	20%	0.16	21%	0.12	15%	0.18	23%

3.3.4 Irreversible losses due to non-ideal behavior of membranes

It could be supposed that the irreversible losses due to non-ideal behavior of the membranes restrict the obtainable energy recovery. At low current densities, the diffusion of co-ions and water transport due to osmosis and electro-osmosis would play an important role. In the current range of our experiments, however, these irreversibilities are supposed to be of minor importance. Even at the start of the experiments when the concentration gradient is maximal, the driving force for co-ion transport is small as indicated by an open-circuit voltage close to the reversible stack voltage. The limited co-ion transport was confirmed by an extensively-sampled experiment with a current density of 10 A/m² where a coulombic efficiency η was found of 105±8%. This is calculated from changes in sodium and chloride content in the diluted solution over 15 time intervals, according to:

$$\eta = \frac{N \cdot I \cdot \Delta t}{F \cdot V_d \cdot \Delta c_d} \quad [8]$$

where the numerator represents the electrical equivalents, and the denominator the ionic equivalents, that are transferred during the time interval Δt (I is the current, V_d the batch volume of the diluted solution, and Δc_d the change in molar concentration of the dilute). Also the water transport was measured. From mass balances over all the experiments, it was determined that a net water transport from the diluted batch to the concentrated batch would give energetic losses at lower current densities. For experiments with a current density of 5 A/m^2 , this transport amounted $58 \pm 7 \text{ mL}$ (i.e., $11 \pm 1\%$ of the batch volumes) where at higher current densities the transport became negligible ($5 \pm 2\%$ for 10 A/m^2 , $2 \pm 2\%$ for the higher current densities).

3.3.5 Irreversible losses due to internal resistance toward ion-transport

The internal losses and the differences between the stacks can be related to the internal resistance of the electrodialytic pile (membranes and solution compartments only). The stack voltage can be defined proportional to the current:

$$V = E - I \cdot R \quad [9]$$

where R is the stack resistance (Ω). This proportionality is confirmed by the measured stack resistance by the method described in the experimental section. The stack resistance appears to be independent of the current density, see Figure 4. For both stacks it was found that the stack resistance is mainly ohmic. The non-ohmic resistances due to concentration polarization at membrane surfaces count for $6 \pm 3\%$ and $16 \pm 3\%$, for the stack with 0.5 mm compartments and the stack with 0.2 mm compartments, respectively. The stack resistance can thus be related to the ionic flow through the membranes and the bulk of the concentrated and diluted salt solutions. Consequently, the stack resistance can be

described as proportional to the sum of the area specific resistances of the cell pairs:

$$R = A^{-1} \cdot \sum_N r \quad [10]$$

where A is the current passing area of a single membrane (m^2), and r the area specific resistance of a single cell-pair (Ωm^2). The area specific resistance of a single cell-pair consists of a four terms: the area specific resistance of a cation-exchange membrane, that of the compartment filled with a spacer and a concentrated salt solution ('sea water'), that of the anion-exchange membrane, and that of the compartment filled with a spacer and a diluted salt solution ('river water'). This can be written as:

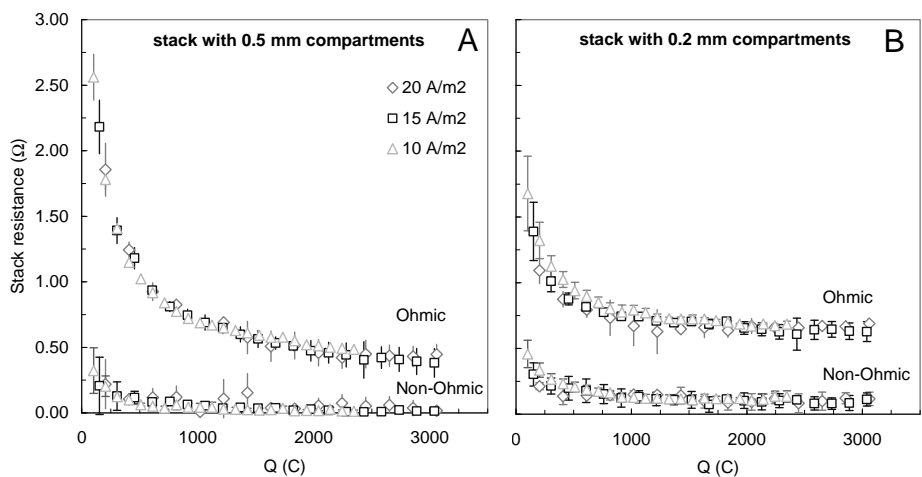


Figure 4: Ohmic and non-ohmic losses with increasing amount of transported charge Q obtained from potential-transients resulting from periodical current-steps, at variable current density (10, 15, 20 A/m^2) for the stack with 0.5 mm spacers (A), and the stack with 0.2 mm spacers (B).

$$r = \frac{r_{cem}}{(1-\beta)} + \frac{h}{\varepsilon^2 \cdot \kappa_c} + \frac{r_{aem}}{(1-\beta)} + \frac{h}{\varepsilon^2 \cdot \kappa_d} \quad [11]$$

where r_{cem} is the area resistance of the cation-exchange membrane (Ωm^2), r_{aem} that of the anion-exchange membrane, β the portion of membrane area that is masked by the spacer (-) referred to as the shadow factor [12], h is the compartment or spacer width (m), ε the porosity (-) of the spacer (the porosity is squared to reflect the tortuous ion transport), κ the conductance of solutions (S/m).

Theoretically, the ohmic losses can be reduced by using membranes with a low resistivity and by minimizing the inter-membrane distance. In both stacks the same membranes were applied, but different compartment thicknesses. The compartment thickness could be considered as the main discriminator between both stacks when we assume the spacer geometries from Table 1 to be comparable with respect to shadow β and tortuosity ε^2 (last term is somewhat higher for the stack with 0.2 mm spacers). At the starting conditions, the stack resistance of the stack with 0.2 mm compartments was indeed lower than of the stack with 0.5 mm compartments. In both cases, the main contributor to the cell-pair resistance is the river water compartment, i.e., the ionic transport through the low-conducting bulk solution and the tortuosity of this ionic transport due to the spacers. However, from a certain amount of transferred charge ($Q > 700$ C, see Figure 4) the resistance of the stack with 0.2 mm compartments became higher than of the stack with 0.5 mm compartments. For the end of charge transfer, it can be derived that the main contributors to the resistance are the membranes and the masked area due to the spacers. Apparently, the shadow factors of the spacers on the membranes are not equal, although this would be suggested from the specifications in Table 1.

From previous analysis, we decided to determine the *apparent tortuosity* ε^2 and the *apparent shadow factor* β . First the apparent tortuosity could be estimated from measurements at low charge transfer, and second the shadow factor β could be estimated from measurements at high charge transfer. For the stack with 0.5 mm spacers, sufficient projections of the stack voltage can be achieved (dotted lines in Figure 3A) with just taking into account the apparent tortuosity $\varepsilon^2 = 0.5$. This is somewhat higher than would be derived from Table 1 ($\varepsilon^2 = 0.6$). For the stack with 0.2 mm spacers, sufficient projections of the stack voltage can be achieved (see dotted lines in Figure 3B) with an apparent tortuosity $\varepsilon^2 = 0.4$ and a shadow factor $\beta = 0.6$. A possible explanation that the shadow factor is of importance in the stack with 0.2 mm spacers and not in the stack with 0.5 mm spacers would be the difference in the manufacturing process. The threads and knits of the 0.2 mm spacer are more extensively calendered and stretched to flatten the fabric. The squashed knits would create a certain contact area on both sides of each membrane. This contact area is masked and thus not available for ion transport.

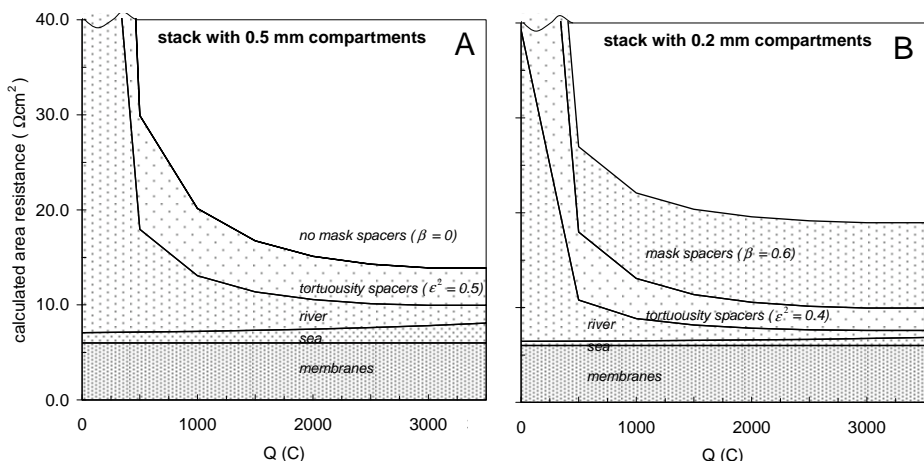


Figure 5: Estimated contributions of cell-pair elements to the cell-pair resistance with increasing amount of transported charge Q for the stack with 0.5 mm spacers (A), and the stack with 0.2 mm spacers (B).

3.4 Future perspectives and outlook

This study shows that reverse electrodialysis is able to obtain a high energy recovery from mixing sea water and river water. The obtainable energy recovery is more than 80% which means an energy yield of $>1.2 \text{ MJ per m}^3$ of river water. The applied method provides a better understanding of the process, especially concerning the mainly-ohmic stack resistance. It can be concluded that for a proper evaluation of a stack design, the proceeding charge transfer should be taken into account. At each stage of charge transfer, the relative contribution of each component to the cell-pair resistance is different. This is indicated in Figure 5 where the cell-pair resistance is given as a function of transferred charge. In this figure, estimations of all contributors are based on the apparent characteristics as mentioned previously (membrane resistances are assumed to be constant, i.e., $3 \Omega\text{cm}^2$ for each membrane). From this figure could be concluded that in the development of reverse electrodialysis, special attention should be given to the development of the compartments. The river compartment thickness was already recognized as an important issue [3, 5, 8-10]. Now the following spacer characteristics can be added as important issues: the tortuosity (porosity) and the shadow.

Together with the development of the compartments and spacers, the entire stack design should be considered regarding the ionic transport. In this study we used a set-up with minor changes in concentrations of the feed waters from the inlet to the outlet (Figure 1). In practice, however, the whole charge transfer should take place during one or few passages through the reverse electrodialysis system. Adjusting one stack voltage will lead to a lower energy recovery near the inlet and a higher energy recovery near the outlet (for V is closer to E at the outlet than to E at the inlet). Accompanying losses could be limited by staging, i.e., applying serial electrode pairs with different stack voltages. Furthermore, the parasitic

system losses for pumping and AC/DC conversion should be investigated. For future work, we also suggest to extend the investigation also to the case of real sea water and river water used as feed solutions.

Acknowledgements

We thank Feiko Reinalda for his help with the experiments and Bertus Nobach for making Figure 1. This work was performed at Wetsus, centre of excellence for sustainable water technology. Wetsus is funded by the ministry of economic affairs. We thank the members of the theme 'Energy' from Wetsus for the fruitful discussions and especially the participating companies Nuon, Magneto, Landustrie, Frisia Zout, Triqua, Dow Chemical, and Waterlab Noord for their support.

3.5 References

1. Lehner, B., G. Czisch, and S. Vassolo, The impact of global change on the hydropower potential of europe: A model-based analysis, *Energy Policy* 33(7) (2005), p. 839-855.
2. Norman, R.S., Water salination: A source of energy, *Science* 186 (1974), p. 350-352.
3. Weinstein, J.N. and F.B. Leitz, Electric-power from difference in salinity - dialytic battery, *Science* 191(4227) (1976), p. 557-559.
4. Wick, G.L. and W.R. Schmitt, Prospects for renewable energy from sea, *Marine Technology Society Journal* 11(5-6) (1977), p. 16-21.
5. Post, J.W., et al., Salinity-gradient power: Evaluation of pressure-retarded osmosis and reverse electrodialysis, *Journal of Membrane Science* 288 (2007), p. 218-230.
6. Forgacs, C., Recent developments in the utilization of salinity power, *Desalination* 40(1-2) (1982), p. 191-195.
7. Audinos, R., Electric-power produced from 2 solutions of unequal salinity by reverse electrodialysis, *Indian Journal Of Chemistry Section A-Inorganic Bio-Inorganic Physical Theoretical & Analytical Chemistry* 31(6) (1992), p. 348-354.
8. Jagur-Grodzinski, J. and R. Kramer, Novel process for direct conversion of free-energy of mixing into electric-power, *Industrial & Engineering Chemistry Process Design And Development* 25(2) (1986), p. 443-449.
9. Veerman, J., et al., Reducing power losses caused by ionic shortcut currents in reverse electrodialysis stacks by a validated model, *Journal of Membrane Science* (310) (2008), p. 418-430.
10. Lacey, R.E., Energy by reverse electrodialysis, *Ocean Engineering* 7(1) (1980), p. 1-47.
11. Larminie, J. and A. Dicks, *Fuel cell systems explained*, 2nd ed. 2005, West Sussex: Wiley.
12. Strathmann, H., *Ion-exchange membrane seperation processes*, 1 ed. Membrane science and technology series. Vol. 9. 2004: Elsevier.

Chapter 3

4 Influence of multivalent ions on power production with reverse electrodialysis

Reverse electrodialysis is a membrane-based technique for production of sustainable electricity from controlled mixing of a diluted electrolyte solution (e.g. river water) and a concentrated electrolyte solution (e.g. sea water). Reverse electrodialysis has been investigated with pure sodium chloride solutions. In practice, however, in most cases also other ions are present in both feed solutions. In the present paper, the effect of multivalent ions on the performance of a reverse electrodialysis stack was investigated. Results show that, besides a higher stack resistance in presence of multivalent ions, especially the presence of multivalent ions in the dilute solution has a lowering effect on the stack voltage. This can be explained by an observed transport of these ions from the diluted electrolyte solution to the concentrated electrolyte solution. In order to prevent or hamper this transport against the activity gradient, monovalent-selective membranes can be used. This shows indeed better results with respect to the stack voltage. Therefore, it would be beneficial to use monovalent-selective membranes in reverse electrodialysis, especially in the case of a relatively high content of multivalent ions in the dilute (i.e., in the first stages of the installation where the sodium chloride content in the dilute is still relatively low).

This chapter has been published as:

Post, J.W., H.V.M. Hamelers and C.J.N. Buisman, Influence of multivalent ions on power production from mixing salt and fresh water with a reverse electrodialysis system, Journal of Membrane Science 330 (2009) 65–72.

4.1 Introduction

4.1.1 Reverse electrodialysis for electricity production

When fresh and saline water mixes, energy is released (Gibbs free energy of mixing). A part of this energy could be used for generation of electrical power by reverse electrodialysis [1]. In a reverse electrodialysis stack, anion- and cation-exchange membranes are used to separate water streams of different salinity. Due to the chemical potential difference between both solutions and an alternating installation of anion- and cation-exchange membranes within the stack, cations are transported in the direction of a cathode and anions in the direction of an anode. This charge transport is counterbalanced by an electron transfer from the anode to the cathode through an external circuit. With this electrical current useful work can be done. The process has been described in more detail by several authors [2-6].

4.1.2 Unknown effect of multivalent ions on performance

In the reported research on reverse electrodialysis, so far, the presence of other ions than sodium and chloride was hardly taken into account. However, in most practical cases also other ions are present in both feed solutions. In sea water, for instance, the most commonly found salt ions are sodium, magnesium, calcium, chloride, sulphate, and bicarbonate. Lacey [4] recommended already to investigate whether reverse electrodialysis behaves differently for solutions that contain other ions than sodium and chloride. His major concern was the possible detrimental effect of traces of ferrous iron and manganese in (geothermal) brines. Jagur-Grodzinski and Kramer [5] performed experiments with Dead Sea water with high magnesium content and they found their cation-exchange membranes to have a high resistivity when equilibrated in with magnesium rich solutions. Finally, Audinos [6] concluded the performance of a reverse electrodialysis

Chapter 4

system to be better for pure sodium chloride solutions than for pure zinc sulphate solutions.

From literature concerning ion-exchange membranes and from preliminary experiments, we know that the presence of multivalent ions may have a lowering effect on stack voltage and consequently on the power density. There are many fundamental and experimental studies for single membrane systems concerning membrane potentials in bi-ionic or multi-ionic solutions. However, contrary to membranes in a reverse electrodialysis system, the membranes in studies on the bi-ionic potential are facing only feed solutions of different composition and not of different concentration [7-9] or feed solutions in absence of multivalent ions [10, 11]. Although Higa et al. [12-15] studied membrane potentials in multi-ionic systems including concentration-gradients, these studies differ from our case as they were carried out at relatively low concentrations on both sides of the membrane (1-10 mmol/L [13, 14]). Besides all these differences, the system of our study has the distinctive characteristic that the chemistry of the concentrated feed solution is dominated by the sodium chloride content. Consequently, the membrane potential is less sensitive to changes in ionic composition of the concentrate and relatively sensitive to changes in concentration and composition of the dilute. Therefore, we decided to vary mainly the dilute feed solution.

4.1.3 Objective

The objective of our study was to investigate the effect of the presence of multivalent ions in the feed solutions on the power density of a reverse electrodialysis system. In the experimental work, we measured the stack voltage with varying concentrations of sodium, magnesium, chloride and sulphate. We also investigated whether monovalent-selective ion-exchange membranes can be used to improve the performance of reverse electrodialysis. We compared a stack with standard-grade ion-exchange

membranes and a stack with monovalent-selective ion-exchange membranes.

4.2 Experimental section

4.2.1 Reverse electrodialysis stacks

The principle of reverse electrodialysis is described in literature (e.g. [3]). The square stacks used in this study are comparable to those previously described by the authors [1]. The compartments between the membranes were formed with 0.5 mm silicone gaskets and spacers (Nitex 06-700/53, Sefar). Ag/AgCl reference electrodes were placed within reservoirs that were connected to capillaries with their tips 1 mm adjacent to the exterior cation-exchange membranes. Anode and cathode were connected to a galvanostat (IviumStat Electrochemical Interface & Impedance Analyser; Ivium Technologies, The Netherlands).

In this study, two reverse electrodialysis stacks were used. One stack contained standard-grade ion-exchange membranes (Neosepta CMX/AMX, Tokuyama Co.), the other stack contained monovalent-selective membranes (Neosepta CMS/ACS, Tokuyama Co.). The CMS membranes are prepared by coating a thin cationic polyelectrolyte layer on both sides of a standard-grade CMX [16]. The monovalent-selectivity is obtained due to the difference of electrostatic repulsion between this thin layer and the cations in solution [17, 18]. The ACS membranes are prepared by deposition of a highly cross-linked layer on both sides of an anion-exchange membrane [16, 18]. The monovalent-selectivity is obtained due to the difference of steric repulsion between this thin layer and the anions in solution [17, 18].

In all experiments, the concentrated salt solution ('sea water'), the diluted salt solution ('river water'), and an electrode rinse solution (0.25 M NaCl, 'brackish water') were fed to the stacks with a flow rate 57.5 mL/min. The

residence time of the solutions in the compartments of the stack, i.e., from inlet manifold to outlet manifold, was estimated to be 0.5 min. Solution samples were taken at the outlets of the stacks. Cations and anions were analyzed with inductive-coupled plasma (Optima 3000XL, Perkin Elmer) and ion chromatography (761 Compact IC, Metrohm), respectively.

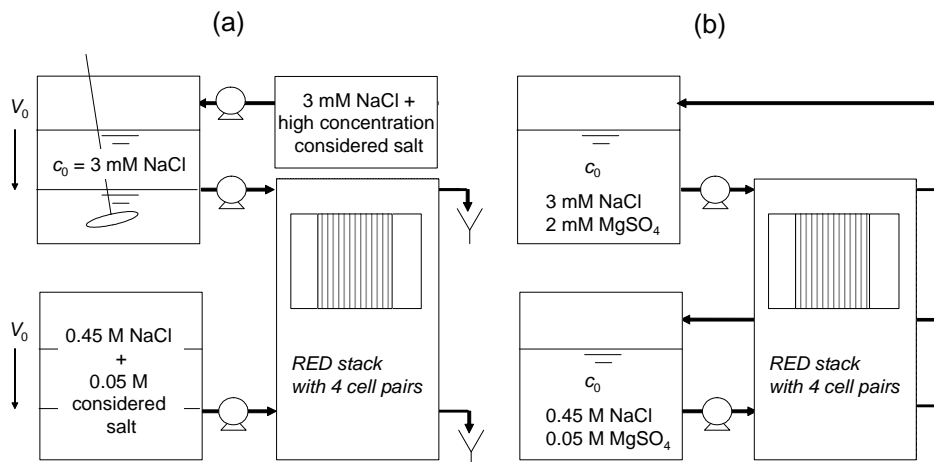


Figure 1: Experimental set-up (a) to determine the effect of different ionic compositions on open-circuit voltage, and (b) to determine the ionic transport under open-circuit conditions and under current-producing conditions.

4.2.2 Experiments with different ionic compositions

To determine the effect of different ionic compositions of the dilute feed water to the stack voltage, four experiments were carried out. Before each experiment, the membranes were brought in the sodium and chloride form and equilibrated in a diluted sodium chloride solution of 3 mmol/L and a concentrated sodium chloride solution of 0.45 mol/L. During each experiment, a different salt was added to these solutions: sodium chloride, magnesium sulphate, sodium sulphate and magnesium chloride, respectively. At the start of each experiment, the concentrated sodium chloride solution was enriched with 0.05 mol/L of the considered salt. During the experiment, the salt was added to the dilute stock solution

(Figure 1a). In all cases, the addition rate was established in the range of 0.2-0.4 mmol/L·min concentration increase in the dilute stock solution (increase in rate due to decrease of stock volume). This addition rate resulted in a sufficient accuracy as determined by some preliminary steady-state experiments. From these preliminary experiments, we concluded that the response period which should be taken into account was approximately 1 min (i.e., two times the estimated residence time). With an addition rate of 0.2 mmol/L·min, this means that the measured stack voltage can be related to the actual concentration at the outlet with an accuracy of ± 0.2 mmol/L.

4.2.3 Experiments with ion-transport

To determine how ion-transport within the stacks takes place, two batch experiments were carried out: (i) under open-circuit conditions and (ii) under current-producing conditions. The solutions were recycled from bottles of 1 L (Figure 1b). The dilute consisted of 3 mmol/L sodium chloride and 2 mmol/L magnesium sulphate, and the concentrate of 0.45 mol/L sodium chloride and 0.05 mol/L magnesium sulphate. For the experiments under current-producing conditions, the bottles were stored in a thermostatic bath (with a temperature of 25 ± 1 °C). Before each experiment, the stacks and tubes were flushed and equilibrated with matching solutions. Each stack with connected tubes had an estimated system volume of 50 mL. The total batch volume of each solution was accordingly 1,050 mL. For the experiments under current-producing conditions, the galvanostat generated a square-wave signal with cycles of a 200 s period of zero-current conditions (open circuit) followed by a 1,000 s period with an adjusted current level of 100 mA (i.e., 10 A/m²).

4.3 Results and discussion

4.3.1 Open-circuit voltage with different ionic compositions

The theoretical non-expansion work that can be produced from mixing is defined by the Gibbs energy of mixing $\Delta_{\text{mix}}G$. For ideal-dilute solutions (i.e., $\Delta_{\text{mix}}H = 0$), it can be shown that the Gibbs energy of mixing is determined by the mole fractions of solutes, no matter the charge and valence of the solutes [1]. Generally for fuel cells, the maximum work that can be done by charge transfer Q (C) is equal to $\Delta G = Q \cdot E_{\text{rev}}$, where E_{rev} (V) is the reversible voltage [19]. In Figure 2 the open-circuit stack voltages are, therefore, presented as measured with an increasing concentration of charge carriers ($\text{meq/L} \approx 10^2 \text{ C/L}$). These charge carriers are the dissolved ions from the added chemicals to the dilute (Figure 1a). An addition of 1 meq/L refers to an addition of 1 mmol/L sodium chloride or to an addition of 0.5 mmol/L for sodium sulphate, magnesium chloride, and magnesium sulphate.

For standard-grade membranes (Figure 2a), we observed that each addition of charge carriers had the same lowering effect on the stack voltage. For the sodium chloride addition, the response of the open-circuit voltage E (V) can be simply predicted by using an adapted Nernst-equation, as proposed by Weinstein and Leitz [3]:

$$E = \alpha \cdot E_{\text{rev}} = \alpha \cdot 2N \cdot \Delta\phi = \alpha \cdot 2N \cdot \frac{RT}{F} \ln\left(\frac{a_c}{a_d}\right)^{\frac{1}{z_i}} \quad [1]$$

Where α is the so-called perm selectivity coefficient (-), $\Delta\phi$ the reversible voltage of a single membrane, N is the number off cell pairs, R the gas constant (J/mol·K), T the temperature (K), a the activity (-), z the valence (eq/mol), F the Faraday constant (C/eq), subscript i refers to an ion, and subscripts c and d to the concentrated and diluted solution, respectively. The perm selectivity coefficient α (-) is used to compensate the calculated

membrane potential for the fact that the membranes do not fully exclude transport of co-ions. For the dilute concentration ranges of the experiment (relatively low concentrations in the dilute compared to high concentration of sodium chloride in the concentrated solution), the stack voltage can be reasonably predicted by equation 1 (see line in *Figure 2a*). In this concentration range, the measured stack voltage is about 93% of the reversible stack voltage, indicating with a mean constant perm selectivity coefficient of 0.93.

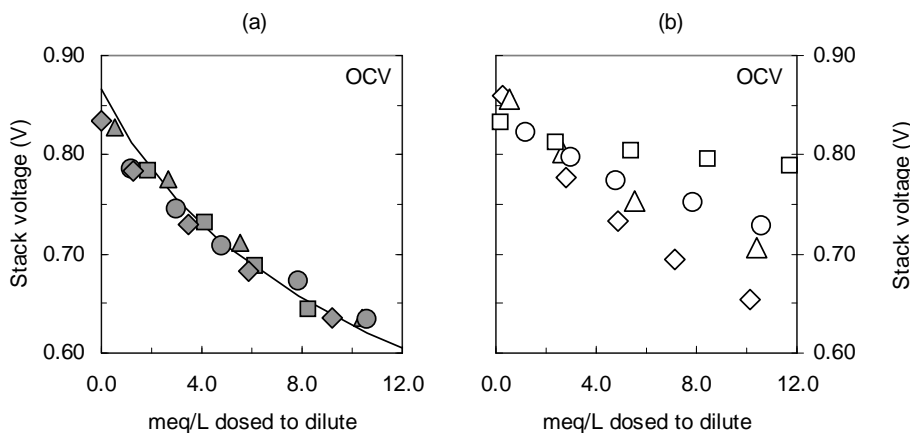


Figure 2: Open-circuit voltage of a stack (a) with standard-grade ion-exchange membranes (closed symbols) and (b) with monovalent-selective membranes (open symbols) at increasing amount of sodium chloride (NaCl , \diamond), sodium sulphate (Na_2SO_4 , \circ), magnesium chloride (MgCl_2 , \triangle), magnesium sulphate (MgSO_4 , \square) added to the sodium chloride feed solutions (a diluted sodium chloride solution of 3 mmol/L and a concentrated sodium chloride solution of 0.45 mol/L + 0.05 mol/L of added chemical). Line gives predicted value (Equation 1).

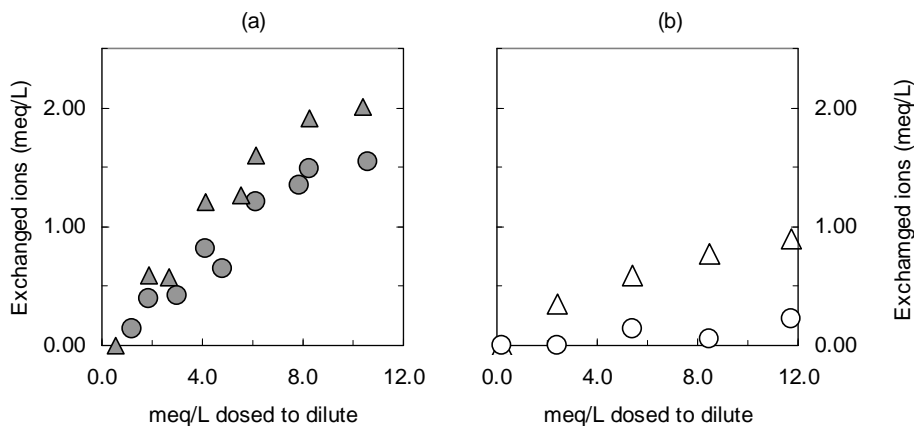


Figure 3: Concentration of exchanged ions (a) with standard-grade ion-exchange membranes (closed symbols) and (b) with monovalent-selective membranes (open symbols) at increasing amount of sulphate (\circ) and magnesium (Δ) added to the sodium chloride feed solutions as declared in caption of Figure 2.

The observed similarity for the other chemicals implicates that for the considered system, the stack voltage apparently can also be predicted by Equation 1 *as if* all multivalent ions in the dilute are exchanged for monovalent ions (e.g. for a cation-exchange membrane: $Mg^{2+} \leftrightarrow 2 Na^+$). Such an ion exchange, however, occurred only to a limited extent. From the samples at the outlet of the stack, it was found that a dosage of e.g. 10 meq/L magnesium actually resulted in an increase of the sodium concentration of <2 meq/L (Figure 3a). Whilst only 20% of the multivalent ions were exchanged for monovalent ions, the stack voltage responded as if all multivalent ions were exchanged.

A physical explanation would be that the exchange of ions takes place in the diffusion boundary layer. In this case, the diffusion boundary layer differs from the sampled bulk solution in a sense that at the membrane surface virtually all multivalent ions have disappeared and monovalent counterions from the membrane matrix are accumulated. From Figure 3a can be

seen that the ion exchange increases with increasing concentration of multivalent ions in the dilute. Assuming the residence time and diffusion boundary layer thickness to be unchanged at constant hydrodynamic conditions (viscosity, cross-flow velocity), this observed increase of ion exchange can be interpreted as an increase of ionic fluxes. With a complete depletion of multivalent ions at the membrane surface, the flux of multivalent ions would be proportional to the concentration in the bulk solution. Apparently, this is not true at higher concentrations of multivalent ions ($> 8 \text{ meq/L}$) added to the bulk dilute solution. Therefore, additional explanations are needed and worthwhile to investigate. One might think of an explanation by the ratio's between diffusivities and valences of the different ions in the membrane matrix as is the case for bi-ionic potentials in relatively concentrated solutions [20].

For monovalent-selective membranes (Figure 2b), we observed that addition of different charge carriers had a different effect on the stack voltage. As expected, for the sodium chloride addition, the response of the stack voltage was comparable to that of the stack with standard-grade membranes. The perm selectivity of monovalent-selective membranes appeared to be a bit higher than of standard-grade membranes.

The addition of magnesium sulphate had a minor effect on the stack voltage. An explanation could be the non-ideal monovalent-selectivity, especially of the cation-exchange membranes. This can be concluded from the observed cation exchange (Figure 3b) and also from the results of the additions of sodium sulphate and magnesium chloride. When sodium sulphate is added, only the membrane potential of the monovalent-selective cation-exchange membranes is supposed to be affected. This means, the effect on the stack voltage should be the half of the effect of the sodium chloride dose. This is indeed in accordance to the experimental results (Figure 2b). However, when magnesium chloride is added, for

which only the membrane potential of the anion-exchange membranes is supposed to be affected, the stack voltage seemed to be more affected. This indicates that the membrane potential of the monovalent-selective cation-exchange membranes is slightly lowered due to the presence of magnesium ions in the dilute solution.

4.3.2 Transport of multivalent ions against the activity gradient

When the solutions were recycled over the stacks under open-circuit conditions (Figure 1b), the ion-concentrations in the dilute were changing with time (Figure 4). For both membrane types, the sodium and chloride content in the dilute increased with time. Since the experiments were carried out under open-circuit conditions, i.e., without net flux of electrical charges, this increase would be the result of co-ion diffusion due to concentration-gradients over the membrane.

For the stack containing standard-grade membranes (Figure 4, closed symbols), magnesium and sulphate concentrations in the dilute decreased with time, which is remarkable as this indicates that these ions were transported against their concentration-gradient (the magnesium sulphate concentration in the concentrate was 0.05 mol/L). Consequently, the back-transport cannot be explained by concentration-gradient driven diffusion. It seems that under open-circuit conditions, ion exchange or inter-diffusion occurs like in Donnan dialysis [21] where monovalent ions from the concentrated ‘draw solution’ are exchanged by multivalent ions from the dilute solution. In our experiment, magnesium ions from the dilute were exchanged for sodium ions from the concentrate, and similarly sulphate ions for chloride ions, in a ratio 1:2 to maintain electro-neutrality. The driving force for this ion-exchange process is a difference in electrochemical potential between the ions. For a cation-exchange membrane, for instance, sodium ions with a relatively higher electrochemical potential tend to permeate through a cation-exchange

membrane from the concentrated solution to the diluted solution, whereas magnesium ions with a relatively lower electrochemical potential tend to permeate in the opposite direction, even against its concentration gradient. Apparently, the back-transport occurred until equilibrium. This equilibrium between the two solutions is achieved when the electrochemical potential gradients of all ions in the two solutions are equated. Thus, in equilibrium:

$$\tilde{\mu}_{i,c} = \tilde{\mu}_{i,d}$$

$$RT \ln a_{i,c} + z_i F \phi_c = RT \ln a_{i,d} + z_i F \phi_d \quad [2]$$

$$\Delta \phi_D = \phi_d - \phi_c = \frac{RT}{F} \ln \left(\frac{a_{i,c}}{a_{i,d}} \right)^{\frac{1}{z_i}}$$

Where μ is the electrochemical potential (J/mol) and ϕ the electrical potential (V). In equilibrium, the potential difference $\Delta \phi_D$ is the so-called Donnan potential, which is the result of all ions that can be transported through the membrane. Theoretically, for cations sodium and magnesium in this experiment, the Donnan equilibrium could be found:

$$\begin{aligned} \Delta \phi_D &= \frac{RT}{F} \ln \left(\frac{a_{Na,c}}{a_{Na,d}} \right) = \frac{RT}{F} \ln \left(\frac{a_{Mg,c}}{a_{Mg,d}} \right)^{\frac{1}{2}} \\ &\quad \left(\frac{a_{Na,c}}{a_{Na,d}} \right) = \left(\frac{a_{Mg,c}}{a_{Mg,d}} \right)^{\frac{1}{2}} \end{aligned} \quad [3]$$

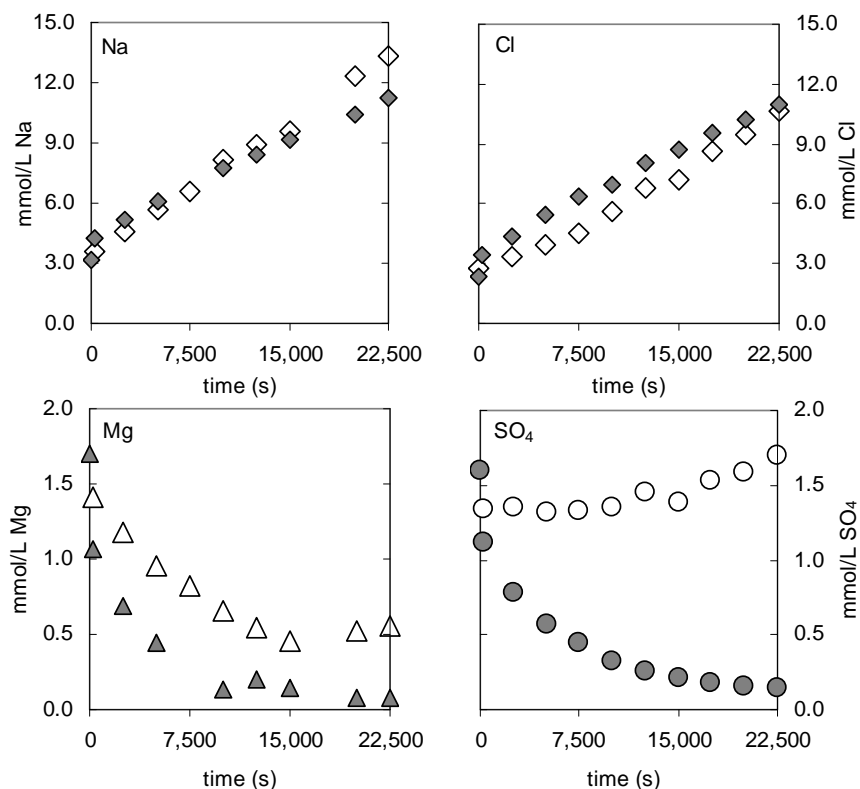


Figure 4: Ion-concentrations in dilute of stack with standard-grade ion-exchange membranes (closed symbols) and with monovalent-selective membranes (open symbols) during recycling offeed solutions under open-circuit conditions.

This derivation assumes the cation-exchange membrane has full exclusion of co-ion transport. However, in practice ion-exchange membranes transport co-ions as well, which was already shown by the fact that diffusion takes place from the concentrated electrolyte solution to the diluted electrolyte solution. To accommodate for this non-perfect exclusion, the permselectivity coefficient was introduced (Equation 1). The perm selectivity coefficient α of ion-exchange membranes is assumed to be close to unity for multivalent ions, where α for monovalent ions was already estimated to be 0.93. Close to equilibrium (at $t = 22,500$ s, where

$c_{Na,c} = 0.45 \text{ mol/L}$, $\gamma_{Na,c} = 0.65$, $c_{Na,d} = 12 \text{ mmol/L}$, $\gamma_{Na,d} = 0.9$, $c_{Mg,c} = 0.05 \text{ mol/L}$, $\gamma_{Mg,c} = 0.3$, $c_{Mg,d} = 0.1 \text{ mmol/L}$, $\gamma_{Mg,d} = 0.65$) it can be confirmed that there is hardly any driving force left to exchange cations anymore, since:

$$\begin{aligned}\Delta\phi_m &= 0.93 \cdot \frac{RT}{F} \ln\left(\frac{a_{Na,c}}{a_{Na,d}}\right) \approx \frac{RT}{F} \ln\left(\frac{a_{Mg,c}}{a_{Mg,d}}\right)^{\frac{1}{2}} \\ &0.93 \cdot \left(\frac{a_{Na,c}}{a_{Na,d}}\right) \approx \left(\frac{a_{Mg,c}}{a_{Mg,d}}\right)^{\frac{1}{2}}\end{aligned}\quad [4]$$

Regarding the ion fluxes, the magnesium and sulphate showed a rapid decrease at the start of the experiment for the experiment with the standard-grade membranes. It can be explained that at the start of the experiment, when the cation-exchange membranes were in sodium-form and the anion-exchange membranes in chloride-form, these free counterions at the surface of the standard-grade membranes are exchanged for magnesium and sulphate from the dilute. Samples were taken at the outlet of the stack, not from the batch-solution. Therefore, results were sensitive for this fast exchange process within the stack (see also Figure 3a).

After the initial rapid increase, the sodium flow of $0.36 \mu\text{eq/s}$ (flux of $9 \mu\text{eq/m}^2\cdot\text{s} \sim 0.9 \text{ A/m}^2$) was counterbalanced by back-diffusion of magnesium ($0.3 \mu\text{eq/s} \sim 0.7 \text{ A/m}^2$, after the rapid decrease) and diffusion of chloride. At the end of the experiment, the sodium flux of $0.3 \mu\text{eq/s} (\sim 0.7 \text{ A/m}^2)$ was counterbalanced just by diffusion of chloride. The same observation can be made for chloride, where the diffusion initially was counterbalanced by back-diffusion of sulphate and diffusion of sodium and at the end just by diffusion of sodium. Obviously, the back-diffusion of multivalent ions and diffusion of co-ions are to certain extent competitive.

For the stack containing monovalent-selective membranes (Figure 4, open symbols), the magnesium concentration also decreased with time, which indicates that the cation-exchange membranes were not completely selective to monovalent cations, and therefore subject to the same ion-exchange phenomenon as described for standard-grade membranes. The sulphate concentration, however, stayed constant (after a rapid initial decrease) or even increased. As expected, the monovalent-selective membranes did show less exchange of counter-ions at the start of the experiment. The flux of sodium stayed constant over the whole period ($0.5 \mu\text{eq}/\text{s} \sim 1.2 \text{ A/m}^2$). At the start of the experiment the diffusion of sodium was counterbalanced by back-diffusion of magnesium ($0.3 \mu\text{eq}/\text{s} \sim 0.7 \text{ A/m}^2$ after the rapid decrease) *and* diffusion of chloride ($0.2 \mu\text{eq}/\text{s} \sim 0.5 \text{ A/m}^2$) whereas at the end of the experiment the diffusion of sodium was counterbalanced just by diffusion of chloride. Without the back-diffusion of sulphate, the chloride flux was just coupled to the sodium flux. Consequently, the flux of chloride increased ($0.2 \mu\text{eq}/\text{s}$ to $0.4 \mu\text{eq}/\text{s}$).

4.3.3 Irreversible loss is limited to first extent of mixing

The described ionic transport under open-circuit conditions should be regarded as an energetic loss due to irreversible mixing. Although this irreversible mixing occurred with low ion-fluxes ($0.3 \mu\text{eq}/\text{s}$ in our experiment is comparable to a current density of only 0.7 A/m^2), the effect on the open-circuit voltage was considerable. During the recycle period, the open-circuit voltage of the stacks decreased due to the increase of sodium chloride concentrations in the dilute (Figure 5). The voltage of the stack with standard-grade membranes can be reasonably predicted over the whole course of the experiment, using Equation 1 with the mentioned apparent exchange of the multivalent ions for their equivalents of monovalent ions. The voltage of the stack with monovalent-selective membranes can be reasonably predicted over the whole course of the

experiment, using Equation 1 with just taking into account the monovalent ions. Initially, the open-circuit voltage of the stack with standard-grade membranes was lower compared to that of the stack with monovalent-selective membranes. After a certain extent of sodium and chloride transport, together with the ion-exchange process, the voltage of the stack with standard-grade membranes became equal to that of the stack with monovalent-selective membranes. At this point, the ion exchange is stopped. As explained, this would mean that the Donnan equilibrium is approached where the electrochemical potentials of monovalent and multivalent cations and anions are equal (no driving force to exchange ions). The stack voltage of the standard-grade membranes seems to be no longer negatively affected by the presence of magnesium or sulphate in the dilute.

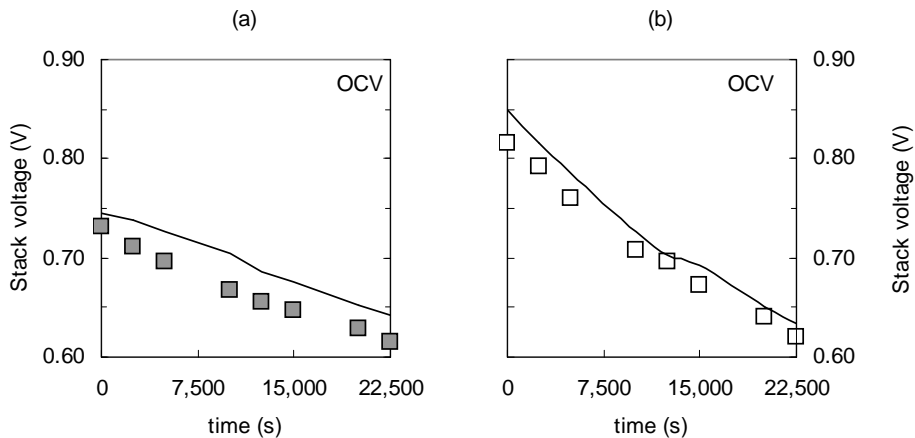


Figure 5: Open-circuit voltage (a) of a stack with standard-grade ion-exchange membranes (closed symbols) and (b) of a stack with monovalent-selective membranes (open symbols) during recycling of feed solutions under open-circuit conditions. Lines give predicted values (Equation 1).

These results of experiments under open-circuit conditions may indicate that the use of monovalent-selective membranes would have a positive effect on the performance of reverse electrodialysis. This positive effect,

however, would be limited to the first stages of the installation where the sodium chloride content in the dilute is still low (and the concentration of multivalent ions is relatively high). For later stages of the installation, i.e., where the sodium chloride content in the dilute is increased, the use of standard-grade membranes would be sufficient.

4.3.4 Transport of multivalent ions under current-producing conditions

In order to check this hypothesis, the solutions were recycled over the stacks under current-producing conditions with a current density of 10 A/m². The ion-concentrations in the dilute were changing with time (Figure 6). For both membrane types, the sodium and chloride content in the dilute increased with time, close to which could be expected from the electrical equivalents (i.e., a Coulombic efficiency close to 100% as for pure sodium chloride solutions [1]). Initially, the sodium and chloride fluxes were higher due to fast exchange with magnesium and sulphate.

For standard-grade membranes (Figure 6, closed symbols), the initial exchange of magnesium occurred at a rate of >5 µeq/s which is comparable to a current density of >12 A/m². After this rapid decrease of magnesium, the equilibrium was reached in a relatively short period due to the fast increase of sodium concentrations in the dilute (4 µeq/s ~ 10 A/m²). After this equilibrium, magnesium starts to contribute to the current production, though to a negligible extent (<0.1 µeq/s ~ <0.2 A/m²). The same observation can be made for sulphate. Compared to the ion transport under open-circuit conditions (Figure 4), the back-transport of multivalent ions under current-producing conditions seems to be accelerated towards an equilibrium. This acceleration is remarkable as the driving force for back-transport of multivalent ions under current-producing conditions is less.

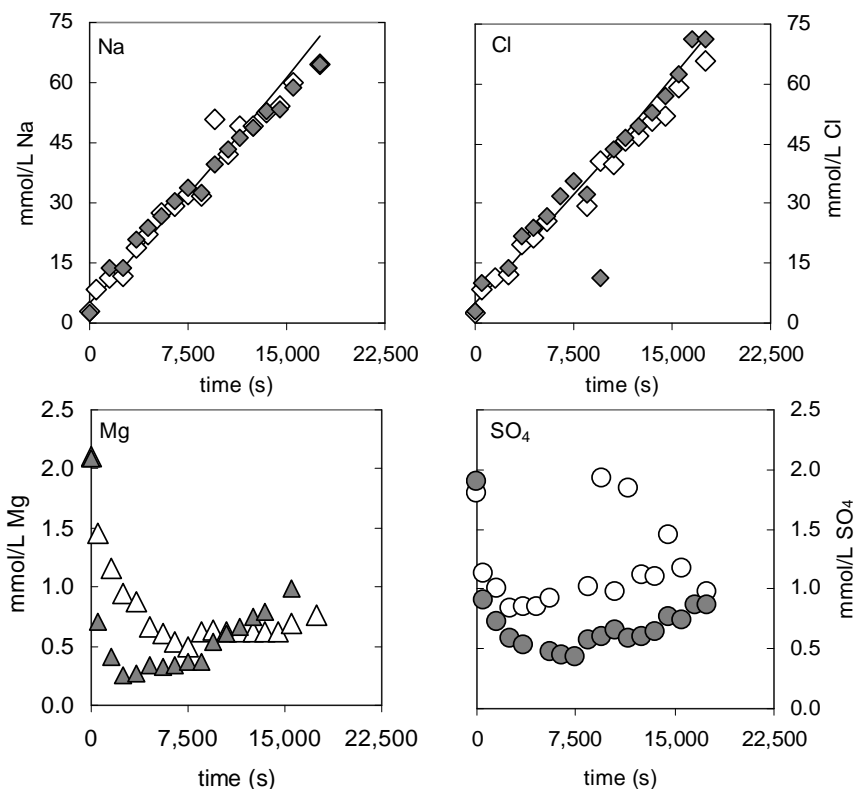


Figure 6: Ion-concentrations in dilute of stack with standard-grade ion-exchange membranes (closed symbols) and with monovalent-selective membranes (open symbols) during recycling of feed solutions under current-producing conditions. Lines give values that can be expected from equivalent electrical transport.

For monovalent-selective membranes (Figure 6, open symbols), the initial exchange of magnesium occurred at a twice lower rate than for standard-grade membranes. Compared to the ion transport under open-circuit conditions (Figure 4), the back-transport of magnesium under current-producing conditions seems to be accelerated towards an equilibrium. Contrary to the experiments under open-circuit conditions, also a back-transport of sulphate was found. Such a remarkable loss of monovalent-selectivity of ACS membranes with increasing current density was also observed in experiments with conventional electrodialysis by Saracco [18].

This loss of monovalent-selectivity might explain the minor differences in performance between the two stacks under current-producing conditions. The voltage of the stack with standard-grade membranes was slightly lower than of the stack with monovalent-selective membranes during the first 5,000 s (Figure 7). The stack resistance of both stacks was comparable, or even a bit lower for the stack with standard-grade membranes. Thus, the suggested beneficial effect of the monovalent-selective membranes on power density is limited.

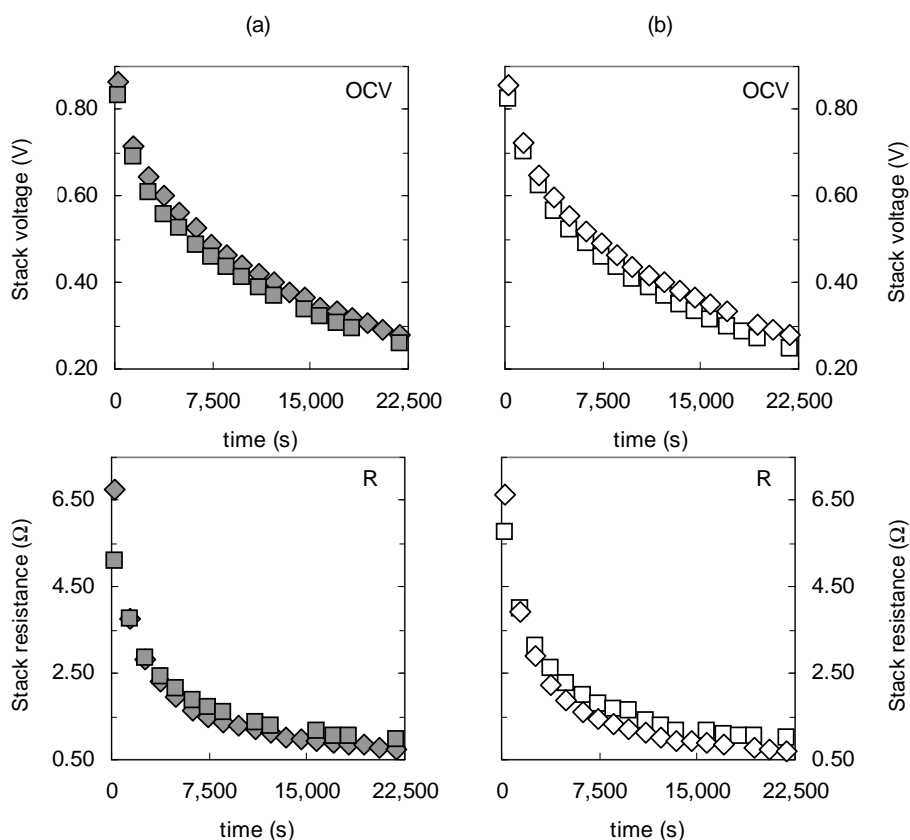


Figure 7: Open-circuit voltage OCV and resistance R , (a) of a stack with standard-grade ion-exchange membranes (closed symbols), and (b) of a stack with monovalent-selective membranes (open symbols) during recycling of feed solutions under open-circuit conditions. Feed solutions were pure sodium chloride solutions (NaCl, \diamond), or with added magnesium sulphate (MgSO₄, \square).

For both stacks the voltage and resistance can be compared to an experiment that was carried out with pure sodium chloride solutions (concentrate 0.5 mol/L, dilute 5 mmol/L). Over the whole range, the stack voltage was slightly lower in presence of magnesium sulphate (Figure 7) when compared to the experiment with pure sodium chloride solutions. At the start of the experiment, the stack resistance was lower in presence of magnesium sulphate as a result of the higher conductivity of the dilute. At a higher extent of mixing, the stack resistance decreased as a result of the increasing conductivity of the dilute. At a higher extent of mixing, the relative contribution of membranes to the stack resistance is considerable [1]. In presence of magnesium sulphate the membrane resistances appeared to be higher than in presence of pure sodium chloride solutions. From this, it can be concluded that multivalent ions have a detrimental effect on the power density. This would especially be the case for better designed reverse electrodialysis stacks, where the membrane resistance is becoming a more important parameter [22].

4.4 Future perspectives and outlook

This study shows that the power density of a reverse electrodialysis system is sensitive to the ionic composition of the feed solutions. The presence of multivalent ions (e.g. magnesium and sulphate) in the feed solutions, particularly in the dilute, gives a lowering effect on stack voltage. Moreover, the stack resistance is higher in the presence of multivalent ions due to higher membrane resistances.

In the first stages of a reverse electrodialysis system, multivalent ions in the dilute are exchanged with monovalent ions from the concentrate. In order to prevent or hamper the transport of multivalent ions against the activity gradient, monovalent-selective membranes can be used. The open-circuit voltage of a stack with these membranes is less affected by the

presence of multivalent ions. Therefore, it would be beneficial to use monovalent-selective membranes in reverse electrodialysis, especially in the case of a relatively high content of multivalent ions in the dilute (i.e., in the first stages of the installation where the sodium chloride content in the dilute is still relatively low). From the experiments, however, the beneficial effect on power density is believed to be limited.

Acknowledgements

This work was performed at Wetsus, centre of excellence for sustainable water technology. Wetsus is funded by the ministry of economic affairs. The authors like to thank the members of the theme 'Energy' from Wetsus for the fruitful discussions and especially the participating companies Nuon, Magneto, Landustrie, Frisia Zout, Triqua, Dow Chemical, Fuji, and Waterlab Noord for their support.

4.5 References

1. Post, J.W., H.V.M. Hamelers and C.J.N. Buisman, Energy recovery from controlled mixing salt and fresh water with a reverse electrodialysis system, *Environ Science Technology* 42 (2008), p. 5785-5790.
2. Pattle, R.E., Production of electric power by mixing fresh and salt water in the hydroelectric pile, *Nature* 174(4431) (1954), p. 660-660.
3. Weinstein, J.N. and F.B. Leitz, Electric-power from difference in salinity - dialytic battery, *Science* 191(4227) (1976), p. 557-559.
4. Lacey, R.E., Energy by reverse electrodialysis, *Ocean Engineering* 7(1) (1980), p. 1-47.
5. Jagur-Grodzinski, J. and R. Kramer, Novel process for direct conversion of free-energy of mixing into electric-power, *Industrial & Engineering Chemistry Process Design And Development* 25(2) (1986), p. 443-449.
6. Audinos, R., Electric-power produced from 2 solutions of unequal salinity by reverse electrodialysis, *Indian Journal Of Chemistry* 31(6) (1992), p. 348-354.
7. Toyoshim.Y and H. Nozaki, Bi-ionic potential across charged membranes, *Journal Of Physical Chemistry* 74(13) (1970), p. 2704-2710.
8. Dammak, L., C. Larchet, B. Auclair, V.V. Nikonenko and V.I. Zabolotsky, From the multi-ionic to the bi-ionic potential, *European Polymer Journal* 32(10) (1996), p. 1199-1205.
9. Tasaka, M., R. Kiyono and D.S. Yoo, Membrane potential across a high water content anion-exchange membrane separating two solutions with a common counterion but two different co-ions, *Journal Of Physical Chemistry* 103(1) (1999), p. 173-177.

10. Tran, S., L. Dammak, C. Larchet and B. Auclair, Bi-ionic potential through a cation exchange membrane separating two electrolyte solutions at different concentrations, *Electrochimica Acta* 44(15) (1999), p. 2515-2521.
11. Tasaka, M., S. Iwaoka, K. Yamagishi and Y. Ikeda, Dependence of bi-ionic potential across membranes on salt concentration, *Journal Of Membrane Science* 24(1) (1985), p. 29-42.
12. Higa, M., A. Tanioka and K. Miyasaka, Simulation of the transport of ions against their concentration gradient across charged membranes, *Journal Of Membrane Science* 37(3) (1988), p. 251-266.
13. Higa, M., A. Tanioka and K. Miyasaka, A study of ion permeation across a charged membrane in multicomponent ion systems as a function of membrane charge-density, *Journal Of Membrane Science* 49(2) (1990), p. 145-169.
14. Higa, M., A. Tanioka and K. Miyasaka, An experimental-study of ion permeation in multicomponent ion systems as a function of membrane charge-density, *Journal Of Membrane Science* 64(3) (1991), p. 255-262.
15. Higa, M., A. Tanioka and A. Kira, A novel measurement method of donnan potential at an interface between a charged membrane and mixed salt solution, *Journal Of Membrane Science* 140(2) (1998), p. 213-220.
16. Firdaous, L., J.-P. Malériat, J.-P. Schlumpf and F. Quéméneur, Transfer of monovalent and divalent cations in salt solutions by electrodialysis, *Separation Science and Technology* 42(5) (2007), p. 931-948.
17. Sata, T., Studies on ion exchange membranes with permselectivity for specific ions in electrodialysis, *Journal Of Membrane Science* 93 (1994), p. 117-135.
18. Saracco, G., Transport properties of monovalent-ion-permselective membranes, *Chemical Engineering Science* 52(17) (1997), p. 3019-3031.
19. Larminie, J. and A. Dicks, Fuel cell systems explained, 2nd ed. 2003, West Sussex: John Wiley & Sons.
20. Dammak, L., C. Larchet and B. Auclair, Theoretical study of the bi-ionic potential and confrontation with experimental results, *Journal Of Membrane Science* 155 (1999), p. 193-207.
21. Strathmann, H., Ion-exchange membrane seperation processes, 1 ed. Membrane science and technology series. Vol. 9. 2004: Elsevier.
22. Długołęcki, P., D.C. Nymeyer, S.J. Metz and M. Wessling, Current status of ion exchange membranes for power generation from salinity gradients, *Journal Of Membrane Science* 319(1-2) (2008), p. 214-222.

Chapter 4

5 Prevention of biofouling by flow reversal in reverse electrodialysis stacks

Reverse electrodialysis is a conversion technique to obtain electricity from salinity gradients. Membrane fouling is a major threat for the feasibility of this technology, because of the extra costs that are a consequence of the fouling. Biofilm formation within the system is probably the most threatening fouling mechanism as it can not be prevented. In this study, we developed a setup in which the biofouling was accelerated by applying high concentrations of biodegradable substances (1.0 mg acetate-C/L). With this setup, we were able to study the effects of biofouling in reverse electrodialysis and the effectiveness of preventive measures under controlled conditions. It appeared that biofouling is primarily causing clogging of the flow channels and spacers. This clogging results in an increase of the energy losses for pumping. Cleaning with biocides or by feed water reversal (osmotic shocks) were applied but appeared to be not able to restore the system performances. It might well be that these measures inactivate the biofilm organisms, however, it did not improve the hydrodynamic resistance and electrical resistance when the inactivated biomass is left where it was. Preventive operational steps, such as a periodically applied feed water reversal (e.g., once per hour) combined with a flow direction reversal, hampered the biofouling significantly. Under worst case conditions as applied to accelerate the biofouling, the possible operational period increased from 5 days to 20 days. In order to answer the question if this can be considered as the final solution against biofouling in practice, the method of accelerated biofouling need to be validated with data from pilots. A combination of redesigned stacks, pre-treatment, additional operational measures, and cleaning procedures may be the way to restrict biofouling at minimum cost.

This chapter is submitted to Journal of Membrane Science

Post, J.W, S. Grasman, J.S. Vrouwenvelder, H.V.M. Hamelers, C.J.N. Buisman,
Prevention of biofouling by flow reversal in reverse electrodialysis stacks
for power generation, Journal of Membrane Science.

5.1 Introduction

5.1.1 Power generation from mixing sea water and river water

Sustainable electricity can be generated from mixing saline sea water and fresh river water by a process that is called ‘dialytic battery’ [1] or ‘reverse electrodialysis (RED)’ [2-4]. Although these expressions are adopted by the authors [5-7], these are not really felicitous terms for the process of direct conversion of free energy of mixing into electric power by means of an electrodialytic pile of ion-exchange membranes. The electrodialytic pile is not like a conventional ‘battery’ with internal energy storage, but more like a ‘flow battery’ or ‘fuel cell’. Electrolytes (river water and sea water) are fed continuously and chemical energy is converted to electricity [8]. This continuous feeding is especially important when pumping requirements and pretreatment are taken into account [1]. In that sense, the term ‘reverse electrodialysis’ is probably a better choice although it may give the impression that power generation with an electrodialytic pile is nothing more than just the reversed operation of an electrodialysis process. However, where electrodialysis is fed from one source (dilute and concentrate have the same origin), reverse electrodialysis is fed from two sources (river water and sea water) with their own specific characteristics. Moreover, the ionic-transport limitations, and thus the process conditions of interest, are different. An example of this is the limiting current for electrodialysis versus the short-circuit current for reverse electrodialysis. In electrodialysis, it is desirable to operate close to the limiting current density in order to get the maximum ion flux [9]. In reverse electrodialysis, it is desirable to operate at a considerable lower current density than the short-circuit current density in order to obtain a reasonable power density and energy recovery [5].

5.1.2 Effects of fouling on performance unknown

Fouling of ion-exchange membranes is considered to be one of the most important limitations for practical use of electrodialysis processes. It limits the competitiveness of the process due to an increase in costs resulting from an increased energy demand, additional labor for maintenance and chemical usage for cleaning as well as shorter membrane lifetime. From this point of view, it is not surprising that a lot is known about the effects of different types of fouling on the electrodialysis process [9-11], and specifically on the characteristics of the ion-exchange membranes [12-18]. However, little is known about the effects of fouling on the reverse electrodialysis process. Ratkje et al. [19], presented the preliminary study on the effect of biofilm formation in a reverse electrodialysis system. Results showed an enormous drop of >70% in power output during an operational period of 26 weeks. It was concluded that the economy of reverse electrodialysis will depend largely on if and how the effects of biofilm formation can be controlled.

From related membrane processes, it is recognized that Potential sources of fouling are: i) particles that may cause clogging of the spacers [11, 20], ii) inorganics that may cause scale formation [12, 21], iii) organic matter that may adsorb to the membrane surfaces [11, 22], iv) biodegradable substances that may be used as feed for microorganisms in the stack in order to grow a biofilm [11, 19], and v) multivalent or large organic ions that may poison the membranes [14, 17].

5.1.3 Objective

In this study we focused on biofouling, i.e., the negative effects of biofilm formation within the stacks on the performance. The purpose of our study was to investigate the effects of biofilm formation within the reverse electrodialysis stack on the efficiency in terms of stack resistance, stack

voltage, and pressure drop. As biofilm formation can not be prevented by any pretreatment process [23] and the use of supplied chemicals or reagents for fouling prevention or cleaning of the stacks should be limited for reasons of sustainability, our challenge was to find operational biofouling control methods that are available from the process itself.

5.2 Experimental

5.2.1 Experimental setup with accelerated biofilm formation

Three reverse electrodialysis stacks were run in parallel. These stacks were continuously fed with the 'sea water' and 'river water'. For making-up of these feed solutions pre-filtered ($> 1 \mu\text{m}$) tap water was used. The tap water was supplied at a temperature of 10-12 °C, without any disinfectant dosage or residual. Each feed stream contained three dosing points in series:

- Addition of brine to increase the sodium chloride concentration of the feed solutions to appropriate levels. For river water the sodium chloride concentration was controlled at 1 g/L, and for sea water at 30 g/L.
- Addition of a concentrated solution of biodegradable compounds. The main nutrient dosed to promote microbial growth was acetic carbon, supplemented by phosphate and nitrate in the m-based ratio of 100:10:20, as commonly found in biomass compositions. For both river water and sea water the sodium acetate concentration was controlled at 1.0 mg C/L. Sodium di-hydrogen phosphate was used as phosphate source and sodium nitrate as nitrate source. In order to prevent any microbial growth prior to the stacks, the pH of the nutrient solutions was leveled to pH 11 by adding sodium hydroxide and the dosing point was relatively close to the inlet of the stacks.

- Addition of inoculates to introduce the microorganisms that may form a biofilm in these salinities. For river water the inoculate was taken from the Van Harinxma Canal (city of Leeuwarden, The Netherlands), and for sea water from the Wadden Sea (harbour of Holwerd, The Netherlands).

The overpressure of the tap water was controlled by a pressure reducing valve at a level of approximately 0.5 bar. The feed flows through the stacks were controlled at 57.5 mL/min with upstream flow controllers (type FCA8842, Brooks Instruments). The pressure drop over the stacks was measured with differential pressure transmitters (type deltabar S PMD70, Endress+Hauser).

5.2.2 Reverse electrodialysis stacks and electrochemical setup

The three square stacks used in this study were identical to those previously described by the authors [6], consisting of four membrane pairs with a current-passing area of 104 cm². Between the membranes, spacers (Nitex 06-700/53, Sefar) were used with a thickness of 0.5 mm. However, a minor adaptation was made concerning the use of separate measurement compartments (*Figure 1*). The reference electrodes were placed within reservoirs that were connected to measurement compartments via Haber-Luggin capillaries. The tips of these capillaries were placed adjacent to the outside membranes (distance of 3 mm). This adaptation was made to prevent the measurement to be disturbed by (i) gaseous products from the working electrodes, (ii) depreciation of the outer membranes by chlorine formed at the anode, and (iii) bended current lines around the tips. Furthermore, the overpressure within the measurement compartments was controlled at 1 bar in order to get a homogeneous tightening of the electrodialytic pile (where the feed water inlets were controlled with an overpressure of 0.5 bar).

The working electrodes are separated from the measurement compartments by chlorine-resistant auxiliary membranes (Ralex cation-exchange membranes; Mega a.s. [7]). The working electrodes were connected to a galvanostat (IviumStat Electrochemical Interface & Impedance Analyser; Ivium Technologies). With the galvanostat a square-wave signal was generated with cycles of a 180 s period of zero current conditions (open circuit) followed by a 3,420 s period with an adjusted current level of 100 mA (i.e. a current density of 10 A/m²). The corresponding stack voltage was measured with an interval of 0.2 s.

After each experiment, the spacers were exchanged for new spacers and the biofilm on the membranes was wiped off with a wetted tissue.

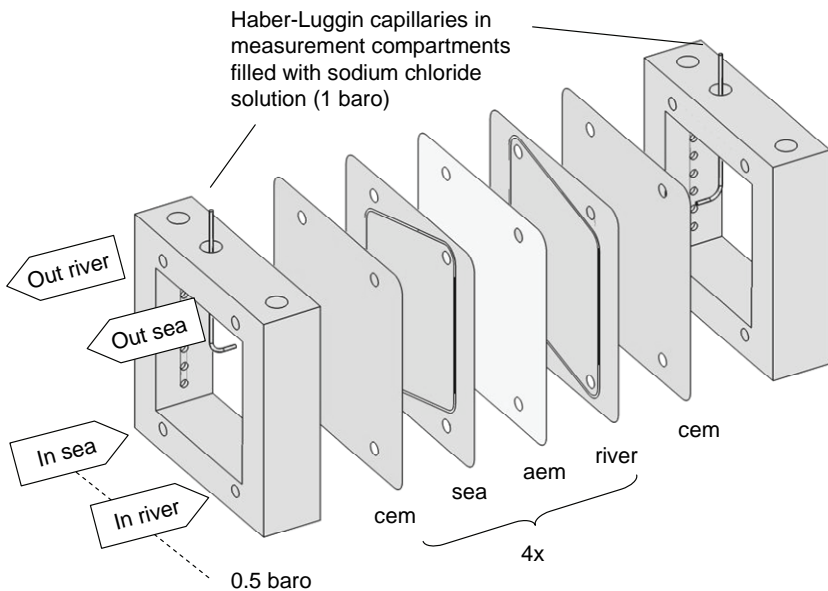


Figure 1: Conceptual representation of a reverse electrodialysis stack used in this study, with Haber-Luggin capillaries placed in measurement compartments; cem is cation-exchange membrane, aem is anion-exchange membrane; repetitive cell pair is drawn only once; auxiliary membranes and working electrodes are not included.

5.2.3 Determination of biomass on membranes and spacers

In order to characterize the accumulated biofouling, defined sections of membranes and spacers were stamped from different locations in the stack. Total organic carbon (TOC) was used as a sum parameter to determine the total biomass amount ($\mu\text{g}/\text{cm}^2$). The activity level of the present biomass was determined in terms of adenosine triphosphate (ATP) (ng/cm^2).

The membrane sections for the TOC analyses were placed in 25 mL of deionized water in capped tubes. The membrane sections for the ATP analyses were placed in 30 mL of autoclaved sea water or river water in capped tubes. For both biomass analyses, the biomass needed to be detached from the membranes and spacers. For the detachment step, an approved procedure of ultrasonic treatment and sonification was used [24]. The capped tubes were stored in ice until the ATP analysis was performed.

5.3 Results and discussion

5.3.1 Effects of biofouling

Effect on parasitic hydrodynamic losses. For membrane processes, biofouling is a term used to describe all instances of fouling where biologically active microorganisms are involved. This could vary from biofilm formation on the feed spacers, biofilm formation on the membrane surface or inside the membrane matrix, to biological degradation of the membranes. The effects of these fouling mechanisms on the performance of reverse electrodialysis would be different.

Due to the biofilm accumulation within the feed spacers, a build-up of the pressure drop may occur [25], comparable to the reported effect of colloidal fouling in a conventional electrodialysis system [11]. For reverse 124

electrodialysis, this clogging of the spacers may be seen as increased pressure drops from inlet to outlet of the stack for both sea water and river water. In our experiment with accelerated biofilm formation, the three stacks showed the same development of pressure drop in time. The pressure drop over the river water compartments increased after 8 days (*Figure 2A*). The salt water side had an operational period that was 5 days longer before the pressure-drop increase occurred (*Figure 2B*), although the growth potentials, expressed in the amount of biodegradable components, is the same for the fresh and salt water side. This difference is probably caused by a lower concentration of microorganisms in the salt water which leads to a lower rate of primary colonization of the stacks internal surface and thereby a slower build-up of biomass [23]. In general, the pressure drop build-up graphs with an exponential rise after a certain operational period are similar to that observed in previous studies with membrane fouling simulators [26].

During sampling and disassembling the stacks after the experiments, it became clear that a biofilm was formed on membranes and spacers. The pressure drop increase can clearly be correlated to the build-up of biomass, *Figure 3A*. The build-up of biomass appeared to be slightly higher at the inlet than at the outlet. At the end of the experiment, after the maximum pressure drop was reached and the feed flow started to decrease, the activity level of the biomass near the outlet appeared to be low (*Figure 3B*). A possible explanation would be that the biomass near the outlet has faced nutrient shortage due to a combination of the starting hydrodynamic failure (e.g., preferential flow paths) and consumption by the preceding biomass.

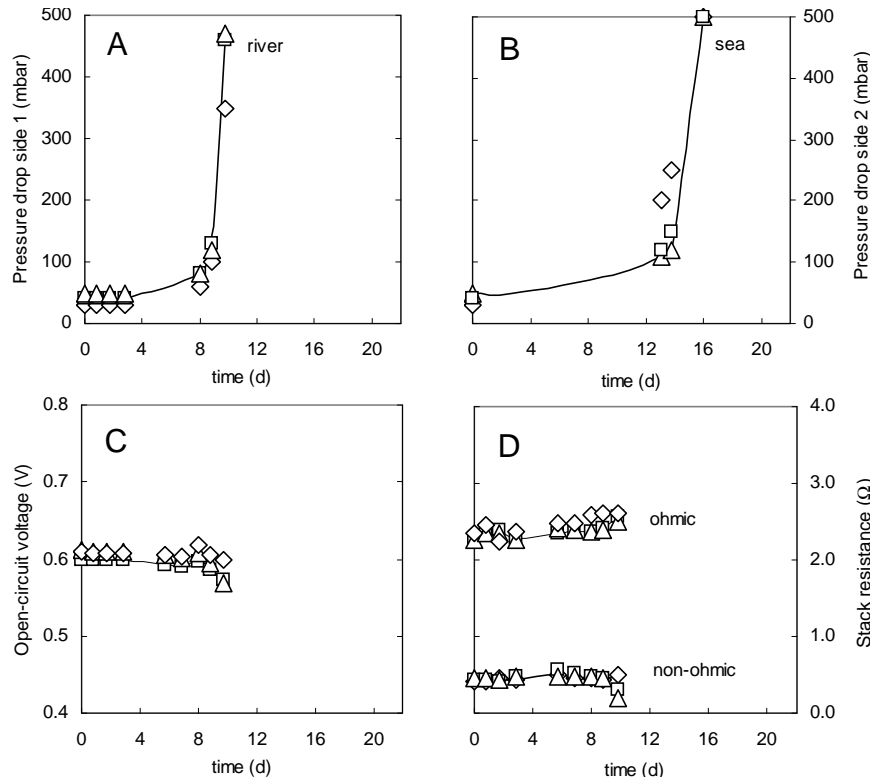


Figure 2: Performances of three parallel stacks: the pressure drops over the feed spacers of the river water compartments (A) and the sea water compartments (B), the open-circuit voltage (C), and the stack resistance (D). The stacks (indicated with symbols \triangle , \diamond , and \square) were operated in parallel under same conditions.

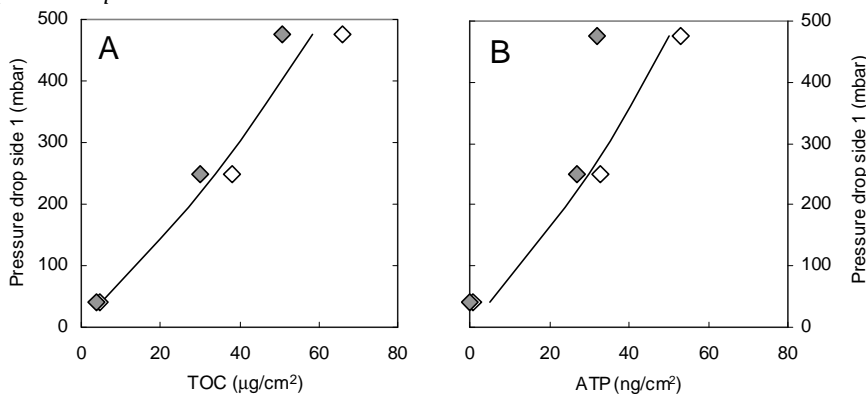


Figure 3: Pressure drop over the river water compartment correlated (A) to the amount of biomass (total organic carbon, TOC in $\mu\text{g}/\text{cm}^2$) and (B) to the activity of the biomass (adenosine triphosphate, ATP in ng/cm^2). Open symbols represent samples taken at the inlet, closed symbols represent samples taken at the outlet.

Effect on thermodynamic efficiency. Microorganisms composing biofilms may directly (via enzymes) or indirectly (via localized pH or redox potential changes) degrade the membrane polymer [27]. If the membranes either foul or decompose during operation, it would mean both a decrease in selectivity and an increase in electrical resistance of the membranes [28]. For reverse electrodialysis, this membrane degradation may be mainly observed as a decreased open-circuit voltage (and a higher stack resistance, as was suggested by Ratkje et al. [19]). The open-circuit voltage in our experiment with accelerated biofilm formation (*Figure 2C*) seemed to be slightly affected after 8 days, i.e., when the rapid increase of the pressure drop occurred at the fresh water side. Likely, the stack was subject to minor internal leakage from the fresh water manifolds to the sea water compartments due to pressure differences over the membrane, or due to salinity gradients within the fouled fresh water compartments, but not due to failure of the membranes. This was confirmed after the experiment had finished as in the next experiment the open-circuit voltage was restored after spacers were replaced and membranes were wiped. After 10 days, i.e., when the pressure drop reached the maximum of 500 mbar and the fresh water flow could no longer be maintained at the same level. Due to this failure of feed water supply, the open-circuit voltage decreased (data not shown in *Figure 2C*).

Effect on ohmic and non-ohmic losses. Besides due to possible membrane degradation, the electrical resistance of a stack could also be increased due to an additional insulating effect of the biofilms adhered to the spacers [6]. For reverse electrodialysis, this additional insulating effect of fouled spacers may be observed as an increased ohmic resistance. In our experiment with accelerated biofilm formation, the ohmic resistance seemed to be slightly increased after 8 days (*Figure 2D*), which again could be explained by mechanic or hydrodynamic failure of the dialytic pile. After

10 days, the ohmic resistance changed due to the decreasing flow of fresh water (data not shown in *Figure 2D*).

As the biofilm comprised not only of single bacteria but also a matrix of EPS, the solutes now have to diffuse through the tortuous path of the deposit [29]. The EPS matrix suppresses turbulent mixing at the membrane surface [27], resulting in enhanced concentration polarization [9, 19, 25]. For reverse electrodialysis, this additional concentration polarization may be observed as an increased non-ohmic resistance. The non-ohmic resistance, however, seemed to be unaffected and even slightly lower just before the feed flows cannot longer be maintained (*Figure 2D*).

5.3.2 Cleaning of stacks

Cleaning with a single reversal of feed waters. After the stacks were fouled, a few cleaning attempts were performed. The first cleaning procedure was a simple reversal of feed waters (during 2 days), followed by a back flush (of 1 day). Microorganisms from a freshwater habitat are exposed to marine conditions, and vice versa. These microorganisms would get a hyper-osmotic shock, or a hypo-osmotic shock, respectively. Only the hyper-osmotic shock is described as cleaning method for reverse osmosis. When water is sucked out from the bacterial cell by osmosis, the cell membranes shrink. This shrinkage may cause the detachment of the microorganisms from the membrane surface [30].

From *Figure 4* can be concluded that indeed a small reduction of the biomass amount (*Figure 4A*) and its activity (*Figure 4B*) can be achieved. However, after the cleaning the pressure drop was not improved at all (data not shown in a figure). Probably, the cleaning was not effective on spots where EPS enhances the survival and robustness of the biofilm microorganisms [27]. Although not effective as a cleaning method, from *Figure 4* it can be concluded that a *periodical* feed water reversal in a

reverse electrodialysis would have a potential retarding effect on the biofilm formation. Experimental results with a periodical reversal are described in next paragraph as a potential preventive operational measure against biofouling.

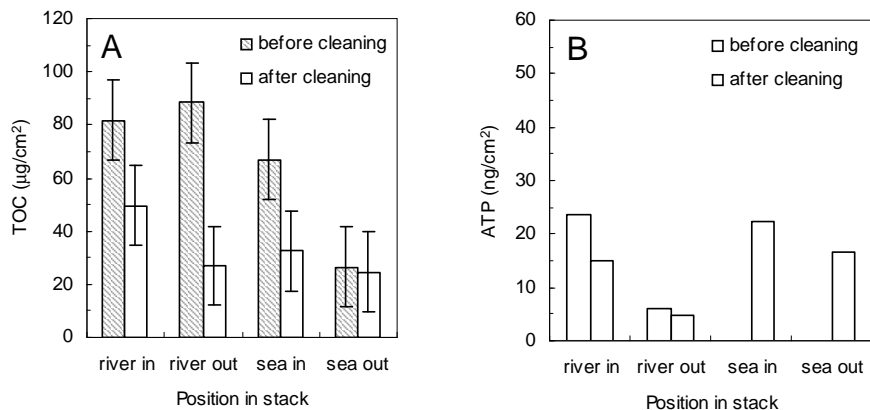


Figure 4: (A) Amount of biomass (total organic carbon, TOC in $\mu\text{g}/\text{cm}^2$) and (B) the activity of biomass (adenosine triphosphate, ATP in ng/cm^2) on membrane and spacer, before and after cleaning with flow reversal.

Chlorine treatment. The second cleaning attempt was performed with 500 ppm sodium hypochlorite at pH 13. Removing a biofilm from a membrane is commonly done with the use of anti-microbial chemicals [31-33]. To clean the membranes and restore the process performance the biomass has to be physically removed [32], in general a two step cleaning strategy is used [31]; first weakening of the biofilm matrix using chemicals (oxidants, enzymes, etcetera) and then the removal of the biofilm using mechanical forces. Liu et al. [33] concluded that caustic and oxidants or a combination of both has the best cleaning effect. The chemicals commonly used in these categories are sodium hydroxide, sodium hypochlorite, peroxide and peroxyacetic acid. The reverse electrodialysis process has the

advantage that the needed chemicals can be produced at the electrodes, e.g., chlorine and acid at the anode and base at the cathode [4].

After half an hour of flushing, the pressure drop decreased from 500 mbar to 100 mbar for the river water compartments, and to 165 mbar for the sea water compartments (data not shown in a figure). The open-circuit voltage was totally recovered. However, the stack resistance was twice higher when compared to the resistance of a clean stack. A possible explanation is the formation of preferential flow paths during cleaning that on the one hand enables a relative low friction loss and a restoration of membrane potentials, but on the other leaves entire regions of membranes and compartments blocked for diffusional and convective transport [34].

5.3.3 Preventive operational measures

Periodical reversal of salt and fresh water. From the cleaning attempts, it can be concluded that the prevention of biofouling by control strategies is preferable over cleaning. A possible control strategy is a periodical reversal of feed streams and consequently of polarity of the stack. The periodical reversal of feed streams for fouling prevention is a well-known measure in electrodialysis which is applied already from the 1950s for groundwater and surface water desalination and waste water reclamation [11, 35]. Allison [11] reported that in 1995 there were six electrodialysis reversal processes in operation on wastewater and none of these faced problems due to biofouling. It was claimed that due to the reversal, the electrodialysis process can withstand water with high concentrations of organic substances, colloidal particles and microorganisms.

Regarding reverse electrodialysis, the cleaning mechanism of a reversal would work in two different ways. Firstly, like in electrodialysis, the electric current is the driving force for the deposition of charged particles. When a current reversal is applied, the driving force for the deposition

changes and thereby would hinder the initial deposition of (negatively charged) microorganisms and would (partially) remove the deposited microorganisms. Secondly, additional to this, the bio-osmotic shock would occur as discussed in previous paragraph.

From *Figure 5A-B* can be seen that the operational period of the stacks before the pressure-drop rise increased with increasing reversal frequency. In next experiment with accelerated biofilm formation, the operational period of the stack without a feed water reversal was limited to 5 days by the pressure drop increase over the river water compartments (8 days for sea water compartments). For the stack with a reversal each twenty-four hours, the operational period before the pressure-drop increase was 14 days. This proofs that the periodical reversal has a beneficial effect and that the extension of the operational period is not simply a matter of a different distribution of biomass. In that case, one would expect the operational period before a pressure-drop rise to be in the range of 7-10 days only, i.e., between the average growth potentials of both feed streams (average of 5 and 8 days) and twice the growth potential of river water (2 times 5 days). Moreover, the cleaning effect of a periodical feed water reversal can be seen from the hitches in the pressure-drop curves (*Figure 5A-B*, stack \diamond).

For the stack with a reversal each hour, the operational period before pressure-drop rise was 17 days (*Figure 5A-B*). Except for one data-point, the build-up of pressure drop seemed to be smoother when compared to that of the stack with the twenty-four hourly reversal. This indicates that at a higher frequency the reversal works becomes more a preventive step and less reliant on the cleaning effect. However, an increase of the frequency would probably not feasible in practice as each feed water switch is associated with a period of sub-optimal power production.

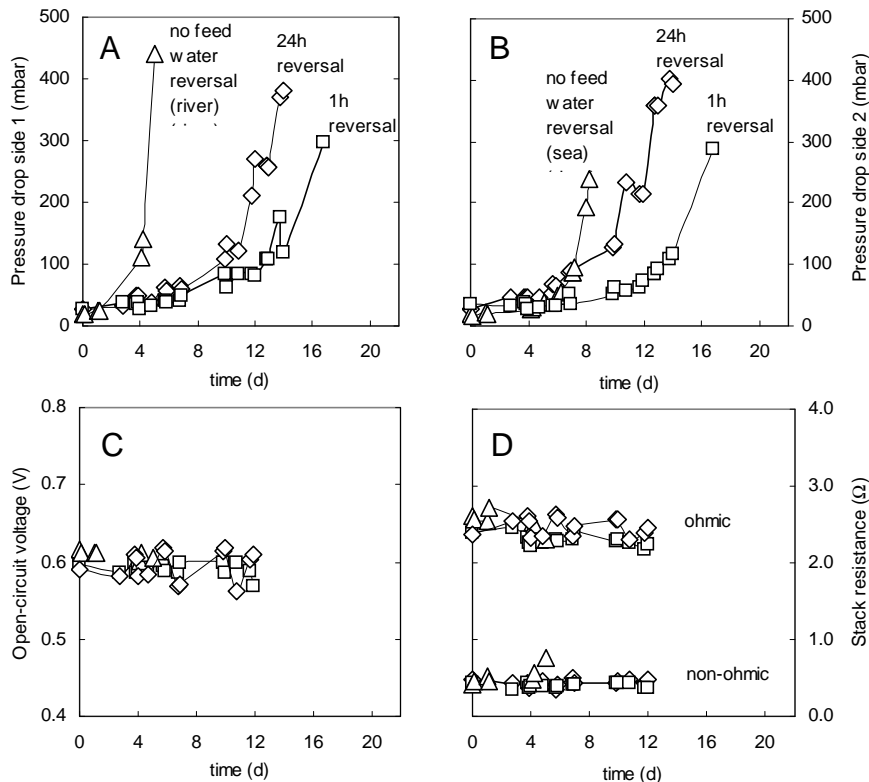


Figure 5: Performances of three parallel stacks: the pressure drops over the feed spacers of the compartments of side 1 (A) and the compartments of side 2 (B), the open-circuit voltage (C), and the stack resistance (D). The stacks faced same circumstances but were operated differently: \triangle without feed water reversal, \diamond with a daily feed water reversal, and \square with an hourly feed water reversal.

The open-circuit voltages of the stacks with the periodical reversal were less stable than of the stack without reversal (Figure 5C). This could be explained by the appearance of zones in the stack where the exchange of feed waters by convection is not effective in changing the salt concentrations. A locally lower salinity gradient decreases the open-circuit voltage of the stack. This may well explain the fact that the stack with the daily reversal is less stable than the stack with the hourly reversal. The more rapid build-up of biomass in the stack with the daily reversal would

increase the heterogeneity of the flow distribution and thus a lower open-circuit voltage. Another point of concern is the fact that the membrane potentials would become less stable due to the fast changes of concentrations (an equilibration period of twenty-four hours is minimal [36]) and compositions of feed streams [37].

The stack resistance of the stacks with feed water reversal decreased slightly during the experiment (*Figure 5D*). This may also be explained by an ineffective exchange of feed waters. When river water compartments locally have a higher salinity, the ohmic resistance of the stack could get lower. In that case, a worsening of the water distribution due to biofouling and thus the effectiveness of feed water exchange would lead to a decrease in stack resistance as can be observed in this experiment.

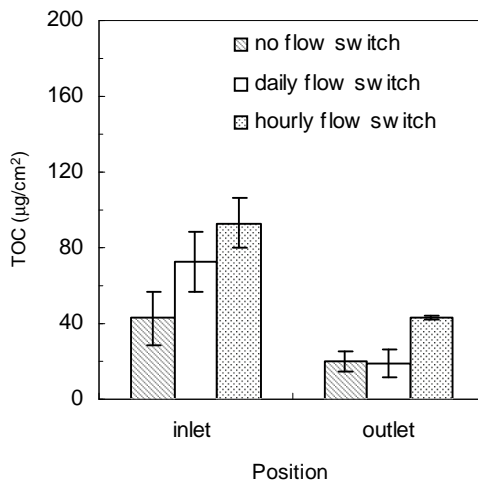


Figure 6: TOC concentrations on membrane and spacer after experiment of Figure 5 for the stack without feed water reversal, with a daily feed water reversal, and with an hourly feed water reversal.

At the end of the experiment, the determination of the biomass was solely based on TOC (*Figure 6*), since especially the stack without reversal and the stack with daily reversal suffered from almost complete blockage of the stack at the end of the experiment. Consequently, the biofilm was exposed to nutrient depletion, which had resulted in a dead biofilm. It was expected that the final amount of TOC would not show a relation with the feed water reversal frequency, since all three the stacks suffered from the same hydraulic resistance in the end. However, *Figure 6* clearly shows that the final amount of TOC increases with increasing reversal frequencies. Apparently, the major effect of the feed water reversal is not on the biofilm development, but on the stacks capability to function well with larger amounts of biofilm on the membranes. This is in line with Allison [11] and Chao and Lang [35], they reported that electrodialysis reversal could cope with water with a higher fouling potential compared to normal electrodialysis.

Periodical reversal of salt and fresh water and change of flow direction. In general, all measures against biofouling are suffering the same problem. It might well be that a measure kill the biofilm organisms, however, it does not help to improve the hydrodynamic resistance and electrical resistance when the inactivated biomass is left where it was [23]. Moreover, it may well be that the remnants of the fouling layer can serve as substrate for new biofilms. As it is recognized that biofouling generally occurs near the inlet of the membrane system [26], a periodical flow direction reversal (i.e., a reversal of inlets and outlets) would be an essential step to flush the residues of the inactivated biofilm out of the stack.

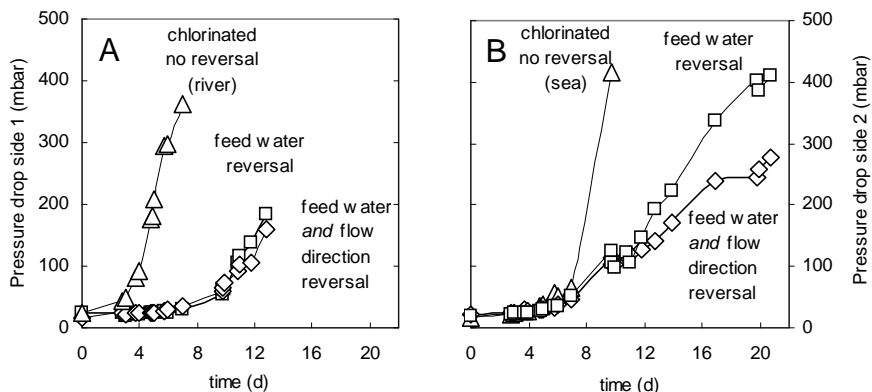


Figure 7: Performances of three parallel stacks: the pressure drops over the feed spacers of the compartments of side 1 (A) and the compartments of side 2 (B); figures for the open-circuit voltage and the stack resistance are not shown as they are comparable to that of Figure 5. The stacks faced same circumstances but were operated differently: \triangle with 50 ppb chlorine addition (without feed water reversal), \square with an hourly feed water reversal (without flow direction reversal), \diamond with an hourly feed water reversal and flow direction reversal.

In next experiment with accelerated biofilm formation, two stacks were operated with an hourly feed water reversal as described in previous experiment, but for one stack also the inlet and outlet were exchanged at each switch event. From Figure 7A-B (stacks \square and \diamond) can be seen that this flow direction reversal hardly had an additional effect. Once the biomass gets a certain density (i.e., at a higher pressure drop), small differences were occurring. From sampling afterwards, it can be concluded that the amount of biomass was the same for both systems. Apparently, the intended wash-out of inactivated biomass was not successfully applied.

Although the amount of biomass was the same for both systems, the distribution was different (Figure 8). For the stack with the one-directional feeding, the biomass build-up was as expected, i.e., a high amount near the inlet and a decreasing amount with increasing distance from the inlet. For the stack with the periodical counter-flow, the biomass build-up showed to be higher at the inlets/outlets and lower in the middle. This different

distribution over the stack length could count for the slightly better performances of the latter. In general, during sampling membranes and spacers were not separated. By occasion, also samples were taken from a membrane only (without spacer). It seemed that less biomass was attached to the membrane than to the spacer. Besides this, the distribution of the biomass on the membrane appeared be more homogeneous than on the spacer but this could well be due to an observed imprint of the spacer on the biofilms on the membrane surface. From pressure drop measurements, from the fact that washout of biomass is not straightforward, together with the observation that the majority of the biomass is attached to the spacer, the conclusion can be drawn that the development of reverse electrodialysis should be in the direction of another hydrodynamic design that is not based on screen spacers (see next paragraph).

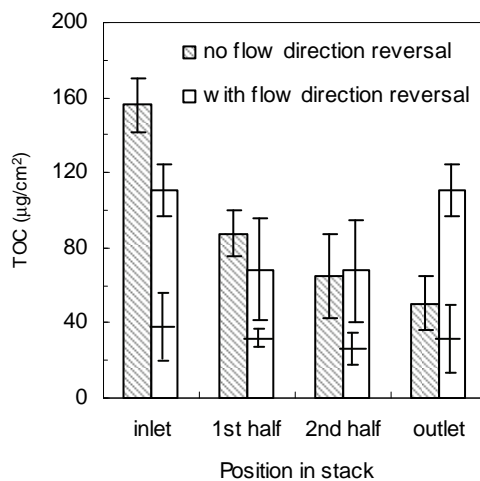


Figure 8: TOC concentrations on membrane and spacer after experiment of Figure 7 for the stack with an hourly feed water reversal (no flow direction reversal) and the stack with an hourly feed water reversal and flow direction reversal. For the latter, a division was made for biomass attached to the membrane (lower part of the blank bars) and the total biomass attached to the membrane and the spacer (total blank bars).

Continuous chlorine addition. Grossman and Sonin [9] reported the use of alkaline or basic solutions as a remedy against biofouling in electrodialysis. The usual approach is to continuously dose biocides to kill the bacteria or to suppress the bacterial activity [31], with chlorine as the most common biocide [23, 33]. The hypochlorite formed at the anode could be used for this purpose. Acid and base can also be produced at the anode and the cathode, respectively, or within the membrane pile by using bipolar membranes as proposed by Zholkovskij et al. [38]. However, it can be calculated that chlorine addition to the feed streams would be in the ppb-scale which is out of range when compared to usual chlorine additions of 0.1-1 ppm [27]. Indeed, in our experiments it appeared that 50 ppb chlorine addition was not effective to prevent a rapid increase of the pressure drop (*Figure 7*, stack Δ).

5.4 Outlook

Impact. In this study, we developed a setup in which the biofouling was accelerated by applying high concentrations of biodegradable substances (1.0 mg acetate-C/L) to the feed waters. With this setup, we were able to study the effects of biofouling in reverse electrodialysis and the effectiveness of preventive measures under controlled conditions. However, in order to answer the question if these measures can be considered as the final solutions against biofouling in practice, the method of accelerated biofouling need to be validated with data from experiences in the field (e.g., from pilot studies).

Redesign of stacks. This study demonstrated that cleanings were not effective in restoring the original performances. Reversal of flows, however, extended significantly the possible operational period before a pressure-drop rise. In practice, a combination of redesigned stacks, pre-treatment, operational measures, and cleaning procedures may be the way to restrict biofouling at minimum cost.

The design of experimental reverse electrodialysis stacks [39] is still based on the common stack design of electrodialysis with the use of screen spacers. These screen spacers, however, were identified not only as undesired insulators [6] and cause of relatively high friction losses [39], but in this study also as a place for biofilm accumulation. Therefore, the reverse electrodialysis stack should be redesigned towards a more robust spacer-less system, using the developed computational fluid dynamics model for flat sheet membrane configurations [40]. One might think not so much in the direction of corrugated membranes as proposed by Brauns [41] but more in the direction of integrated flow paths with a more open design and with fewer crevices for physical entrapment of solids [11].

Pre-treatment. Although a redesigned stack with flow paths would be less sensitive to fouling, reverse electrodialysis still requires a filtration step to prevent the stacks from clogging. Biofilm formation can not be prevented by filtration [23], but several studies showed that nutrient control by biological filtration can be effective to reduce the effects of biofouling [24, 42].

Additional operational measures. Additional operational measures and cleaning procedures need to be investigated in practical situations as these certainly have a beneficial effect on the performance. For instance, detachment of biofilms (and other foulants) can also be achieved by a periodically applied electrical back-pulse [43, 44]. This back-pulse can be generated within the reverse electrodialysis system itself, e.g., by charging and discharging capacitors in the electrical circuit in a much higher frequency and amplitude than possible with a periodical feed flow reversal as discussed previously. Therefore, a pulsed reversed current is probably able to prevent the initial deposition of (charged) microorganisms [44].

Acknowledgements

This work was performed at Wetsus, centre of excellence for sustainable water technology. Wetsus is funded by the ministry of economic affairs. The authors like to thank the members of the theme 'Energy' from Wetsus for the fruitful discussions and especially the participating companies Nuon, Eneco, Magneto, Landustrie, Frisia Zout, Triqua, Dow Chemical, and Fuji for their support.

5.5 References

1. Weinstein, J.N. and F.B. Leitz, Electric-power from difference in salinity - dialytic battery, *Science* 191(4227) (1976), p. 557-559.
2. Audinos, R., Reverse electrodialysis - study of the electrical energy obtained from 2 solutions of different salinity, *Journal Of Power Sources* 10(3) (1983), p. 203-217.
3. Lacey, R.E., Energy by reverse electrodialysis, *Ocean Engineering* 7(1) (1980), p. 1-47.
4. Jagur-Grodzinski, J. and R. Kramer, Novel process for direct conversion of free-energy of mixing into electric-power, *Industrial & Engineering Chemistry Process Design And Development* 25(2) (1986), p. 443-449.
5. Post, J.W., J. Veerman, H.V.M. Hamelers, G.J.W. Euverink, S.J. Metz, D.C. Nijmeijer and C.J.N. Buisman, Salinity-gradient power: Evaluation of pressure-retarded osmosis and reverse electrodialysis, *Journal of Membrane Science* 288 (2007), p. 218-230.
6. Post, J.W., H.V.M. Hamelers and C.J.N. Buisman, Energy recovery from controlled mixing salt and fresh water with a reverse electrodialysis system, *Environ Science Technology* 42 (2008), p. 5785-5790.
7. Veerman, J., J.W. Post, S.J. Metz, M. Saakes and G.J. Harmsen, Reducing power losses caused by ionic shortcut currents in reverse electrodialysis stacks by a validated model, *Journal of Membrane Science* (310) (2008), p. 418-430.
8. Larminie, J. and A. Dicks, Fuel cell systems explained, 2nd ed. 2003, West Sussex: John Wiley & Sons.
9. Grossman, G. and A.A. Sonin, Membrane fouling in electrodialysis: A model and experiments, *Desalination* 12 (1973), p. l07- I25.
10. Van der Hoek, J.P., D.O. Rijnbende, C.J.O. Lokin, P.A.C. Bonné, M.T. Loonen and M.H. Hofman, Electrodialysis as an alternative for reverse osmosis in an integrated membrane system, *Desalination* 117 (1998), p. 159-172.
11. Allison, R.P., Electrodialysis reversal in water reuse applications, *Desalination* 103(1-2) (1995), p. 11-18.
12. Atamanenko, I., A. Kryvoruchko and L. Yurlova, Study of the scaling process on membranes, *Desalination* 167(1-3) (2004), p. 327-334.
13. Bazinet, L., D. Ippersiel, D. Montpetit, B. Mahdavi, J. Amiot and F. Lamarche, Effect of membrane permselectivity on the fouling of cationic membranes during skim milk electroacidification, *Journal Of Membrane Science* 174(1) (2000), p. 97-110.

Chapter 5

14. De Körösy, F. and E. Zeigerson, Breakthrough of poisoning multivalent ions across a permselective membrane during electrodialysis, *Journal of Physical Chemistry* 71(11) (1967), p. 3706-3709.
15. Lee, H.J., J.H. Choi, J.W. Cho and S.H. Moon, Characterization of anion exchange membranes fouled with humate during electrodialysis, *Journal Of Membrane Science* 203(1-2) (2002), p. 115-126.
16. Lee, H.J., D. Kim, J. Cho and S.H. Moon, Characterization of anion exchange membranes with natural organic matter (nom) during electrodialysis, *Desalination* 151(1) (2003), p. 43-52.
17. Lindstrand, V., A.S. Jonsson and G. Sundstrom, Organic fouling of electrodialysis membranes with and without applied voltage, *Desalination* 130(1) (2000), p. 73-84.
18. Lindstrand, V., G. Sundstrom and A.S. Jonsson, Fouling of electrodialysis membranes by organic substances, *Desalination* 128(1) (2000), p. 91-102.
19. Ratkje, S.K., T. Holt and L. Fiksdal. Effect of biofilm formation on salinity power plant output on laboratory scale, in *Industrial Membrane Processes* (Aiche Symposium Series). 1986.
20. Lee, H.J. and S.H. Moon, Influences of colloidal stability and electrokinetic property on electrodialysis performance in the presence of silica sol, *Journal Of Colloid And Interface Science* 270(2) (2004), p. 406-412.
21. Bazinet, L. and M. Araya-Farias, Effect of calcium and carbonate concentrations on cationic membrane fouling during electrodialysis, *Journal Of Colloid And Interface Science* 281(1) (2005), p. 188-196.
22. Kim, D., S.H. Moon and J. Cho, Investigation of the adsorption and transport of natural organic matter (nom) in ion-exchange membranes, *Desalination* 151(1) (2003), p. 11-20.
23. Flemming, H.C., G. Schaule, T. Griebel, J. Schmitt and A. Tamachkiarowa, Biofouling - the achilles heel of membrane processes, *Desalination* 113 (1997), p. 215-225.
24. Vrouwenvelder, J.S., S.A. Manolarakis, J.P. van der Hoek, J.A.M. van Paassen, W.G.J. van der Meer, J.M.C. van Agmaal, H.D.M. Prummel, J.C. Kruithof, and M.C.M. van Loosdrecht, Quantitative biofouling diagnosis in full scale nanofiltration and reverse osmosis installations, *Water Research* (42) (2008), p. 4856-4868.
25. Tanaka, Y., Ion exchange membranes: Fundamentals and applications. *Membrane science an technology series*. Vol. 12. 2007, Amsterdam: Elsevier. 531.
26. Vrouwenvelder, J.S., C. Hinrichs, A.R. Sun, F. Royer, J.A.M. Van Paassen, S.M. Bakker, W.G.J. Van der Meer, J.C. Kruithof, and M.C.M. Van Loosdrecht, Monitoring and control of biofouling in nanofiltration and reverse osmosis membranes, *Water Science & Technology: Water Supply* 8.4 (2008), p. 449-458.
27. Ridgway, H.F., Membrane biofouling, in *Water treatment membrane processes*, J. Mallevialle, P.E. Odendaal, and M.R. Wiesner, Editors. 1996, American Water Works Association, McGraw-Hill Inc.
28. Hansen, H.K., L.M. Ottosen and A. Villumsen, Electrical resistance and transport numbers of ion-exchange membranes used in electrodialytic soil remediation, *Separation Science and Technology* 34(11) (1999), p. 2223-2233.
29. Chong, T.H., F.S. Wong and A.G. Fane, The effect of imposed flux on biofouling in reverse osmosis: Role of concentration polarisation and biofilm enhanced osmotic pressure phenomena, *Journal of Membrane Science* 325 (2008), p. 840-850.
30. Fritzmann, C., J. Löwenberg, T. Wintgens and T. Melin, State-of-the-art of reverse osmosis desalination, *Desalination* 216 (2007), p. 1-76.
31. Flemming, H.C., Reverse osmosis membrane biofouling, *Experimental Thermal and Fluid Science* 14 (1997), p. 382-391.

32. Cornelissen, E.R., J.S. Vrouwenvelder, S.G.J. Heijman, X.D. Viallefont, D. Van der Kooij and L.P. Wessels, Periodic air/water cleaning for control of biofouling in spiral wound membrane elements, *Journal of Membrane Science* 287 (2007), p. 94-101.
33. Liu, C., S. Caothien, J. Hayes, T. Caothuy, T. Otoyo and T. Ogawa, Membrane chemical cleaning: From art to science. 2008 (access date 2009-01-28), Scientific and Laboratory Services, Pall Corporation: Port Washington, available from www.pall.com/pdf/mtcpaper.pdf.
34. Graf von der Schulenburg, D.A., J.S. Vrouwenvelder, S.A. Creber, M.C.M. Van Loosdrecht and M.L. Johns, Nuclear magnetic resonance microscopy studies of membrane biofouling, *Journal of Membrane Science* 323 (2008), p. 37-44.
35. Chao, Y.M. and T.M. Liang, A feasibility study of industrial wastewater recovery using electrodialysis reversal, *Desalination* 221 (2008), p. 433-439.
36. Długołęcki, P., D.C. Nymeyer, S.J. Metz and M. Wessling, Current status of ion exchange membranes for power generation from salinity gradients, *Journal Of Membrane Science* 319(1-2) (2008), p. 214-222.
37. Post, J.W., H.V.M. Hamelers and C.J.N. Buisman, Influence of multivalent ions on power production from mixing salt and fresh water with a reverse electrodialysis system, *Journal of Membrane Science* 330 (2009), p. 65-72.
38. Zholkovskij, E.K., M.C. Müller and E. Staude, The storage battery with bipolar membranes, *Journal of Membrane Science* 141 (1998), p. 231-243.
39. Veerman, J., M. Saakes, S.J. Metz and G.J. Harmsen, Reverse electrodialysis: Performance of a stack with 50 cells on the mixing of sea and river water., *Journal Of Membrane Science* 327 (2008), p. 136-144.
40. Dirkse, M.H., W.P.K. van Loon, J.D. Stigter, J.W. Post, J. Veerman and G.P.A. Bot, Extending potential flow modelling of flat-sheet geometries as applied in membrane-based systems, *Journal Of Membrane Science* 325 (2008), p. 537-545.
41. Brauns, E., Salinity gradient power by reverse electrodialysis: Effect of model parameters on electrical power output, *Desalination* 237 (2009), p. 378-391.
42. Griebel, T. and H.C. Flemming, Biocide-free antifouling strategy to protect ro membranes from biofouling, *Desalination* 118 (1998), p. 153-156.
43. Lee, H.J. and S.H. Moon, Enhancement of electrodialysis performances using pulsing electric fields during extended period operation, *Journal of Colloid and Interface Science* 287 (2005), p. 597-603.
44. Lee, H.J., S.H. Moon and S.P. Tsai, Effects of pulsed electric fields on membrane fouling in electrodialysis of nacl solutions containing humate, *Separation and Purification Technology* 27 (2002), p. 89-95.

5 Appendix: Pulsed reversed currents

Introduction

Additional operational measures and cleaning procedures need to be investigated in practical situations as these certainly have a beneficial effect on the performance. In chapter 5 it was mentioned that detachment of biofilms (and other foulants) may also be achieved by a periodically applied electrical back-pulse [43, 44]. This back-pulse can be generated within the reverse electrodialysis system itself, e.g., by charging and discharging capacitors in the electrical circuit in a much higher frequency and amplitude than possible with a periodical flow-switch as discussed previously in chapter 5. Therefore, a pulsed reversed current is probably able to prevent the initial deposition of (charged) microorganisms [44]. In order to prove this hypothesis, we performed experiments with and without electric back-pulse.

Experimental

Two stacks were run in parallel, one with and one without an electric back-pulse. These flow cells were continuously fed with ‘river water’ and ‘sea water’. A comparable methodology was used as in chapter 5 to accelerate the biofilm formation, except that in this experiment 0.2 mg acetate-C/L was dosed instead of 1.0 mg acetate-C/L), supplemented by phosphate and nitrate in the ratio of 100:10:20 (m-base).

In a first experiment, a square-wave signal was generated with a back-pulse of 2 ms per 1 s with amplitude of 75 A/m² (i.e., 7.5 times the operational current density of 10 A/m²), see Figure 9. The power density during the pulse is -25 W/m². The related energy loss in practice would 142

thus be 2-4% (in the experiment it is about 10%). In a second experiment, the back-pulse was 5 times longer, i.e., 10 ms per 1 s. The latter was applied for scientific reasons to prove the concept.

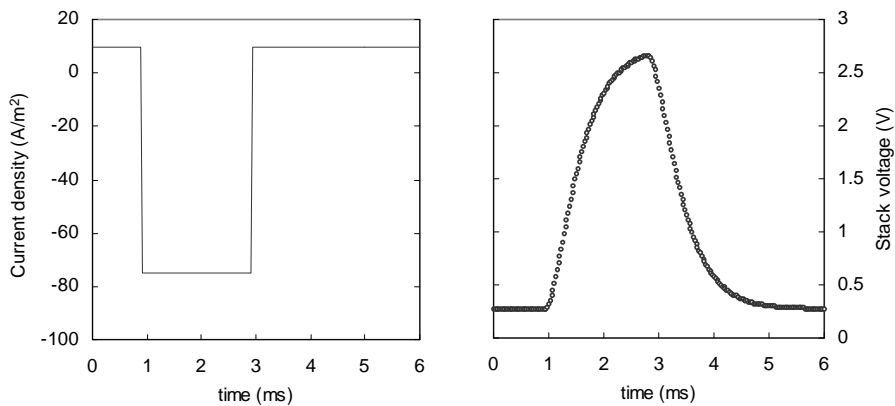


Figure 9. Electric back-pulse of 2 ms per 1 s with a current density of 75 A/m² (left) and the stack voltage response (right).

Results and discussion

In both cases, the electric backpulse had a small effect on the operational period before the pressure-drop rise (Figure 10 and Figure 11). It should be noticed that the electric backpulse would only work on the active (current-passing) membrane area and not near the inlets of the compartments. In other words, in the current design (as in all designs for electrodialysis stacks) this method would not be effective to prevent biofouling near the inlet.

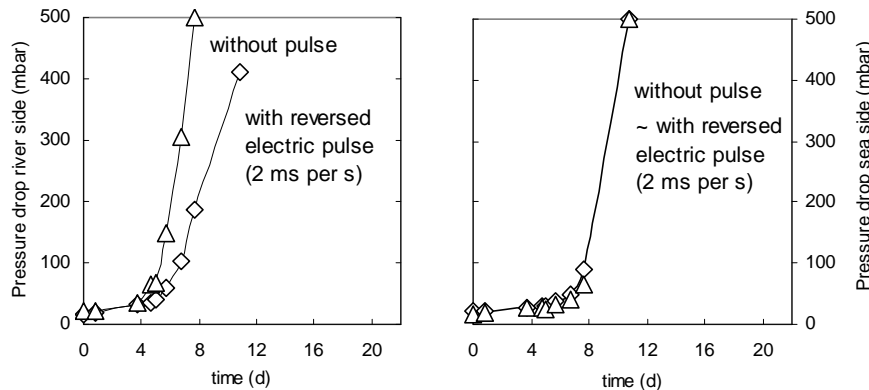


Figure 10. Pressure drops over the 0.5 mm feed channels with river water (left), and with sea water (right), for stack without an electric backpulse \triangle and with an electric backpulse of 2 ms per s \diamond .

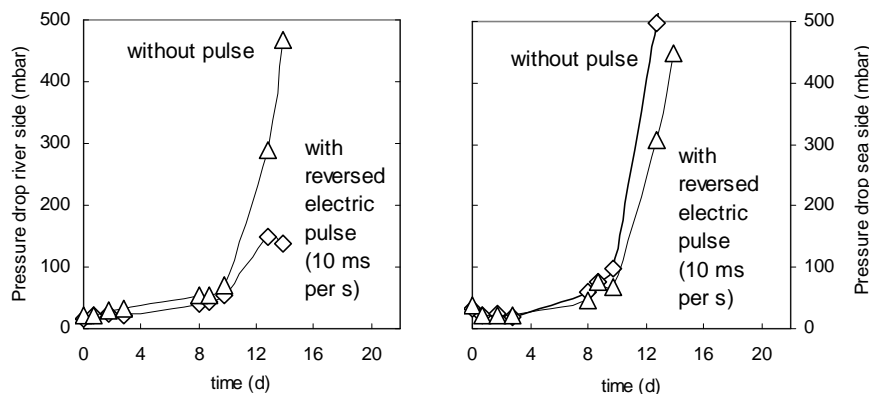


Figure 11. Pressure drops over the 0.5 mm feed channels with river water (left), and with sea water (right), for stack without an electric backpulse \triangle and with an electric backpulse of 10 ms per s \diamond .

The question, therefore, was whether this method was effective to hamper biofilm formation on the active membrane area. From sampling afterwards, however, no differences in amount nor distribution of attached biomass was observed (Figure 12).

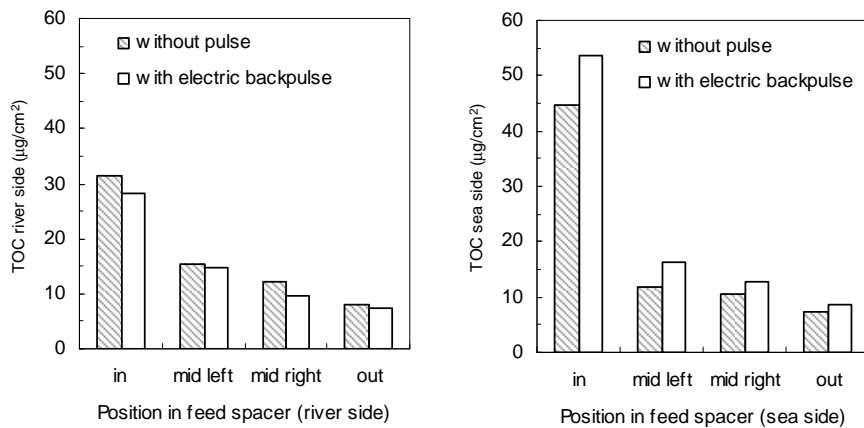


Figure 12. Amount of biomass (TOC, $\mu\text{g}/\text{cm}^2$) over the feed spacers within the stack without an electric backpulse and with an electric backpulse of 10 ms per s.

An electric backpulse as applied in this experiment seemed not a successful method to prevent biofouling. Nevertheless it may be useful to prevent other types of fouling (e.g., organic fouling).

Chapter 5

6 Proof-of-principle of a reverse electrodialysis stack without spacers

Concerning the internal losses of reverse electrodialysis, it was well-recognized that the main contribution comes from the resistance to ionic transport in the compartments filled with the dilute, because of its low conductivity. From Chapter 3, we may conclude that a spacer is an undesired isolator in all (reverse) electrodialysis processes. This statement would be even further supported when also the parasitic energetic losses associated to screen spacers are taken into account, due to friction losses and fouling. The application of a spacer-free stack design would be advantageous for all (reverse) electrodialysis processes. However, a spacer-free stack design is not yet available. Therefore, we invented a stack design in which membranes are separated by two thin gaskets that form together an open non-woven structure. This resulted indeed in a remarkable lower ohmic resistance of about a factor 2. However, the non-ohmic resistance of the stack without spacers was significantly higher, possibly due to a higher concentration polarization than in a stack with spacers (turbulence promoters). This concentration polarization could be prevented by other measures, e.g. with surface heterogeneities and gas sparging. Also from the perspective of biofouling, it was experimentally proven that obtaining a stack design without spacers is a good direction for further development of reverse electrodialysis.

6.1 Introduction

6.1.1 Stack design with spacers between the membranes

Electrodialysis (reversal) is a membrane-based technique for desalination or mineral recovery [1]. *Reverse electrodialysis* is a membrane-based technique for generation of sustainable energy (e.g. electric power) from controlled mixing of river water and sea water [2]. In both cases ion-exchange membranes are stacked in an alternating pattern between a cathode and an anode. The compartments between the membranes are alternately filled with a concentrated salt solution and a diluted salt solution. Due to an applied electrical potential (electrodialysis) or a salinity gradient between dilute and concentrate (reverse electrodialysis), a transport of ions occurs through the membranes. For sodium chloride solutions, sodium ions permeate through the cation-exchange membrane in the direction of the cathode, and chloride ions permeate through the anion-exchange membrane in the direction of the anode. Electroneutrality of the solution in the anode compartment is maintained via oxidation at the anode surface. Electro-neutrality of the solution in the cathode compartment is maintained via reduction at the cathode surface.

Although a schematic overview of conventional electrodialysis (reversal) and reverse electrodialysis looks similar, the hydrodynamic requirements of a stack would be totally different [3]. The design of a conventional electrodialysis stack is intended for turbulent flow conditions in order to obtain a reasonable limiting current. These turbulent conditions are obtained with relatively big distances between the membranes of one millimeter or more, relatively high cross-flow velocities in the range of 5-40 cm/s, and the use of screen spacers for turbulence promotion. For reverse electrodialysis, however, it is not likely and, in fact, not preferred to operate the system with high Reynolds numbers. It is not likely, given that the distance between the membranes should be decreased to less than one

millimeter in order to cut down the internal ohmic resistance and the cross-flow velocities should be lower to keep the parasitic energy losses for pumping to a reasonable level. It is not preferred, given that the diffusion layers do play a minor role in reverse electrodialysis [4] as it is not operated at its limiting current.

The spacers in a reverse electrodialysis are, therefore, not primarily applied for turbulence promotion but mainly to keep distance between the adjacent membranes. Although these differences are recognized, the existing design of a reverse electrodialysis is still based on the common stack design of electrodialysis. However, the stack design needs to be reconsidered when the technology comes beyond its experimental phase [3].

6.1.2 Problems associated with spacers

In Chapter 3, we showed that the screen spacers are of major importance regarding the internal losses of reverse electrodialysis. We introduced the equations for the ohmic internal electrical resistance of a stack [5]. In these equations we showed that the spacers (i) reduce the active membrane area due to coverage, and (ii) that the spacers not only inhibit the volume for ion-transport but also cause a lengthening of the mean ion-transport length due to tortuosity. Besides the spacer width h (m), we introduced two parameters to reflect these additional spacer properties: (i) β as the portion of membrane area that is masked by the spacer (-) referred to as the shadow factor [6], (ii) ε^2 as the tortuosity factor (the porosity ε (-) of the spacer is squared to reflect the tortuous ion transport). From available spacer geometries, we can derive the ε^2 to be in the range of 0.4-0.6, and β to be 0.1-0.5. If our equation and assumptions are correct, we can conclude that a spacer is an undesired isolator in all (reverse) electrodialysis processes.

Although a possible solution would be to use ion-conductive spacer materials, from Chapter 5 it can be concluded that it is anyhow unfavorable to apply screen spacers for reverse electrodialysis. Screen spacers cause relatively high friction losses [7], but moreover they form a place for biofilm accumulation causing pressure drop increases [8] and a subsequent decline of the electrical performances. Instead of spacers, flow paths should be formed in the membranes providing a more open design with fewer crevices for physical entrapment of solids. At present, however, it is not possible to construct a spacer-free stack with use of commercial available materials.

For a spacer-free design, one would need corrugated membranes, i.e., with integrated channels for distribution of water across the membranes [9]. These membranes are not (yet) available on the market. Another option would be the use of so-called tortuous path spacers instead of screen spacers [6]. This tortuous path spacer is in fact a gasket with a long winding path from inlet to outlet and has following disadvantages: (i) a high pressure drop and (ii) a high voltage drop. In order to obtain a certain degree of mixing between the membranes, the linear velocity should be extremely high. This fact, together with the length of the path and the presence of numerous bends, results in an unacceptable flow resistance of the stack (i.e. a high pressure drop over the stack). Membranes should have a certain flexural strength to span the path. Consequently, these membranes should be relatively thick. This thickness results in an undesired electrical resistance of the stack (i.e. a high voltage drop over the stack).

6.1.3 Objective

The objective of this study was to give a proof of principle of a spacer-free reverse electrodialysis system, firstly on performance and secondly on biofouling behaviour. In order to achieve the first, we designed a spacer-
150

free stack in such a way that commercially available membranes and gaskets can be applied without the use of spacers or a tortuous pathway. The performance of this newly designed spacer-free system can be compared with a conventional designed system as previously used in this thesis. In order to achieve the second, we made use of available ‘membrane fouling simulators’ [10]. These simulators can be easily run with and without a spacer, enabling us to compare the biofouling behaviour of a spacer-free system with the conventional designed system.

6.2 Experimental

6.2.1 Performance experiments

From Chapter 3, it can be expected that without a spacer, considerable ohmic losses in the system can be avoided. To prove this hypothesis, two types of reverse electrodialysis stacks were used. The difference between the stacks was the applied gasket and spacer. One stack was provided with a PET fabric with a thickness of 500 µm (Nitex 06-700/53, Sefar) in a 500 µm silicone gasket, the other was not provided with a spacer. The latter design is explained in next section.

Table 1: Characteristics of stack with spacer and stack without spacer

		Stack with spacers	Stack without spacers
Inter membrane distance	µm	500	300+200
Porosity, ϵ	-	80%	>90%
Tortuosity, ϵ^2	-	0.64	0.8-0.9
Open area	-	53%	>80%
Shadow, β	-	0.47	<0.2

Main characteristics of the stacks with respect to porosity and open area are summarized in Table 1. The characterization method, solution compositions, flow rates, and further operational conditions and measurement procedures were identical to those described in Chapter 3 [5]. The placement of the reference electrodes was identical as in Chapter 4 [11].

6.2.2 Biofouling experiments

From Chapter 5 and other published studies on biofouling at our institute, we know that “in the presence of a feed spacer the absolute feed channel pressure drop increase caused by biomass accumulation was much higher than when a feed spacer was (...). Biofouling is dominantly a feed spacer problem” [12]. To prove this hypothesis, two flow cells ('membrane fouling simulators' as described in [10]) were run in parallel, one with and one without a spacer. These flow cells were continuously fed with 'river water'. A comparable methodology was used as in Chapter 5 to accelerate the biofilm formation, except that in this experiment 0.2 mg acetate-C/L was dosed instead of 1.0 mg acetate-C/L), supplemented by phosphate and nitrate in the ratio of 100:10:20 (C:P:N, m-base).

In a first biofouling experiment, the flow channel (spacer thickness) was 0.5 mm. The flow rate was maintained at 11.5 mL/min in order to get comparable conditions as in a stack as described in Chapter 5 (also with 0.5 mm spacers) in terms of flow rate per area. In a second experiment, the flow channel (spacer thickness) was 0.2 mm which is closer to the application of reverse electrodialysis. The flow rate was maintained at 11.5 mL/min in order to get a similar nutrient load per area of membrane.

6.3 Results and discussion

6.3.1 Design and performance of a spacer-free system

Design of a spacer-free experimental setup. Our aim was to design a spacer-free stack in such a way that commercially available membranes and gaskets can be applied without the use of screen spacers or a tortuous pathway. We invented a system consisting of two thin gaskets between the membranes that form together an open non-woven structure (an example is given in *Figure 1*). A first gasket contains vertical ribbons that allow the solution to flow in a vertical direction, a second gasket contains horizontal ribbons that allow the solution to flow in a horizontal direction.

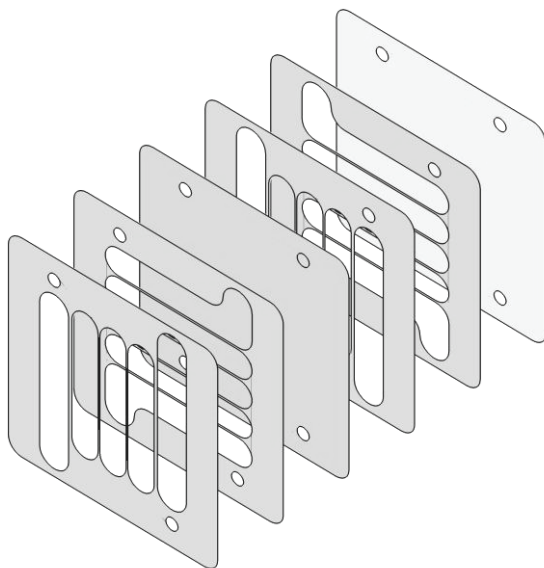


Figure 1: spacer-free design with two-layers of gaskets: a gasket with horizontal ribbons on top of a silicone gasket with vertical ribbons

The strength of the stack is obtained by the outside gaskets and also by the crossings of the horizontal and vertical ribbons. The membranes obtain extra strength due to the adjacent ribbons. This is an advantage compared

to a tortuous path design. The obstruction of the ribbons in either horizontal or vertical direction enhances the flow distribution like in a stack with screen spacers. This means that with this design it is possible to use just a few manifolds as sources and shrinks (or inlets and outlets) for the solution flows. Although the functionality of screen spacers as turbulence promoters is lost, the obstruction of the ribbons in both horizontal and vertical direction still enhances the flow velocities in the direction perpendicular to the membranes. This would enhance the mixing between the membranes and thus decrease concentration polarization effects (which might play a major role in a tortuous path design). The distances between the ribbons and the thicknesses of the ribbons can be adjusted locally, e.g. for a higher strength near the manifolds or for a better flow distribution, etc. This is an advantage compared to screen spacers that are often woven structures with given warp and weft distances (defined by the used loom).

Proof of principle. The internal stack resistance decreases during the experiments, as the concentration of the concentration and thus the conductivity of the diluted solution is increasing with the amount of transferred charge (Q , in C), see *Figure 2*. At the starting conditions, the main contributor to the stack resistance is the diluted solution compartment, i.e. the ionic transport through the low-conducting bulk solution and the tortuosity of this ionic transport due to the spacers. As expected from the differences in tortuosity in *Table 1*, the design without spacers resulted in a remarkable lower ohmic resistance of about a factor 2 compared to the design with spacers. This proves that potentially the power density of reverse electrodialysis can be doubled by applying a spacer-free design.

At a higher extent of charge transfer, it can be derived that the main contributors to the resistance are the membranes and the masked area due

to the spacers. Apparently, the shadow factor of the spacer-free design on the membranes is lower, as was suggested from the specifications in *Table 1*.

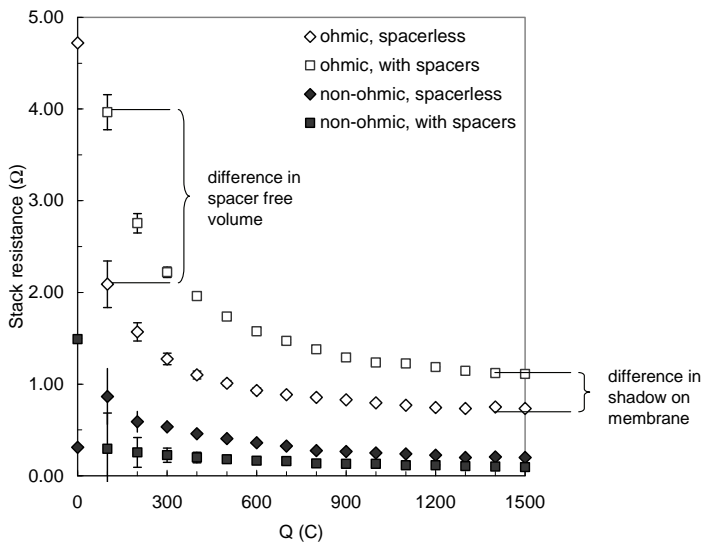


Figure 2: Stack resistance with proceeding charge transfer (Q).

The potential increase of power density, however, is not fully harvested. As can be seen from *Figure 2*, the net benefit is lower due to the higher non-ohmic resistance of the spacer-free stack than in a stack with spacers. This can be explained with a higher concentration polarization in the spacer-free stack, indicating that the hydrodynamic design should be carefully examined and improved. The obstructions for the solution flow decrease when the dense structures of the spacer are replaced with the more open structure in the spacer-free design. This causes a decrease in turbulence of the solution flow through the compartments. This means that the solution flow through the compartment flows more direct from the inlet to the outlet without dispersing the solution throughout the compartment. Therefore the concentration of ions at the solution surface layer of the membrane at

the concentrated side decreases and at the dilute side increases (concentration polarization), i.e., resulting in an increase of the non-ohmic voltage drop.

In order to prevent this polarization and to enhance mixing of these boundary layers, one may think of engineered inhomogeneity of the membranes surfaces [13]. Another possible solution for the increase of the non-ohmic resistance is the introduction of a gas flow (for example air) along the membranes (in the same direction as the solution flows), flowing through the compartments between two membranes [14]. This can be achieved by creating gas inlets on the bottom side of the solution compartments for dispersing the gas-flow through the solution flow. By this, the dispersion of the solution flow through the compartments can be improved. The gas bubbles can increase the speed of the flow through the compartment, and may result in better mixing of the surface layers. One should assure that this possible benefit of gas sparging compensates for the increase of the ohmic voltage drop due to the presence of bubble curtains and the additional power consumption.

6.3.2 Biofouling behavior of a spacer-free system

The biofouling behaviour was studied with flow channel heights of 0.5 mm and 0.2 mm. In both cases, it was confirmed that biofouling is causing clogging of the feed spacers (Figure 3). In the flow cells without spacers, this clogging is not occurring. From this perspective, obtaining a stack design without spacers is indeed a good direction for further development of reverse electrodialysis.

Surprisingly, the problem of spacer clogging was more pronounced in the experiment with a 0.5 mm spacer. A possible explanation would be that, although the nutrient load in both experiments was the same, the linear cross-flow velocity in the second experiment was 2.5 times higher than in 156

the first experiment. The accumulation of micro-organisms may be lower at an elevated cross-flow velocity due to a higher shear stress on the biofilm [15]. In this experiment, this can be seen as a prolongation of the operational period until clogging from 4 days for the 0.5 mm spacer up to 12 days for the 0.2 mm spacer.

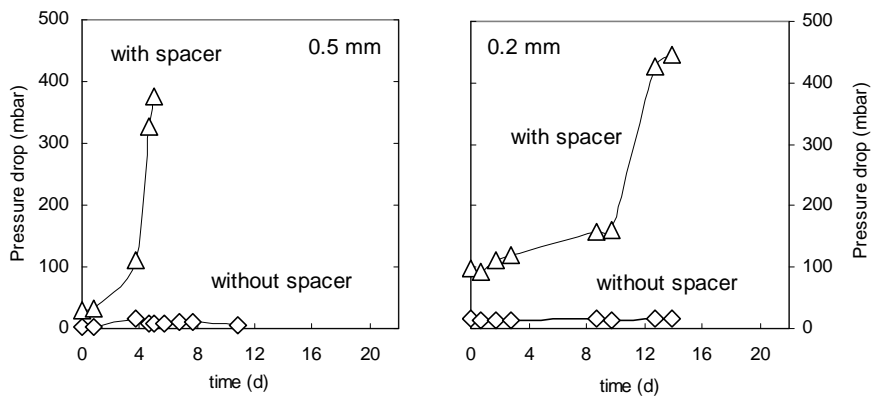


Figure 3. Pressure drops over the flow cells with 0.5 mm flow channels (left), and with 0.2 mm flow channels (right).

After the experiments were finished, the flow cells were sampled. The amount of biomass was analyzed as Total Organic Carbon mass per unit area (Figure 4). In both cases, the flow cells without spacers had comparable amount of biomass as the flow cells with spacers, except for the inlets. At the inlets, the amount of attached biomass in the flow cells with spacers was much higher than in the flow cells without spacers.

At the end of the experiments, when the pressure drop reached the upper limit of 0.5 bar, the amount of biomass attached to the 0.2 mm spacer was slightly bigger than to the 0.5 mm spacer. Firstly, this confirms the hampering effect of an elevated cross-flow velocity on the accumulation of biomass. Despite the difference in operational period and thus the cumulative nutrient supply, the amount of accumulated biomass is

relatively unaffected. Secondly, however, it clearly shows that the relative pressure drop increase due to the biofilm formation is much lower in case of the 0.2 mm spacers with the higher cross-flow velocity. Apparently, the cross-flow velocity determines the biofilm characteristics, e.g. the density (thickness, porosity) and the structure (morphology, roughness) [16].

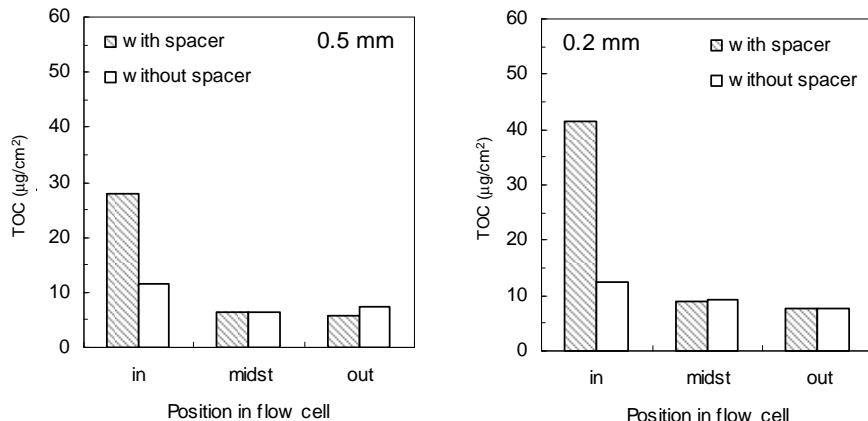


Figure 4. Amount of biomass (TOC, $\mu\text{g}/\text{cm}^2$) over the flow cells with 0.5 mm flow channels (left), and with 0.2 mm flow channels (right).

6.4 Outlook

This study showed that obtaining a stack design without spacers is a good direction for further development of reverse electrodialysis. Firstly, the proof-of-principle showed that a reverse electrodialysis stack without spacers has about a twice times lower ohmic resistance compared to a reverse electrodialysis stack with spacers. Secondly, the proof-of-principle showed that a stack without spacers is free sensitive for biofouling compared to a reverse electrodialysis stack with spacers.

Acknowledgements

We thank Watse Hoekstra for his inventive idea of the spacer-free design of the experimental setup, Piet Leijstra for his contribution to the experimental work, and Sybrand Metz for his contribution to the patent application. This inventive experimental setup was patented by Wetsus, centre of excellence for sustainable water technology. Wetsus is funded by the ministry of economic affairs. The inventors like to thank the members of the theme 'Energy' from Wetsus for the fruitful discussions and especially the participating companies Nuon, Eneco, Magneto, Landustrie, Frisia Zout, Dow Chemical, and Fuji for their support.

6.5 References

1. Allison, R.P., Electrodialysis reversal in water reuse applications, Desalination 103(1-2) (1995), p. 11-18.
2. Weinstein, J.N. and F.B. Leitz, Electric-power from difference in salinity - dialytic battery, Science 191(4227) (1976), p. 557-559.
3. Dirkse, M.H., W.P.K. van Loon, J.D. Stigter, J.W. Post, J. Veerman and G.P.A. Bot, Extending potential flow modelling of flat-sheet geometries as applied in membrane-based systems, Journal Of Membrane Science 10.1016/j.memsci.2008.08.022 (2008), p.
4. Lacey, R.E., Energy by reverse electrodialysis, Ocean Engineering 7(1) (1980), p. 1-47.
5. Post, J.W., H.V.M. Hamelers and C.J.N. Buisman, Energy recovery from controlled mixing salt and fresh water with a reverse electrodialysis system, Environ Science Technology 42 (2008), p. 5785-5790.
6. Strathmann, H., Ion-exchange membrane seperation processes, 1 ed. Membrane science and technology series. Vol. 9. 2004: Elsevier.
7. Veerman, J., M. Saakes, S.J. Metz and G.J. Harmsen, Reverse electrodialysis: Performance of a stack with 50 cells on the mixing of sea and river water., Journal Of Membrane Science 327 (2009), p. 136-144.
8. Vrouwenvelder, J.S., S.A. Manolarakis, J.P. van der Hoek, J.A.M. van Paassen, W.G.J. van der Meer, J.M.C. van Agmaal, H.D.M. Prummel, J.C. Kruithof, and M.C.M. van Loosdrecht, Quantitative biofouling diagnosis in full scale nanofiltration and reverse osmosis installations, Water Research (42) (2008), p. 4856-4868.
9. Brauns, E., Salinity gradient power by reverse electrodialysis: Effect of model parameters on electrical power output, Desalination 237 (2009), p. 378-391.
10. Vrouwenvelder, J.S., C. Hinrichs, A.R. Sun, F. Royer, J.A.M. Van Paassen, S.M. Bakker, W.G.J. Van der Meer, J.C. Kruithof, and M.C.M. Van Loosdrecht, Monitoring and control of biofouling in nanofiltration and reverse osmosis membranes, Water Science & Technology: Water Supply 8.4 (2008), p. 449-458.

Chapter 6

11. Post, J.W., H.V.M. Hamelers and C.J.N. Buisman, Influence of multivalent ions on power production from mixing salt and fresh water with a reverse electrodialysis system, *Journal of Membrane Science* 330 (2009), p. 65-72.
12. Vrouwenvelder, J.S., D.A. Graf von der Schulenburg, J.C. Kruithof, M.L. Johns and M.C.M. van Loosdrecht, Biofouling of spiral-wound nanofiltration and reverse osmosis membranes: A feed spacer problem, *Water Research* 43 (2009), p. 583-594.
13. Balster, J.H., Membrane module and process development for monopolar and bipolar membrane electrodialysis. 2006, University of Twente: Enschede.
14. Sedahmed, G.H., M.M. Naim and M.Y. Haridi, Mass transfer in gas sparged membrane cells, *Journal Of Applied Electrochemistry* 20 (1990), p. 145-149.
15. Wills, A., T.R. Bott and I.J. Gibbard, The control of biofilms in tubes using wire-wound inserts, *Canadian Journal of Chemical Engineering* 78 (2000), p. 61-64.
16. Vrouwenvelder, J.S., C. Hinrichs, W.G.J. van der Meer, M.C.M. van Loosdrecht and J.C. Kruithof, Pressure drop increase by biofilm accumulation in spiral wound ro and nf membrane systems: Role of substrate concentration, flow velocity, substrate load and flow direction, *Biofouling* 25 (2009), p. 543-555.

7 Technical and economic prospects of reverse electrodialysis

Reverse electrodialysis is a conversion technique to obtain electricity from salinity gradients. Over the past few years, the performance of reverse electrodialysis on laboratory scale has improved considerably. In this paper, we discuss the challenges we are still facing concerning the economic and technological feasibility and the developing path of reverse electrodialysis. We focus on the following issues: (i) the development of low-cost membranes, (ii) the pre-treatment in relation to stack design and operation, and (iii) the economics of reverse electrodialysis. For membranes, the challenge is to increase availability ($>\text{km}^2/\text{year}$) at reduced cost ($<2 \text{ €}/\text{m}^2$). The membranes should be manufactured at high speeds to meet this challenge. For pre-treatment, a capital-extensive microscreen filter with $50 \mu\text{m}$ pores was selected and tested. Such a straightforward pre-treatment is only sufficient given the fact that the reverse electrodialysis stack was redesigned towards a more robust spacer-less system. For the economic feasibility, a 200 kW repetitive unit was designed. The cost price is estimated to be less than 0.08 €/kWh (excl. any subsidy or compensation), comparable with that of wind energy. The feasibility of the technology should be proven with a scaled-up system under practical conditions. The intended pilot facility at the Afsluitdijk (The Netherlands) will be an essential step towards implementation of reverse electrodialysis for power generation.

This chapter is submitted in revised form to Desalination & Water Treatment:

J.W. Post, C.H. Goeting, J. Valk, S. Goinga, J. Veerman, H.V.M. Hamelers,
P.J.F.M. Hack, Towards implementation of reverse electrodialysis for power
generation from salinity gradients.

7.1 Introduction

7.1.1 From scientific research to technical development

Salinity-gradient energy is the energy that can be gained by mixing two flows of water with different salinity. The idea is formulated for the first time in 1954 by R. Pattle in Nature [1]. The potential of salinity-power has been estimated in the 1970s on the basis of average ocean salinity and annual global river discharges to be between 1.4 and 2.6 TW [2, 3]. In The Netherlands, river water discharge and sea water are abundantly available. On average the river Rhine discharges 2,200 m³/s. Assuming an energy potential of 1.5 MJ per m³ of river water, this means an electricity potential of over 6 million households (>80% of all households). Even when this river discharge can be used only to some extent, it is an enormous source of renewable energy. Furthermore, it is inherently clean and sustainable. There is no emission of CO₂ and no thermal pollution. Moreover, in principle, energy can be generated continuously 24 hrs per day and 365 days a year, unlike wind or solar energy. In theory, there are different techniques to obtain this energy. The most promising are reverse electrodialysis (RED) and partially retarded osmosis (PRO). In chapter 2 [4] we have pointed out that in the case of sea water and river water, the reverse electrodialysis technique would be the best choice (see process scheme in Figure 1, for explanation see chapter 1).

Wetsus - centre for sustainable water technology in the Netherlands - started in 2005 with the project 'Blue Energy' with a focus on reverse electrodialysis. At that time only a few scientific papers were published over a period of 50 years [1, 3, 5, 6] concerning experimental reverse electrodialysis systems. In the past few years, the performance of reverse electrodialysis on laboratory scale has improved considerably (Table 1). The specific power or power density is probably the most important measure for performance. Although it was recognized for a long time that

the power density was mainly determined by the inter-membrane distance [7], no real attempts were made to minimize the spacer thickness. The first recent attempt by Turek and Bandura [8] was not quite successful as only a power density of 0.4 W/m^2 was obtained. However, this could be caused by ionic short-circuits in the system due to the small current-passing area of their setup as can be seen from the low obtained open-circuit voltages. We were the first to report a much higher power density of 0.95 W/m^2 [9] and more recently [10] an even higher power density of $>1.2 \text{ W/m}^2$. Furthermore, in chapter 3 [11] we showed that from mixing sea water and river water using reverse electrodialysis, in principle, a high energy recovery of more than 80 % can be obtained, which means an energy yield of $>1.2 \text{ MJ per m}^3$ of river water.

The first steps to practical use were made in chapter 4 [12], in which reverse electrodialysis was applied to feed waters of different chemical compositions. In chapters 5 and 6, we even introduced biofilm formation in the system to investigate the effects of biofouling and preventive operational steps.

Table 1: Obtained power density (W/m^2) and spacer thickness (mm); experiments with sodium chloride solutions, typical concentrations 0-1 g/L and 30-35 g/L NaCl [10].

Author	Year	Power density	Spacer
		(W/m^2)	thickness (mm)
Pattle	1954	0.05	0.7
Weinstein and Leitz	1976	0.17	1.0
Jagur-Grodzinski and Kramer	1986	0.41	0.55
Turek	2007	0.46	0.19
Suda	2007	0.26	1.0
Veerman et al.	2008	0.95	0.2
Veerman et al.	2009	1.18	0.2

Thus far, reverse electrodialysis experiments have typically been performed on a laboratory scale, varying from current-passing areas of just a few square centimeters [8] to hundreds of square centimeters [9] and from four cell-pairs [11] to fifty cell-pairs [10]. State-of-the-art is a stack with an active membrane area of 25x75 cm² and 50 cell-pairs with a power output of about 16 Watt (Figure 1; manufactured by REDstack B.V., The Netherlands). To achieve practical implementation, reverse electrodialysis still need to be scaled-up by several orders of magnitude. This scaling-up and practical implementation are beyond the academic expertise and need to be done by specialized companies. For this reason REDstack B.V. was founded by Magneto and Harlingen Holding Industries (owner of Landustrie/Hubert), two companies participating within the Blue Energy research project of Wetsus.

7.1.2 Development challenges

Before starting the scale-up, the following hurdles should be overcome by the companies: (i) there are no specially developed low-cost membranes available for the reverse electrodialysis process, (ii) there is no vision on

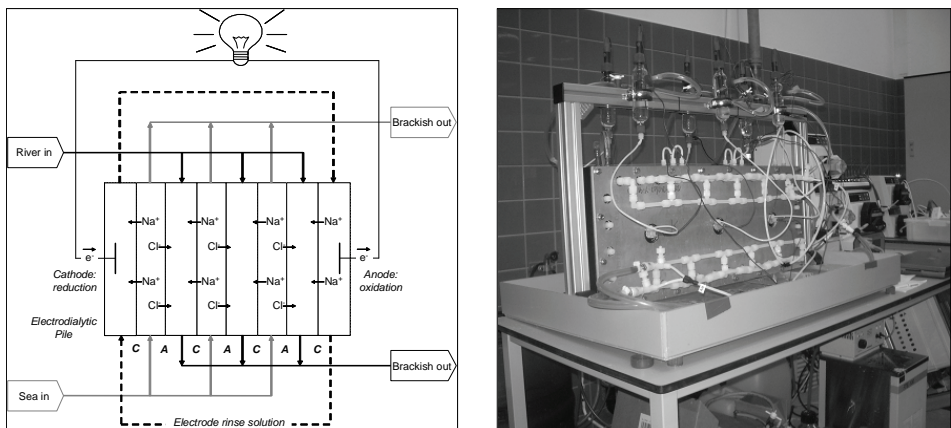


Figure 1: Process scheme and picture of a reverse electrodialysis stack (membrane area of 25x75 cm² and 50 cell-pairs as manufactured for research purposes by REDstack B.V., The Netherlands).

the requirements for stack design in relation to pre-treatment and friction losses, and (iii) there is no project to be evaluated to get the economic figures.

Ion-exchange membranes are the key components in a reverse electrodialysis system. In the 70s, Weinstein and Leitz [3] concluded that large-scale energy conversion by reverse electrodialysis may become feasible, but only with major advances in the manufacturing of ion-exchange membranes and with careful optimization of the operating conditions. Given a proper stack design, the membrane characteristics directly influence the power output [13] and energetic efficiency [11]. Moreover, the membrane price is a key issue for successful market introduction of the reverse electrodialysis technology [8].

Although mentioned in scientific papers, challenges such as the pre-treatment of river water and sea water [11], and the hydrodynamic aspects of reverse electrodialysis [14] are often ignored or underestimated. Regarding the pre-treatment, Lacey [7] assumed activated-carbon filtration as pre-treatment, just to perform economic calculations. However, until now there is neither experimental basis nor a clear vision on the feed water quality requirements. This lack is probably mainly due to the fact that the pre-treatment requirements can not be seen separately from the hydrodynamic design of the reverse electrodialysis stacks. Regarding the hydrodynamics, Lacey [7] modeled the friction losses. Jagur-Grodzinski and Kramer [5] and Turek and Bandura [8] measured the these friction losses and reported both the gross power output and net power output. These studies showed considerable energy losses for pumping, even under laboratory conditions without membrane fouling.

At this moment, electricity of salinity-gradient energy is still costly compared to electricity of other renewable energy sources due to high

membrane prices of commercially available membranes. Reverse electrodialysis has never been applied before at commercial scale. An economic evaluation can, therefore, be only done on realistic assumptions and expectations.

7.1.3 Objective

In this chapter, we discuss the economic and technological challenges we are facing in the scale-up of reverse electrodialysis. We take the achievements of the academic research as presented in this introduction as starting point. We focus on the following issues: (i) the development of low-cost membranes (section 7.2), (ii) the pre-treatment in relation to stack design and operation (section 7.3), (iii) an economic evaluation (section 7.4). Further steps towards application in practice are presented in section 7.5.

7.2 Development of low-cost membranes

7.2.1 Membrane requirements

Audinos [6] already mentioned explicitly the importance of membranes specially developed for reverse electrodialysis. Nevertheless, most research was done with standard electrodialysis membranes (e.g., [3, 5, 9]). As a result, nowadays available homogeneous ion-specific membranes may be used (e.g. from Asahi Glass, Tokuyama or Fumatech [13]) as a benchmark for the development of tailor-made membranes. The requirements for the ion-exchange membranes for reverse electrodialysis are summarized in Table 2.

During the development process, it may be sufficient to use a straightforward model to evaluate the performance of the membranes with respect to the maximum power density [13]. However, we are aware that this evaluation is just a guideline to give direction to the development of

Chapter 7

membranes for reverse electrodialysis. Absolute values as calculated by a simple model are likely to overestimate the specific power since numerous assumptions (e.g. total effective membrane area available for ion transport, ideality of solutions, no depletion of feed streams) and simplifications are made. The most important uncertainty is the translation of membrane characteristics as measured by the standard characterization methods to apparent characteristics of the same membranes when applied in a reverse electrodialysis stack.

Table 2: Membrane requirements for reverse electrodialysis.

Criterion	Requirement	Comments
Perm-selectivity	> 95% (this can be measured as in [13])	The perm-selectivity determines the membrane potential which is available as a driving force for the process, and the transport of co-ions which is in fact energy dissipation [11]
Electrical resistance	< 3 Ωcm ² (this can be measured as in [13])	The internal resistance of the stack should be as low as possible, and the lower the electrical resistance of the membranes, the lower the electrolytic shortcircuits are through the manifolds [10])
Mechanical stability	Enables construction of a stack	The membranes should have enough strength to be used for stack construction. This measure is hard to be quantified, but should be part of the evaluation.
Chemical stability	Lifetime > 5 years	Mild membrane environment, no special requirements (neutral pH's, no free chlorine), although certain resistivity for cleaning agents is preferred, etc.
Cost price	< 2 €/m ²	Explained in section 7.4

As can be seen from the desired characteristics in Table 2, our focus is on the development of membranes with high perm-selectivity and low cost price.

electrical resistance. It is difficult to optimize these characteristics of ion-exchange membranes for reverse electrodialysis since the different properties (thickness, swelling degree, ion-exchange capacity) often have a counteracting effect on these characteristics. For instance, thin membranes have a relatively low area resistance (desired) but also a low perm-selectivity (not desired).

7.2.2 Challenges are cost-price and production scale

Although the technical requirements are already met by currently available membranes, the cost-prices are out-of-range to make reverse electrodialysis affordable. According to Turek and Bandura [8], it is hard to believe that the price of low-resistance ion-exchange membranes may be reduced a hundred times, which seems to be the desired cost level [8].

Nevertheless, after a look at related markets, we are more optimistic that membrane prices for (reverse) electrodialysis can be reduced tremendously [4]. One should be aware of the fact that electrodialysis membranes have never had a considerable market share. Even then, on the global market, heterogeneous ion-exchange membranes can be found with very low cost-prices (< 5 US\$/m²). Of course, low-resistance ion-exchange membranes have higher prices of 100 US\$/m² or more [8], but even these prices can be expected to fall, as manufacturing techniques improve, and the range of applications expands. Market research for related membrane applications show unit prices of installed membranes falling by an order of magnitude in 10 years, and this made Sutherland [15] to predict that the 1 US\$/m² of installed membrane is not far off.

It should be noted that, even when the total current membrane manufacturing capacity is considered (neglecting the differences in technical specifications of membranes), this global production capacity would never be able to match the demand of membranes for power

Chapter 7

production. The global turnover in 2003 for sales and after-sales of desalination membrane modules was 1814 million US\$ [15]. Assuming a cost price of <10 US\$/m² installed membrane, this means a market of >180 km² of membrane per year, i.e., equivalent to the demand of one medium-sized salinity-gradient power plant. For the development of low-cost manufacturing of ion-exchange membranes and stacks, this means that besides the expertise in manufacturing of membranes also the expertise of mass production is needed.

Therefore, a comparison with the market of ionites – or more specifically of synthetic ion exchange resins - would be more appropriate than a comparison with the membrane market. The chemistry of ion exchange polymers in bead-shaped materials is comparable of that of ion-exchange membranes. Besides, ion-exchange resins can be directly used for preparation of heterogeneous membranes when they are mixed in a basically uncharged polymer membrane matrix [16, 17]. Regarding the market, ion exchangers for deionization and water softening applications can be considered commodity chemicals (excess of production capacity, limited market growth, and intense competition) with a global market volume that exceeds 0.15 million m³ per year [18]. To get an idea, this would be comparable to a market volume of >1.500 km² of ion-exchange membrane per year (i.e., equivalent to several medium-sized salinity-gradient power plants), if we assume 100 µm thick membranes. Current prices for commodity ion-exchange resins are in the order of 3,000-6,000 US\$/m³ [18], indicating that a membrane price in the order of 1 US\$/m² is indeed within reach [15].

While at the start of the membrane development for reverse electrodialysis, we paid much attention to the technical requirements and cost prices of base materials, nowadays we are focusing on high-volume manufacturing. Given the enormous amount of membrane area needed for

large-scale energy conversion by reverse electrodialysis, the scalability of the production processes becomes more and more important. In our vision, the membranes should be manufactured on labour-extensive reel-to-reel production lines operating at high speeds. The post-processing such as alternating piling of the cation-exchange membranes and anion-exchange membranes in the required stack configuration should be automated as well.

7.3 Stack design related to friction loss and pre-treatment

7.3.1 Process design

The required water quality parameters are still unknown. Like in previous section about the membrane prices, it is tempting to look at experiences with desalination membranes. However, the usually applied pre-treatment steps [19] are probably excessive and certainly too capital-intensive to be viable for reverse electrodialysis. Besides the quality and cost aspects, also the footprint, energy consumption, and use of chemicals, would be important factors regarding the feasibility of reverse electrodialysis. We defined these requirements in Table 3.

On forehand, it should be mentioned that these requirements, are based on the assumption that the reverse electrodialysis stacks are redesigned toward a system *without* spacers between the membranes. If spacers were used, the question remained whether these requirements would be sufficient. Reverse electrodialysis stacks *with* spacers would require an even more extensive pre-treatment than conventional flat-sheet membrane systems as the distance between the membranes is less than 0.5 mm. The design of experimental reverse electrodialysis stacks were still based on the common stack design of electrodialysis with the use of screen spacers. These screen spacers, however, were identified not only as undesired insulators [11] and cause of relatively high friction losses [10], but

Chapter 7

moreover as a place for biofilm accumulation causing pressure drop increases [20] and a decline of the electrical performances. Therefore, the reverse electrodialysis stack was redesigned towards a more robust spacer-less system, using the developed computational fluid dynamics model for flat sheet membrane configurations [14]. Instead of spacers, now flow paths are formed in the membranes providing a more open design with fewer crevices for physical entrapment of solids. With a cross flow velocity of 3 cm/s it was confirmed using model calculations and experiments with an non-fouled system, that the friction loss is less than 2-3 m water column (\sim 6-7 Wh/m³). Assuming that each 1 m³ water (i.e., 0.5 m³ sea water and 0.5 m³ river water) yields 130 Wh [11], the related pumping energy loss accounts only for 5%.

Table 3: Pre-treatment requirements for reverse electrodialysis.

Criterion	Requirement	Comments
Separation cut-off	<50 µm	Sufficient to prevent fouling with Common or Blue Mussel (<i>Mytilus edulis</i>). Fertilized eggs are 60-90 µm in diameter [26].
Costs	< 1 €ct/m ³	Each 1 m ³ pre-treated water (i.e., 0.5 m ³ seawater and 0.5 m ³ river water) could yield 130 Wh \sim 1 €ct [11]
Energy consumption	< 6-7 Wh/m ³ (<2-3 m water column)	Our arbitrary aim to limit parasitic losses to < 10% of yielded energy, with a maximum of 50% for pre-treatment.
Footprint	> 15 m ³ /h of capacity per m ³ reactor	Our arbitrary aim to limit the footprint. Obtained flux (m ³ /m ² .h) times packing density of the reactor (m ² /m ³) could be used for indication.
Chemical use	No dosage	May be incidentally used for cleaning

For the selection of a suitable pre-treatment technology, our aim was to find commercially available operational units that meet the self-defined criteria in Table 3. We assumed that floating coarse debris such as weed, reed, and plastics were removed from the surface water at the intake by using weirs and bar-screens. For further pre-treatment all kind of separation processes were reviewed: settling, decanting, centrifugation, filtration, hydro-cyclone, flotation, elutration, flocculation, biological treatment. Based on the criteria as given in Table 3 it was concluded that two types of filtration technologies would be suitable as pre-treatment: (i) river/sea-bank filtration or (ii) mechanical filtration. Most technologies were expelled as they are too expensive and have too low fluxes or too high residence times, leading to a huge footprint and building volume.

River/sea-bank filtration also has also low fluxes ($0.1\text{-}1 \text{ m}^3/\text{m}^2\cdot\text{h}$), but this open-field extraction process requires no big building volumes and could well be combined with other functions (e.g. recreation, landscape development). Sea-bank filtration is used for desalination systems with reverse osmosis membranes. The use of (vertical) beach-wells has the benefit that bank-filtrated sea water needs minimal additional pre-treatment prior to the reverse osmosis. We did not further design this pre-treatment as the applicability of beach wells is very site-specific, e.g. depending on the soil morphology. For desalination plants with a high capacity an open sea water intake is in many cases the only feasible option [21, 22]. Nowadays, new techniques are available to increase the capacity of beach wells by using drainage pipes installed in horizontally drilled holes [23].

Mechanical filtration is a more generic pre-treatment step than bank filtration. Filter media are used to remove or separate particles by steric rejection. The configuration of the micro-screen filter may have different configurations and screen fabrics. Hubert Stavoren B.V., one of the

companies in our consortium, has an extensive track record on micro-screen rotating drum filters for pre-treatment of cooling water. In their configuration, the micro-screen consists of a drum, fitted along the circumference with screen panels. The drum is placed in a concrete pit or tank and rotates on a stationary hollow shaft which is provided with one or more funnel-shaped debris collectors. The feed water enters the drum axially and flows radially through the panels by gravitation (typically a level difference in the order of 10-20 cm), the dirt particles being trapped in the mesh. In order to prevent clogging of the fabric by particles, the drum rotates and the rows of screen panels subsequently pass a set of high-pressure water nozzles at the top of the drum. The dirt particles are washed from the screen and discharged through the funnel-shaped debris collector(s) and the hollow shaft.

Looking at the criteria in Table 3, the most critical factors for these drum filters are energy consumption and footprint. The high-pressure pump needed to supply the water to the high pressure nozzles (e.g., 8 bar overpressure) is the most energy consuming part of this system although the amount of pressurized backwash water is only a few percent of the filtrated water. Assuming 2% of pressurized backwash water, the net head loss is 1.6 m water column (and thus the criterion is met). In order to minimize energy consumption, the high-pressure pump is controlled by a level differential meter over the filter. Regarding the footprint, obtainable net fluxes are reasonable high even with a fabric with 50 µm pores, e.g. in the order of 20-40 m³/m².h. The packing density of the reactor, however, is quite low (~0.5-1 m²/m³). The cylindrical drums with a filter area $A = \pi D L$ (diameter $D < 5$ m, length $L < 6$ m) are placed in a rectangular tank with a volume $V > D^2 L$, resulting in a packing density $<\pi/D$. Consequently, the treated flow rate is 10-40 m³/h per m³ reactor. Depending on obtainable flux and design of drum and tank, the footprint criterion can be met.

7.3.2 Experimental validation

In the harbour of Stavoren (Lake IJssel, The Netherlands), we tested the effectiveness of the pre-treatment. The experimental setup consisted of a rotating drum with a filter area of 1.1 m^2 . The filtrate is fed to a flow-cell that represents the hydrodynamic design of a single membrane in a full-scale reverse electrodialysis stack with membrane-integrated flow patterns (Figure 2). During successive experimental runs, the screen panels were covered with different types of fabrics to test the flux and energy consumption of the pre-treatment. Also the pressure-drop over a flow cell was measured to test the effectiveness of the pre-treatment.

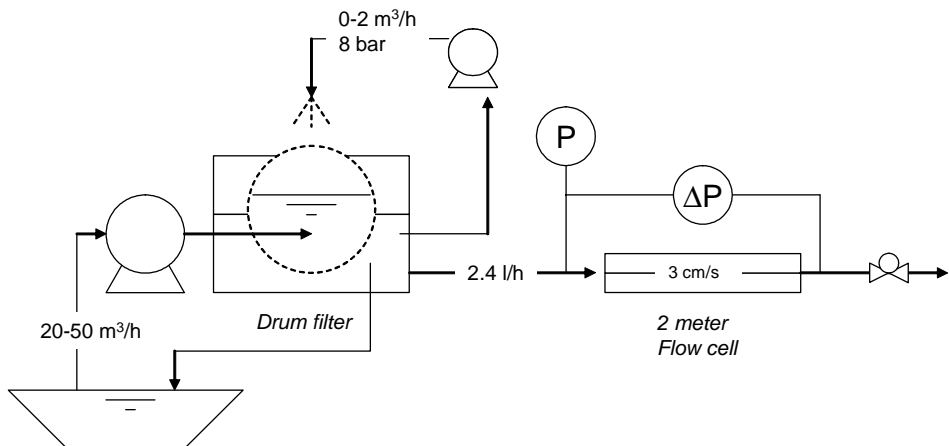


Figure 2: Experimental setup to test the capacity and energy consumption of a drum filter and the effectiveness of this pre-filtration on a flow cell which represents the hydrodynamic design of a single membrane in a full-scale reverse electrodialysis stack.

The capacity of the filter was depending strongly on the chosen fabric and the pore size. We took comparable synthetic fiber materials with pore sizes of $20 \mu\text{m}$ and $50 \mu\text{m}$ and tested the maximum flux to be $22 \text{ m}^3/\text{m}^2\cdot\text{h}$ and $50 \text{ m}^3/\text{m}^2\cdot\text{h}$, respectively. These filter fabrics, however, were not reliable enough as pre-treatment as in cases of failures with the backwash. When a support layer is added to the $50 \mu\text{m}$ fabric to gain mechanical strength and robustness, the maximum flux decreased to $21 \text{ m}^3/\text{m}^2\cdot\text{h}$. This is worse

Chapter 7

when compared to a stainless steel fabric with 40 µm pores with a maximum flux of 43 m³/m².h.

With the latter two fabrics (i.e., the reinforced synthetic fabric with 50 µm pores and the stainless steel fabric with 40 µm pores), we were able to measure the energy consumption and the effectiveness of the filter over longer periods without interruptions (Table 4). The energy consumption of the filter drum was very much dependent on the seasonal water quality. During summer season with elevated water temperature (17-19 °C) the high-pressure pump was switched on more frequently than during the winter season with low water temperatures (5-7 °C), causing a monthly average net head loss of 1.87±0.17 and 0.36±0.34 meter of water column, respectively. Even in summer period, the criterion for the energy consumption is met (Table 3), not only with the monthly average, but even with a once measured maximum of a net head loss of 2.92 meter water column.

During the test periods, the pressure drop over the flow cell (membrane) did not increase, indicating that the filter drum was effective as pre-treatment. The pressure drop appeared to be dependent on seasonal temperature fluctuations, the lower the water temperature, the higher the head loss across the flow paths in the membrane. The total energy consumption in all cases met the objectives for pumping power losses.

Table 4: Pre-treatment experimental results.

Season 24-31 days	Water temp °C	Filter drum		Head losses (meter water column)					
		pores µm	flux m/h	filter drum		membrane		total	
		Avg	max	Avg	max	avg	max	avg	max
summer	17-19	50	21	1.87±0.17	2.92	1.23±0.05	1.30	3.10±0.70	4.12
winter	5-7	50	18	0.36±0.34	1.18	2.06±0.27	2.70	2.41±0.45	3.30
spring	12-14	40	27	0.96±0.46	1.69	1.80±0.19	2.09	2.75±0.58	3.55

7.4 Economic feasibility

7.4.1 Designing a 200 kW module

To get a view on construction costs, we designed a module of 200 kW (net) in 40ft sea container frames. A full-scale plant can contain multiple of these modules. A modular design has the advantage that a localized breakdown can be fixed very soon, and only a small part (200 kW) of the total plant capacity has to be stopped in case of maintenance. One frame contains six reverse electrodialysis stacks (Figure 3) with a total effective membrane area of 100,000 m².

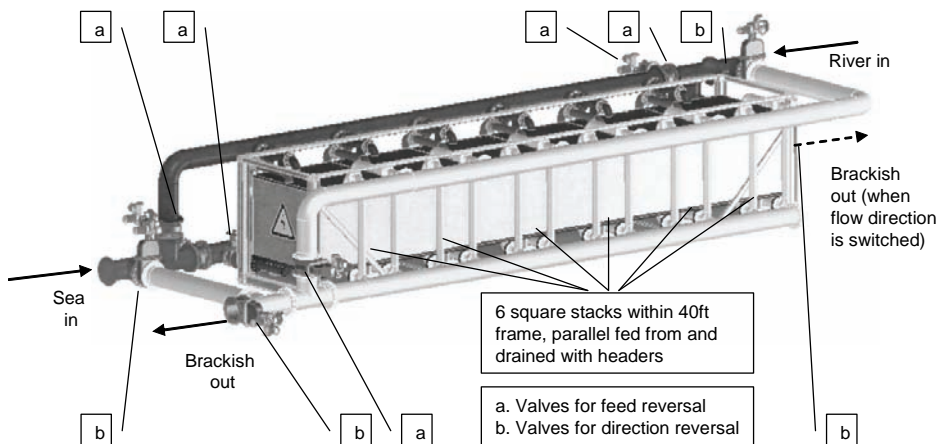


Figure 3: A 200 kW (net) unit with six reverse electrodialysis stacks in a 40 ft sea container frame.

The calculated power density is 2 W/m², according to the model presented by Post et al. [4, 11], with an energy recovery of 70%. The gross power output is 220 kW, but about 10% of this is subtracted for pumping power losses and DC/AC conversion. Most piping and fittings are located outside the frame. These are sufficiently dimensioned for the supply and distribution of 0.2 m³/s fresh water and 0.2 m³/s salt water, and for the discharge of 0.4 m³/s brackish water. The interconnecting pipes between

the feed headers and included valves enable a reversal of feed flows (salt water side becomes fresh water side, and vice versa) and a reversal of feed direction (supply header becomes collection header, and vice versa). This provides the possibility to clean the systems by applying osmotic shocks and to wash out the remnants of detached biofilms, respectively. Furthermore, each unit has its own electrical connection.

Another frame contains two rotating drum filters for the pre-treatment of both feed flows. Assuming a diameter $D = 1.7$ m and a length of $L = 4.5$ m per filter, the area per filter is 31 m^2 . Assuming a flux of $30 \text{ m}^3/\text{m}^2\cdot\text{h}$, the filter can easily supply the required $0.2 \text{ m}^3/\text{s}$. Since the filtrate comes out at atmospheric pressure, it is logical to locate the filter drums on a little higher level than the stacks (e.g., stacks on the first floor and stacks on the ground floor), enabling a gravitational flow from drum filter through the stacks to the outlet. With this hydraulic line, the feed pumps raise the level of the water from the inlet water surface to the water level within the filter drums, i.e., to a level of 5 m above the water level of the brackish water outlet. The actual head which has to be delivered by the pumps depends on the water level differences between intake and outlet.

A cost break-down was made (Table 5) by using detailed cost calculations from the supplying companies Hubert (drum filters) and Landustrie (piping, fittings and pumps). For the reverse electrodialysis stacks, the assumption was made of an installed membrane price of $2 \text{ €}/\text{m}^2$ (i.e., including end plates and electrodes). The mechanical and electrical construction for components of a 200 kW unit is less than 900,000 €. The cost price is less than $0.08 \text{ €}/\text{kWh}$. It appears that each component has about an equal contribution to the cost-price. However, it should be noted that the cost price is most sensitive to changes in the assumed membrane price and lifetime expectancy (all other components contain proven technologies with less uncertainties).

Table 5: Cost break-down for a 200 kW reverse electrodialysis unit on surface waters (in case of very clean industrial feed waters the costs for pre-treatment might be lower, resulting in a lower kWh-price).

Part	Construction costs (€)	Annual costs (€/y)			Cost price (€/kWh)⁵
		Capex³	Opex⁴	Total	
Frame with RED stacks ¹	200,000	37,000	6,000	43,000	0.027
Piping, fittings & pumps ²	320,000	28,000	10,000	38,000	0.024
Frame with filter drums ²	370,000	32,000	11,000	43,000	0.027
Total	890,000	97,000	27,000	124,000	0.079

¹Membrane lifetime 7 years; ²Depreciation in 20 year; ³Annuity depreciation: discount rate 6%;

⁴Operation and maintenance: 3% of construction costs; ⁵Production of 8,000 hours per year (base load)

7.4.2 Cost estimation for a 200 MW plant

With the 200 kW unit as a repetitive unit, a cost estimation could be made for a 200 MW plant consisting of 1,000 units. For the mechanical and electrical part, the investment costs of such a plant would benefit to a certain extent from the economy of scale. Instead of two small feed pumps per module, two pumping stations can be built for the total plant, for instance, each with 16 screw pumps of 12.5 m³/s with an average lift of 5 m. The mechanical and electrical investments for a 200 MW plant would, therefore, not exceed 900 million € (i.e., 1,000 times the construction costs of a 200 kW module).

However, on the other hand, a site should be purchased and industrial building needs to be built. The total volume of buildings is in the order of 200,000 m³. Taking into account a heavy construction and foundation due to the large amounts of water, the construction costs could be as high as 100 million € (i.e., a cost price of 500 €/m³). Moreover, site-specific additional infrastructure could be a large investment. However, these costs

for buildings and infrastructural works do not influence the overall cost price too much. This can be explained by the long lifetime expectancy of 40 years and relatively expenditures for operation and maintenance. For a 200 MW power plant, each 100 million € of investment in civil engineering would add 0.005 € to the cost price of a kWh.

7.4.3 Comparison with wind energy

In order to valuate the impact of 200 MW salinity-gradient power plant, a comparison is made with wind energy. With a load factor of ~90% (8,000 hours per year base load), such a reverse electrodialysis plant delivers on annual basis 1.6 billion kWh to the public network, which is enough for over 0.5 million households. In 2007, all 1,800 existing wind turbines in The Netherlands produced on annual basis 3.7 billion kWh [24]. A salinity-gradient power plant of this size would have a significant contribution to the green electricity production of the country.

Meanwhile, also in wind energy a lot of technical progress has been made. In the near future, new wind turbines will be able to produce 3-5 MW at peak power [24, 25]. These modern wind turbines have a diameter of approximately 100 meters, and the height of the axis is found 80 meters above ground level. When calculating the number of new wind turbines that are necessary to produce the same amount of electricity as the salinity-gradient power plant of 200 MW, the differences in load factors should be taken into account (25-30% for wind turbines; 90% for salinity-gradient power). One can find that 140-240 wind turbines are needed. With a mutual distance of approximately 200 m this would imply a line of 30-50 kilometres. The impact on the landscape is obviously bigger than that of a salinity-gradient power plant. Assuming the investment costs for wind turbines to be 1-2 €/W [25], the investment costs are 700-1.400 million €. Investment costs and cost prices of both technologies are thus comparable.

7.5 Further steps

7.5.1 Aimed location for first power plant

In the Netherlands, five locations have been identified for salinity-gradient energy. Two of these locations provide the opportunity for a large scale application, being the Afsluitdijk and the Dutch Delta. The Dutch Delta is interesting because of the enormous fresh water discharge, but requires more complicated infrastructural works. Despite of initial skepticism about applicability in the Dutch Delta [25], a recent model study showed that several alternative locations for salinity-gradient power plants of over 500 MW each are available [24]. On the shorter term, however, the ideal spot to realize reverse electrodialysis is the 30-km long Afsluitdijk in the North of The Netherlands (Figure 4).

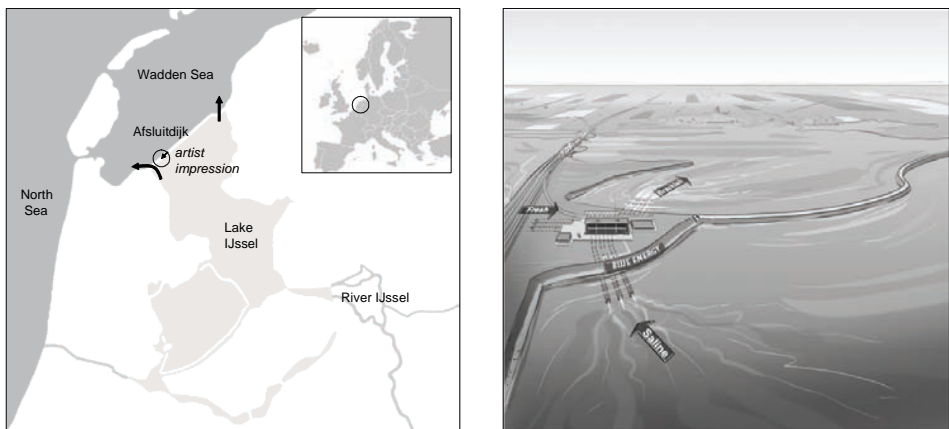


Figure 4: Map and artist impression of a salinity-gradient power plant at the Afsluitdijk (source: Rijkswaterstaat).

This dyke separates the 1100-km² fresh Lake IJssel from the saline Waddensea. In 1932 the lake was formed by closing of the Zuiderzee, the estuary of a couple of rivers with an average flow of 450 m³/s. The dike provides a strict separation of salt and fresh water. Large outlet sluices

Chapter 7

discharge water from the lake onto the Waddensea. Discharging the fresh water is not a continuous process but depends on tide levels on the Waddensea.

The flow that can be used for salinity-gradient energy at this location is quite large, i.e. on average $450 \text{ m}^3/\text{s}$. Statistic model calculations should verify that this flow can be made available for power generation during the main part of the year (in summer time less fresh water is available than in winter time). This should, however, not be a big issue given the fact that upstream the discharge distribution can be regulated to guarantee this discharge. Moreover, given the fact that Lake IJssel already serves as a fresh water storage, the lake can be used to absorb differences in the availability of fresh water.

The salinity of Lake IJssel is very low, around $0.2\text{-}0.5 \text{ g/L}$. The salinity of the Waddensea is difficult to determine due the discontinuous discharging process of the outlet sluices. Every time the sluices open their gates, a large fresh water bubble builds up. This bubble influences salt concentrations in the sea. Hydraulic models should be used to verify that in case all water from the Lake IJssel is continuously mixed with water from the Waddensea in a salinity-gradient power plant, the salinity would be almost as high as that of the North Sea of around 28 g/L . This salinity could be reached due to a better mixed Waddensea (continuous discharge of brackish water instead of fresh water bubbles) and due to the use of dominant flows at the Waddensea along the dike that provides the possibility of an upstream sea water intake and downstream brackish water release. Eventually, an additional embankment perpendicular to the Afsluitdijk is needed to enhance the separation of salt water and brackish water (Figure 4).

7.5.2 Scale-up: from pilot to full-scale

Before implementing reverse electrodialysis on a commercial scale, the feasibility of the technology should be proven in practice. The promising research and development of the technology raised interest of different industrial and energy companies and water authorities to invest in pilot facilities at the Afsluitdijk. Thus far, we are happy to find suppliers that are really prepared to take the opportunity to develop a prototype of a production line without an actual order for square km's of membranes. At this stage of the project, we focus on consortium building, with customers entering into technical development agreements with suppliers, joint design and test programs. The involved parties agreed on the following development path for scale-up of the system Table 6.

Table 6: Development path of reverse electrodialysis scale-up.

Project	Scale	Aim
2008-2010 Pilot on industrial water flows	kW-scale	First step out of the laboratory. Pilot on saline flows in a salt factory of Frisia in Harlingen (Financial supported by SenterNovem, Innovator project).
2008 Engineering of pilot on surface waters	-	Feasibility study and definition of requirements for a communal pilot on the Afsluitdijk (Private funding, 2008).
2010-2012 Pilot on surface waters	20-50 kW	Communal pilot on sea water and river water at the Afsluitdijk. Focus on 'design to work'.
2013-2015 Demonstration plant on surface waters	1 MW	Communal demonstration on sea water and river water at the Afsluitdijk. Focus on 'design to cost'.

7.5.3 Other issues for study

Reverse electrodialysis is a clean and sustainable technology. The sustainability should be further analyzed and proven in the near future based on the experiences from these pilots and demonstration plants. Currently, expectations are based on the construction and production of a power plant and its components; however, also attention should be drawn to the processing of the used materials (especially the membranes) at the end of their lifetime.

When applying salinity-gradient energy at a large scale it might be necessary to change the hydraulic system and water management rules, because a lot of fresh and salt water is needed. These measures should fit within legislation and regulations. The impact on the environment and ecological system (e.g., flora and fauna, water quality, bank morphology) of changing nutrient flows, sediment transport, changing local salinities and gradients, building a power plant etc., should be entirely studied on short notice. Also other interests of the water system (shipping, recreation) and infrastructural works (protection, water management) should be taken into account. These aspects will be crucial for the decision making process. Therefore, we recommend to take care of partnering with knowledge institutes of different disciplines, like hydraulic engineering and water resources management.

Acknowledgements

We thank Sjoerd Stelwagen (Landustrie) for preparing Figure 3. We thank Mr. Bernard B. Bligh, thermodynamics expert and inventor of several patents on reverse electrodialysis (GB 2197116, GB 2195818 and GB 2194855), for his valuable comments. The Senter Novem organization is gratefully acknowledged for their grants within the New Energy Research programme. We thank the European Membrane Institute and Kema for 184

their work for REDstack B.V. on membrane development. We thank Wetsus and especially the other participating companies Nuon, Frisia Zout, Eneco, Dow Chemical, and Fujifilm, for their partnership.

7.6 References

1. Pattle, R.E., Production of electric power by mixing fresh and salt water in the hydroelectric pile, *Nature* 174(4431) (1954), p. 660-660.
2. Wick, G.L. and W.R. Schmitt, Prospects for renewable energy from sea, *Marine Technology Society Journal* 11(5-6) (1977), p. 16-21.
3. Weinstein, J.N. and F.B. Leitz, Electric-power from difference in salinity - dialytic battery, *Science* 191(4227) (1976), p. 557-559.
4. Post, J.W., J. Veerman, H.V.M. Hamelers, G.J.W. Euverink, S.J. Metz, D.C. Nijmeijer and C.J.N. Buisman, Salinity-gradient power: Evaluation of pressure-retarded osmosis and reverse electrodialysis, *Journal of Membrane Science* 288 (2007), p. 218-230.
5. Jagur-Grodzinski, J. and R. Kramer, Novel process for direct conversion of free-energy of mixing into electric-power, *Industrial & Engineering Chemistry Process Design And Development* 25(2) (1986), p. 443-449.
6. Audinos, R., Electrodialyse inverse. Etude de l'énergie électrique obtenue à partir de deux solutions de salinités différentes, *Journal of Power Sources* 10 (1983), p. 203-217.
7. Lacey, R.E., Energy by reverse electrodialysis, *Ocean Engineering* 7(1) (1980), p. 1-47.
8. Turek, M. and B. Bandura, Renewable energy by reverse electrodialysis, *Desalination* 205 (2007), p. 67-74.
9. Veerman, J., J.W. Post, S.J. Metz, M. Saakes and G.J. Harmsen, Reducing power losses caused by ionic shortcut currents in reverse electrodialysis stacks by a validated model, *Journal of Membrane Science* 310 (2008), p. 418-430.
10. Veerman, J., M. Saakes, S.J. Metz and G.J. Harmsen, Reverse electrodialysis: Performance of a stack with 50 cells on the mixing of sea and river water., *Journal Of Membrane Science* 327 (2009), p. 136-144.
11. Post, J.W., H.V.M. Hamelers and C.J.N. Buisman, Energy recovery from controlled mixing salt and fresh water with a reverse electrodialysis system, *Environ Science Technology* 42 (2008), p. 5785-5790.
12. Post, J.W., H.V.M. Hamelers and C.J.N. Buisman, Influence of multivalent ions on power production from mixing salt and fresh water with a reverse electrodialysis system, *Journal of Membrane Science* 330 (2009), p. 65-72.
13. Długołęcki, P., D.C. Nijmeijer, S.J. Metz and M. Wessling, Current status of ion exchange membranes for power generation from salinity gradients, *Journal Of Membrane Science* 319(1-2) (2008), p. 214-222.
14. Dirkse, M.H., W.P.K. van Loon, J.D. Stigter, J.W. Post, J. Veerman and G.P.A. Bot, Extending potential flow modelling of flat-sheet geometries as applied in membrane-based systems, *Journal Of Membrane Science* 325 (2008), p. 537-545.
15. Sutherland, K., *Profile of the international membrane industry: Market prospects to 2008*. 2003, Amsterdam: Elsevier. 184.

Chapter 7

16. Schauer, J., L. Brozova, Z. Pientka and K. Bouzek, Heterogeneous ion-exchange polyethylene-based membranes with sulfonated poly(1,4-phenylene sulfide) particles, Desalination 200 (2006), p. 632-633.
17. Molau, G.E., Heterogeneous ion-exchange membranes, Journal of Membrane Science 8 (1981), p. 309-330.
18. Volesky, B., Markets for ion exchange resins and biosorbents, in "Biosorption technology" Company Brochure - Business Plan Summary. access date 2009-04-16, BV Sorbex, Inc.: St. Lambert (Montreal), available from <http://www.bvsorbex.net/sxMarkets.pdf>.
19. Van der Hoek, J.P., D.O. Rijnbende, C.J.O. Lokin, P.A.C. Bonné, M.T. Loonen and M.H. Hofman, Electrodialysis as an alternative for reverse osmosis in an integrated membrane system, Desalination 117 (1998), p. 159-172.
20. Vrouwenvelder, J.S., S.A. Manolarakis, J.P. van der Hoek, J.A.M. van Paassen, W.G.J. van der Meer, J.M.C. van Agmaal, H.D.M. Prummel, J.C. Kruijthof, and M.C.M. van Loosdrecht, Quantitative biofouling diagnosis in full scale nanofiltration and reverse osmosis installations, Water Research (42) (2008), p. 4856-4868.
21. Malfeito, J.J., J. Diaz-Caneja and A. Jimenez, Innovative sea water intake for reverse osmosis desalination plants, International journal of nuclear desalination (2008), p. 3-10.
22. Anderson, D.J., W.A. Timms and W.C. Glamore, Optimising subsurface well design for coastal desalination water harvesting, Australian journal of earth sciences (2009), p. 53-60.
23. Peeters, T. and D. Pintó, Seawater intake and pre-treatment/brine discharge - environmental issues, Desalination 221 (2008), p. 576-584.
24. Quak, R.W., Blue energy in dutch delta: Feasibility of a power plant, in Faculty of Civil Engineering and Geosciences, Department of Hydraulic Engineering. 2009, Delft University of Technology: Delft. p. 119.
25. Duurzaamheid duurt het langst. 2007, Amsterdam: Koninklijke Nederlandse Akademie van Wetenschappen.
26. Tyler-Walters, H., *Mytilus edulis*. Common mussel, in Marine Life Information Network: Biology and Sensitivity Key Information Sub-programme. 2008 (access date 2009-01-14), Marine Biological Association of the United Kingdom: Plymouth, available from <http://www.marlin.ac.uk/species/Mytilusedulis.htm>.

8 Global and national prospects of salinity-gradient energy

Salinity gradient power (or blue energy) is a renewable energy source mentioned in the literature since the 1950s. It refers to the production of electricity from mixing of two solutions with different salt concentrations, for example river and sea water. The global potential of salinity power has been estimated in the 1970s as substantial, but the state of the membrane technology at that time – crucial for energy recovery – did not permit practical use of this resource. More recently, the interest in salinity power has been growing, because of the need for carbon neutral, renewable sources of electricity. This chapter aims to assess the potential of salinity-gradient power. Firstly, we discuss the global potential, i.e. the theoretical and technical amount of energy that could be retrieved at river mouths. The analysis is based on global datasets of annual river discharges for 5,472 world rivers. The theoretical potential for salinity-gradient power is estimated at 1,724 GW. The technical potential – the share that can be recovered with current technology – is estimated at 983 GW. Secondly, the technical and economic potential of the rivers Rhine and Meuse (with their river mouth located in The Netherlands) is described in more detail. The technical potential for these rivers - as derived from the global datasets – is 2.4 GW. The economic potential is estimated to be 1.5 GW, when looking into more detail to the Dutch Delta.

Section 8.1 and 8.2 are based on the following MSc thesis and manuscripts:

Kuleszo, J.T., The global and regional potential of salinity-gradient power, Dept. Environmental Sciences, Environmental Systems Analysis Group. 2008, Wageningen University and Research centre: Wageningen [1].

Kuleszo, J.T., C. Kroese, J.W. Post, B.M. Fekete. The potential of Blue Energy to reduce emissions of CO₂ and non-CO₂ greenhouse gases, in Proceedings of the 5th International Symposium on Non-CO₂ Greenhouse Gases: Science, Control, Policy and Implementation. 2009. Wageningen, The Netherlands [2].

Section 8.3 is based on the following MSc thesis:

Quak, R.W., Blue energy in dutch delta: Feasibility of a power plant, in Faculty of Civil Engineering and Geosciences, Department of Hydraulic Engineering. 2009, Delft University of Technology: Delft [3].

8.1 Introduction

Salinity-gradient energy is a renewable energy source that was recognized already in the 1950s [4]. The energy can be made available from mixing of two solutions with different salt concentrations. When two salt solutions with different concentrations are brought into contact, they mix to form a homogeneous mixture. An example is the natural process of mixing river water with low electrolyte concentration and seawater with high electrolyte concentration. This natural process is irreversible; no work is attained from it. However, if the mixing is done (partly) reversibly, some work can be obtained from the mixing process. The mixing process should then be controlled by means of selective membranes. The use of selective membranes secures that the mixing is limited to one of the components, either the solvent (i.e. water molecules diffuses through semi-permeable membranes) or solutes (i.e. ions diffuses through perm-selective membranes). The energy obtained in this way is called salinity-gradient power, or according to the development program in The Netherlands: "Blue Energy".

The concept of using the salinity gradients for energy generation was being developed mainly in the 70's and 80's but the state of the membrane technology at that time – crucial to energy recovery – did not allow practical use of this resource. More recently, however, the salinity power has come back into focus as the need for renewable, carbon neutral power sources grows and need for membranes for other applications has advanced the technology. Until now several systems for retrieving energy from salinity gradients have been proposed, two of which seem to be in the most advanced stage: pressure-retarded osmosis [5-10] and reverse electrodialysis [11-13].

The power available globally in form of salinity gradients has been estimated in the 1970s (on the basis of average ocean salinity and annual

global river discharges) to be between 1.4 and 2.6 TW [14, 15]. These numbers give an idea of how substantial the resource is. Compared to other forms of marine energy, salinity gradient resources are in the same order as wave energy or thermal gradients and are 100 times higher than those of the tidal energy [16]. Or, 1.4 TW (12,279 TWh/y) should be able to satisfy over 80% of the current global electricity demand (15,746 TWh/y [17]). Replacing current and projected coal-fired power plants with salinity power plants could reduce global greenhouse gas emissions by 10 Pg CO₂-eq/year ($\sim 10^{10}$ tonnes/year), when calculated with standard emission factors [18, 19] and an efficiency for coal-fired power plants of 40%. This means a potential reduction of 40% of current global energy-related greenhouse gas emissions (40% of 28.9 Pg CO₂-eq/year [20]).

As an outlook to this thesis, we re-examine the prospects of the new technology more accurately and detailed. Such a re-examination is needed as our insight in the performance of the technology has grown and spatially referenced datasets and processing software are available that enable a study that was not possible in 1970's. When geographical location of the rivers and local sea salinities and temperatures are taken into consideration, the result is bound to be more accurate. Besides the spatial variation in the theoretical potential, calculated from the important parameters for salinity-gradient energy (i.e., volume, salinity and temperature), also the technical characteristics influencing the salinity gradient power potential were introduced. For these technical characteristics (e.g., obtainable energy recovery, pumping losses) estimates were made based on the experiences and research as presented in this thesis. Combining the increased insight in the performance of the technology and the now available datasets and software, we are now able to make estimates that were not possible before: (i) with a refined calculation of the global potential as no globally averaged values are used,

(ii) with a distinction between theoretical, technical, economic and exploitable potential, and (iii) with insight in regional and spatial patterns.

8.2 Estimating the global potential

8.2.1 Estimates of global and regional energy potential in literature

Apart from the two global salinity power assessments, some country-level estimations were done and a few assessments of selected rivers were performed. Recently, an assessment for Europe was done within the Salinity Power Project of Statkraft [21], however, this was a private estimate and was not published in scientific literature. Most research in the field of salinity-gradient power focused on the conversion techniques, but a more detailed and spatially explicit study on the global or regional potential of salinity power has not yet been conducted. In section 2.2 an overview is given from literature. Today, spatially referenced datasets and processing software are available. This makes it possible to assess the global potential in a spatially explicit way. In section 2.3 a more accurate study is presented to estimate the global and regional potential.

The difference between the two global salinity power potential estimates published by Isaacs and Seymour (1.4 TW; [15]) and by Wick and Schmitt (2.6 TW; [14]) shows that the figures are only approximate. The calculation method, assumptions and standards differed between authors. Isaacs and Seymour [15] did not specify how they obtained their result. Wick and Schmitt [14] used a standard osmotic pressure difference between fresh water and sea water (of 24 atm., after [22]). Other authors based calculations on the assumption that all of the ocean and river water is of uniform salinity and temperature. For the standard sea salinity, some used 0.5 mol/L and some 35ppt (\sim 0.6 mol/L). For the standard temperature, 20°C or 25°C were commonly used. As an example obtained from the datasets as we used (see next paragraph), the average sea water salinity is

Chapter 8

indeed close to 35 ppt but locally varies from 5ppt to 40ppt (with the highest values at the tropical latitudes) and the sea temperature ranges from -2°C to 30°C (with the highest temperatures at the equator). Also, the local salinities and temperatures change seasonally. The seasonal variation in salinity can reach up to 10ppt (in the northern basins) and the differences in temperature up to 28°C (Caspian Sea). Moreover, hypersaline basins are often associated with low river discharges, and big rivers with lower salinities of coastal waters.

Table 1: Estimates of the salinity-gradient power potential

Authors	Year	Region	Estimate	Estimate
			(original units)	(GW)
Isaacs and Seymour	[15]	1973	World	1,400 billions kW
Wick and Schmitt	[14]	1977	World	2.6 TW
Salinity Power Project	[21]	2004	Europe ^a	200 TWh/y
Norman	[23]	1974	US	120 \pm 10 ⁹ W
Jones and Finley	[24]	2003	Norway	25 TWh/y
Salinity Power Project	[21]	2004	Norway ^a	12 TWh/y
Isaacs and Schmitt	[16]	1980	Congo River (Zaire)	10 ⁵ MW
Loeb	[8]	2001	Jordan River (US)	66,300 kW
Norman	[23]	1974	Mississippi (US)	40,000 MW
Loeb	[25]	2002	Mississippi ^b (US)	9,800 MW

^a Economic potential, ^b Technical potential

Besides the estimates for the global potential, recently an estimate was done for Europe [21]. Also some country-level estimations have been done and a few assessments of selected rivers were performed. These estimates are presented in *Table 1*. Also on this level, remarkable differences of estimates can be found. These differences are not only caused by different assumptions and standards, but mainly due to different definitions of the potential. Implicitly or explicitly, some authors noted that not all potential energy can be used: for technical, environmental, economical or political

reasons. Therefore, a clear definition is required how these aspects affect the potential. We used a division of theoretical, technical, economic, and exploitable potential (based on Lehner et al. [26]), see *Table 2*.

8.2.2 More accurate estimate of global and regional energy potential

When geographical locations of rivers, their discharge as well as local sea salinities and temperatures are taken into consideration, the estimate is bound to be more accurate. This would also allow for identification of promising locations, where salinity gradients could be a significant source of energy. The energy dissipated at the river mouths (theoretical potential) as well as the maximum amount of energy that could be retrieved at the current state of technology (technical potential) were calculated with the use of data derived from spatial models. The result is a geographically referenced database of 5,472 world rivers with their respective theoretical and technical energy potentials [1]. Here, we summarize the approach and the results.

The amount of electricity that can be produced from a river flowing into the sea depends on a number of factors, including river and sea salinity and temperature, river water quantity and quality, river to sea water volume ratios, sea salt composition, salinity gradient steepness, infrastructure and local energy demand, and environmental impacts. We calculated the *theoretical potential* as a function of the annual river discharges, average sea salinities and temperatures at the river mouth, see *Table 2*. Taking all these parameters into account, the equations as presented by Forgacs [27] were used to calculate the theoretical energy potential¹.

¹ Equations are presented in chapter 2 and 3

Chapter 8

Table 2: Definitions and assumptions to calculate the energy potential

Potential	Definition	Assumptions
Theoretical potential	Energy that is potentially available if all energy being dissipated at the river mouths was harnessed without any energy losses	- Annual averaged river water discharge - Average sea salinity and temperature at river mouth (as if pure sodium chloride solutions) - 1 m ³ of river water mixing with 1 m ³ of sea water
Technical potential	Share of the theoretical energy that can be recovered with current technology, regardless other restrictions.	- Minimum monthly energy density (determined by monthly averages) - Energy recovery by current technologies ^[2] of 70% ^[3] - 50 kJ per m ³ water (13 Wh per m ³) is subtracted for transport and pre-treatment, i.e., for energy consumption of pumping ^[6]
Economic potential	Part of technical potential that can be developed at costs competitive with other energy sources.	- Chemical composition of feed water ^[4] - Fouling characteristics, dependent on water quality related to technology ^[5-6] - Site-specific study to identify required civil infrastructural works
Exploitable potential	Fraction of economical potential that can be used if the environmental, political and other unique constraints are accounted for.	- Site-specific study to identify the environmental impact, political agendas, and other specific constraints

^[2-6] Validated or investigated in this thesis: numbers refer to chapters

Two data sources were used. These are the World Ocean Database 2005 (WOD05) for salinity and temperature [28], and the global water balance model (WBM_{plus}) for river discharges and water quality [29-31].

The global *theoretical potential* for salinity-gradient power is 1,724 GW, see *Table 3*. For most continents the potential is about 300 GW. The continent with largest potential is Asia with 374 GW. Only Europe (94 GW) and Australia (30 GW) have significantly lower potentials.

We estimated the *technical potential* by accounting for the minimum monthly energy densities (energy available from 1 m³ of river water mixing with 1 m³ of sea water and determined by the monthly temperatures and salinities of sea water), annual river discharge, energy retrieval efficiencies (70%) and energy requirements of the power plants (50 kJ/m³), see *Table 2*. It should be noted that the latter assumptions, i.e., for energy recovery and energy requirements, are validated in chapter 3 and 7, respectively. The global *technical potential* is 983 GW, *Table 3*. This is nearly 60% of the theoretical potential (1,724 GW). This percentage changes slightly among regions, being highest for Australia (65%) and lowest for South America (47%).

For individual rivers the technical potential is 3 to 65% of the theoretical potential. Three quarters of the world technical salinity power potential is distributed evenly over Africa, Asia, North America and Oceania, with each an approximately 20% share in the total (175 - 206 GW). Among the rivers with high technical potentials for salinity power are the Zaire (57 GW), Orinoco (36 GW), Ganges (25 GW), Nile (21 GW), Mississippi (18 GW), St. Lawrence (16 GW), Parana (16 GW), Zambezi (15GW), and the Mekong (15 GW). We identified 123 rivers with technical potential exceeding 1 GW. These are usually large rivers. However, not all rivers with high discharge rates have high potentials for salinity power. For instance, the Amazon discharges three times more water as the Zaire. Yet, the Amazon is not among the ten rivers with the largest technical potential for salinity power.

Chapter 8

Table 3: Theoretical and technical potential of salinity gradient power by world region

Region	Number of rivers	Average discharge	Theoretical potential		Technical potential		
			% of total		GW	% of total	% of theoretical
			#	m ³ /s			
Africa	391	170,294	311	18	190	19	61
Asia	1,243	236,769	374	22	206	21	55
Australia	251	15,818	30	2	20	2	65
Europe	779	74,569	94	5	56	6	59
North America	1,878	191,434	321	19	189	19	59
Oceania	540	149,748	278	16	175	18	63
South America	390	320,078	316	18	148	15	47
World	5,472	1,158,709	1,724	100	983	100	57

A clear spatial pattern in salinity power potential can be observed: the rivers with low technical potential compared to their theoretical potential are the ones in the North, where generally salinity and temperature variation (the two factors influencing energy density) is high and energy density is low. Similarly, for the rivers draining into the Baltic and Caspian Sea the percentage of the theoretical potential can be technically recovered is low. However, because the theoretical potential of these rivers is small their impact on the overall technical potential is not large. South American rivers draining at the equatorial latitudes have a substantial lower technical potential relative to theoretical potential. The Amazon, for instance, is a river that may not be as useful as others for salinity gradient power generation because of the very low energy density (both technical and theoretical). Particular geomorphologic characteristics (shape of the coastline and a large number of other rivers draining in that area) cause less mixing with sea water at the river mouth and formation of a fresh water plume. A similar, but much smaller, plume can be also observed at the Zaire. Such effect can easily take place on a smaller scale at other river

mouths, not noticeable at the used data resolution. Therefore, the specific characteristics of the river mouths would be an important factor for more detailed technical potential assessments in future research.

When considering geographical sites suitable for salinity power plants, Charlier [32] wrote that “the most promising locations are those at the mouths of powerful rivers [and] hypersaline basins [...]. This is only partially true. Hypersaline basins are associated with low river discharges, and big rivers with lower salinities of coastal waters. It might be necessary to choose between high energy density or high power retrievable when looking for a good location for a salinity-gradient power plant.

It should be noted that our estimates for the technical potential only consider the technical limitations associated with physical and technical characteristics of the rivers and the power plants. We did not consider that water quality may also affect the actual potential of salinity power. We also did not assess the many economical, institutional and practical issues that determine the actual feasibility of salinity gradient power. And we ignore morphological aspects. Our estimates of the technical potentials as in *Table 3* must, therefore, be considered as upper estimates.

8.3 Economic potential of rivers Rhine and Meuse

The river Rhine is amongst the most ‘energetic’ rivers from Europe. The estimated technical potential is 2.0 GW, which is 62% of the theoretical potential. The Rhine enters The Netherlands at Lobith near the city of Arnhem at the border with Germany. Before entering the sea, it is combined with the river Meuse (technical potential 0.4 GW). So the total technical potential of Rhine and Meuse is 2.4 GW. In order to see how the technical potential can be translated to an economic potential (as defined in Table 2), we studied the river mouth of the Rhine and Meuse in more detail to identify physical locations for power plants [3].

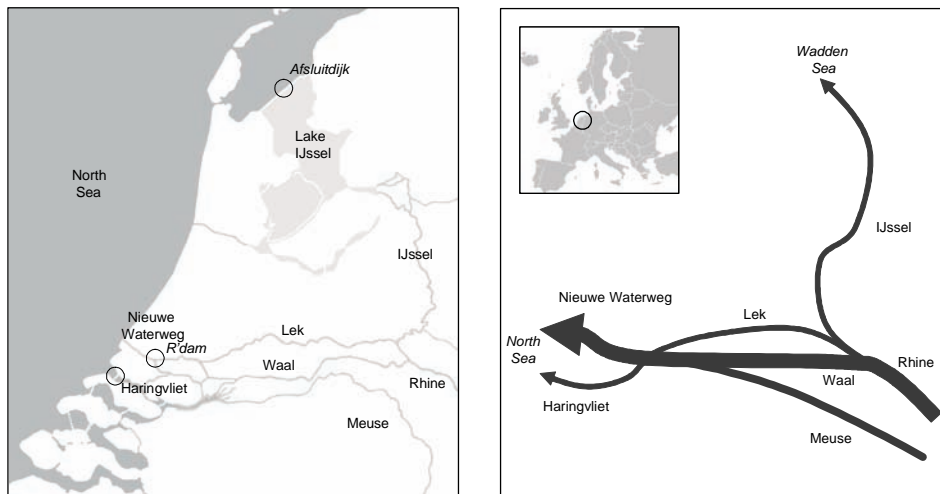


Figure 1: Map and schematic overview of river mouth of Rhine and Meuse

The river mouth of Rhine and Meuse is schematically divided in three branches (*Figure 1*): IJssel, Nieuwe Waterweg, and Haringvliet. The first branch is the river IJssel, which ends in the Lake IJssel. When at present the water level at the Wadden Sea is low enough, the stored water in Lake IJssel is discharged through sluices with an average discharge of $450 \text{ m}^3/\text{s}$. A big advantage of this location is the availability of the strict separation between salt and fresh water. Furthermore, fresh water is abundantly available, and with Lake IJssel there is a large buffer which can be used. A level fluctuation on the lake of 50 cm provides a buffer of 0.55 km^3 , which is enough to ensure the average fresh water flow for more than 14 days. A disadvantage of this location might be the lack of availability of really salt water. Calculations have to show to what extent the Wadden Sea is able to refresh the brackish water, which is discharged by the power plant, fast enough. On this location, it might well be possible to use the full technical potential of 450 MW [3].

The main part of the Rhine water flows through the Lek and the Waal. These two rivers split in the eastern part of the country, and converge

again in the western part of the country. Within the Dutch Delta the water can be discharged to the North Sea in two different ways. The northern branch is called Nieuwe Waterweg with an average discharge of 1,300 m³/s. This is an open connection for the harbor of Rotterdam with the North Sea. The availability of fresh water at this location is questionable as salt intrusion makes the Nieuwe Waterweg brackish over a long distance. To make this huge flow of Rhine water available for a power plant, the water management system should be changed significantly. The feasibility of this location is dependent on the impact on shipping activities as the Nieuwe Waterweg is extensively used by seagoing vessels and inland navigation. At first sight, this makes the Nieuwe Waterweg unsuitable for a salinity power plant. However, a detailed hydraulic study [3] showed that at an upstream location at the Botlek, in the Port of Rotterdam, has promising prospects. Fresh water can be diverted from river Oude Maas (average discharge is 600-700m³/s). Salt water at this location can be provided by the Hartelkanaal by changing its flow regime to an inland directed salt water discharge. This canal allows a supply of 500-700m³/s. The brackish water can be discharged via the Nieuwe Waterweg. The study showed that there is hardly a recirculation between the salt water inlet of the Hartelkanaal and the brackish water outlet of the Nieuwe Waterweg. The influence on the total hydraulic system is considerable, but not insuperable. The implementation of a power plant at this location certainly causes economic damage to inland navigation due to the need of shipping locks in the Oude Maas and Hartelkanaal. The study concluded that a power plant of 500MW in the Botlek is possible.

Furthermore, the water of the Rhine can be discharged via the southern branch through the Hollands Diep and Haringvliet. At the mouth of the Haringvliet, large outlet sluices are located with an average discharge of 800 m³/s. When the water level at the North Sea is low enough, these sluices can be opened to discharge water from the Haringvliet into the

Chapter 8

North Sea. These sluices are the main instrument to direct the flow of the Rhine to the northern or the southern branch. In closed situation almost the total flow will pass through Rotterdam and the Nieuwe Waterweg. When opened, part of the flow is directed to the Haringvliet. When keeping the Delta in its present state, it might be possible to build a power plant at this location. The challenge for this location is the separation of the inlet of salt water and the outlet of brackish water. When taking salt water directly from the North Sea, recirculation will definitely occur. Another issue is the availability of fresh water at low Rhine discharge. Maintaining the flow in the southern branch (Haringvliet) to a certain level would mean a decreasing flow through the northern branch (Nieuwe Waterweg). The salt intrusion might than increase in the Nieuwe Waterweg. Besides this, neither other drastic hydraulic changes nor undesirable additional barriers for shipping have to be introduced. A technical potential of 500-600 MW at Haringvliet sluices could be achieved [3].

If all these options are aggregated and interactions between the locations are neglected, the economic potential of the river mouth of the Rhine and Meuse could be 1.5 GW, which is >60% of the estimated technical potential (and 40% of the theoretical potential). This economic potential is quite substantial for The Netherlands, as it could cover the electricity demand of over 4 million households (>50% of the total). In order to find out the exploitable potential, for each site an entire study should be made to the impact on the environment and ecological system (e.g., flora and fauna, water quality, bank morphology) due to changing nutrient flows and sediment transport, changing local salinities and gradients, building infrastructural works for the power plant, etc.

8.4 Conclusion of the thesis

We started this thesis with the promising – but highly theoretical - estimates of the global potential of salinity-gradient energy or Blue Energy. The scope of this thesis was to investigate and solve the identified technical constraints of reverse electrodialysis that are crucial for the successful exploitation of salinity gradient energy. With the improved technology and the gained technical expertise, we were able to end this thesis with a thorough re-examination of the prospects of this new technology, on global and national level. The promising prospects, especially for Netherlands where salinity gradients could become a significant source of energy, lead to a strong recommendation to policy makers, captains of industry, and principal scientists to proceed with research and development of reverse electrodialysis.

Acknowledgements

This chapter was written based on the excellent MSc-theses of Joanna Kuleszo and Rutger Quak. Joanna Kuleszo obtained her MSc-degree in Environmental Science in May 2008 from the Department Environmental Sciences, Environmental Systems Analysis Group, Wageningen University and Research Centre. Rutger Quak obtained his MSc-degree in Civil Engineering in April 2009 from the Department of Hydraulic Engineering, Faculty of Civil Engineering and Geosciences, Delft University of Technology. Their departments and supervisors are fully acknowledged for their supervision and for giving me the opportunity to supervise their students as well.

8.5 References

1. Kuleszo, J.T., The global and regional potential of salinity-gradient power, in Dept. Environmental Sciences, Environmental Systems Analysis Group. 2008, Wageningen University and Research centre: Wageningen. p. 71.
2. Kuleszo, J.T., C. Kroese, J.W. Post and B.M. Fekete. The potential of blue energy to reduce emissions of co₂ and non-co₂ greenhouse gases, in 5th International Symposium on Non-CO₂ Greenhouse Gases: Science, Control, Policy and Implementation. 2009. Wageningen.
3. Quak, R.W., Blue energy in dutch delta: Feasibility of a power plant, in Faculty of Civil Engineering and Geosciences, Department of Hydraulic Engineering. 2009, Delft University of Technology: Delft. p. 119.
4. Pattle, R.E., Production of electric power by mixing fresh and salt water in the hydroelectric pile, *Nature* 174(4431) (1954), p. 660-660.
5. Jellinek, H.H.G. and H. Masuda, Osmo-power. Theory and performance of an osmo-power pilot plant, *Ocean Engineering* 8(2) (1981), p. 103-128.
6. Loeb, S., Osmotic power plants, *Science* 189(4203) (1975), p. 654-655.
7. Loeb, S., Production of energy from concentrated brines by pressure-retarded osmosis: I. Preliminary technical and economic correlations, *Journal of Membrane Science* 1 (1976), p. 49-63.
8. Loeb, S., One hundred and thirty benign and renewable megawatts from great salt lake? The possibilities of hydroelectric power by pressure-retarded osmosis, *Desalination* 141(1) (2001), p. 85-91.
9. Loeb, S., F. Van Hessen and D. Shahaf, Production of energy from concentrated brines by pressure retarded osmosis. II. Experimental results and projected energy costs, *Journal of Membrane Science* 1(3) (1976), p. 249-269.
10. Panyor, L., Renewable energy from dilution of salt water with fresh water: Pressure retarded osmosis, *Desalination* 199(1-3) (2006), p. 408-410.
11. Lacey, R.E., Energy by reverse electrodialysis, *Ocean Engineering* 7(1) (1980), p. 1-47.
12. Weinstein, J.N. and F.B. Leitz, Electric-power from difference in salinity - dialytic battery, *Science* 191(4227) (1976), p. 557-559.
13. Jagur-Grodzinski, J. and R. Kramer, Novel process for direct conversion of free-energy of mixing into electric-power, *Industrial & Engineering Chemistry Process Design And Development* 25(2) (1986), p. 443-449.
14. Wick, G.L. and W.R. Schmitt, Prospects for renewable energy from sea, *Marine Technology Society Journal* 11(5-6) (1977), p. 16-21.
15. Isaacs, J.D. and R.J. Seymour, The ocean as a power resource, *International Journal of Environmental Studies* 4(1) (1973), p. 201-205.
16. Isaacs, J.D. and W.R. Schmitt, Ocean energy: Forms and prospects, *Science* 207(4428) (1980), p. 265-273.
17. IEO, International energy outlook 2007. Office of integrated analysis and forecasting, energy information administration. 2007, Washington D.C.: U.S. Department of energy.
18. IPCC, Guidelines for national greenhouse gas inventories. Vol. 2. 2006.
19. Boudri, J.C., L. Hordijk, C. Kroese, M. Amann, J. Cofala, I. Bertok, L. Junfeng, D. Lin, Z. Shuang, H. Runqing, T.S. Panwar, S. Gupta, S. Singh, A. Kumar, M.C. Vipradas, P. Dadhich, N.S. Prasad, and L. Srivastava, The potential contribution of renewable energy in air pollution abatement in china and india, *Energy Policy* 30 (2002), p. 409-424.

20. Olivier, J.G.J., J.A. Van Aardenne, F. Dentener, V. Pagliari, L.N. Ganzeveld and J.A.H.W. Peters, Recent trends in global greenhouse gas emissions: Regional trends 1970-2000 and spatial distribution of key sources in 2000, *Env. Sc.*, 2(2-3) (2005), p. 81-99.
21. The salinity power project. 2004.
22. Bromley, L.A., D. Singh, P. Ray, S. Sridhar and S.M. Read, Thermodynamic properties of sea salt solutions, *American Institute of Chemical Engineering Journal* 20(2) (1974), p. 326-335.
23. Norman, R.S., Water salination: A source of energy, *Science* 4161 (1974), p. 350-352.
24. Jones, A.T. and W. Finley. Recent development in salinity gradient power, in proceedings of Oceans 2003. 2003.
25. Loeb, S., Large-scale power production by pressure-retarded osmosis, using river water and sea water passing through spiral modules, *Desalination* 143 (2002), p. 115-122.
26. Lehner, B., G. Czisch and S. Vassolo, The impact of global change on the hydropower potential of europe: A model-based analysis, *Energy Policy* 33(7) (2005), p. 839-855.
27. Forgacs, C., Recent developments in the utilization of salinity power, *Desalination* 40(1-2) (1982), p. 191-195.
28. Boyer, T.P., J.I. Antonov, H.E. Garcia, D.R. Johnson, R.A. Locarnini, A.V. Mishonov, M.T. Pitcher, O.K. Baranova, and I.V. Smolyar, *World ocean database 2005*. 2006, U.S. Government Printing Office: Washington, D.C.
29. Fekete, B.M., D. Wisser, C. Kroeze, E. Mayorga, A.F. Bouwman and W.M. Wollheim, Scenario drivers (1970-2050): Climate and hydrological alterations, *Global Biogeochemical Cycles*, submitted (2009), p.
30. Vorosmarty, C.J., B.M. Fekete, M. Meybeck and R.B. Lammers, Geomorphometric attributes of the global system of rivers at 30-minute spatial resolution, *Journal of Hydrology* 237(1-2) (2000), p. 17-39.
31. Vorosmarty, C.J., B.M. Fekete, M. Meybeck and R.B. Lammers, Global system of rivers: Its role in organizing continental land mass and defining land-to-ocean linkages, *Global Biogeochemical Cycles* 14(2) (2000), p. 599-621.
32. Charlier, R.H., Oceans and electrical power (part i), *International Journal of Environmental Studies* 18(3) (1982), p. 159-168.

Summary and discussion

Blue Energy

Blue energy is a popular term for salinity-gradient energy, indicating the theoretical non-expansion work that can be produced from mixing two salt solutions with different concentrations. In thermodynamics, it is defined by the Gibbs energy of mixing, see **chapter 1**. The theoretically available amount of energy from mixing 1 m³ sea water (comparable to 0.5 mol/L NaCl) and 1 m³ river water (comparable to 0.01 mol/L NaCl) both at a temperature of 293 K, is 1.4 MJ. Blue Energy is a promising renewable energy source for the future. In densely populated delta areas, where rivers with a low salinity flows in to the saline sea, the potential is enormous. Estimates from literature predicted coverage of over 80% of the current global electricity demand. This means a potential reduction of 40% of global energy-related greenhouse gas emissions.

Selection of reverse electrodialysis for Blue Energy

Pressure-retarded osmosis and reverse electrodialysis are the most frequently studied membrane-based processes for energy conversion of salinity-gradient energy. In **chapter 2** both techniques are described. One technique is based on the transport of water molecules, the other on the transport of ions. In pressure-retarded osmosis, the water molecules move through semi-permeable membrane from the fresh water to the saline water until the ion concentrations on both sides of the membrane are equal. This creates a high pressure in the compartment with the saline water. With this pressure, a turbine can be driven to produce electricity. In reverse electrodialysis, the ions move through ion-selective membranes from the saline water to the fresh water until the ion concentrations on both sides of the membranes are equal. The anions are transported in the

Summary / Samenvatting

direction of an anode, the cations in the direction of a cathode. This charge transport can be converted to electricity by electrochemical reactions at these electrodes. From the literature, a comparison is not possible since the reported performances are not comparable. A method was developed which allows for a comparison of both techniques at equal conditions, with respect to power density and energy recovery. Based on the results from the model calculations, each technique has its own field of application. Pressure-retarded osmosis seems to be more attractive for power generation using concentrated saline brines because of the higher power density combined with higher energy recovery. Reverse electrodialysis seems to be more attractive for power generation using sea water and river water. Keeping in mind the huge energy potential of river mouths, reverse electrodialysis was selected for further investigation in this thesis.

Over 80% of energy can be recovered

In practice, the feed waters should be pumped up and pre-treated before entering the reverse electrodialysis stacks. These energy-consuming and capital-intensive efforts should be paid back by the production of sustainable electricity. A main question, therefore, is how much of this salinity-gradient energy can be converted into sustainable electricity. From the review in chapter 2, however, we found that actually hardly attention was paid to the energetic efficiency. Described experiments focused on power output or power density whereas the energy recovery was never directly measured. In **chapter 3** we proved that no fundamental obstacle exists to achieve an energy recovery of >80%. This number was obtained with taking into account no more than the energetic losses for ionic transport. Regarding the feasibility, it was assumed to be a necessary but not sufficient condition that these internal losses are limited. The internal losses could be minimized by reducing the inter-membrane distance, especially from the compartments filled with the low-conducting river

water. It was found that a reduction from 0.5 mm to 0.2 mm indeed could be beneficial, although not to the expected extent. From an evaluation of the internal losses, it was supposed that besides the compartment thickness, also the geometry of the spacer affects the internal resistance.

First steps to application: chemical composition and fouling

In the research on reverse electrodialysis, so far, the presence of other ions than sodium and chloride was hardly taken into account. However, in most practical cases also other ions are present in both feed solutions. In **chapter 4** we investigated the influence of multivalent ions on stack voltage and ion transport in the stack. We also investigated whether monovalent-selective ion-exchange membranes can be used to improve the performance of reverse electrodialysis. Results show that, besides a higher stack resistance in presence of multivalent ions, especially the presence of multivalent ions in the dilute solution has a lowering effect on the stack voltage. This can be explained by an observed transport of these ions from the diluted electrolyte solution to the concentrated electrolyte solution. In order to prevent or hamper this transport against the concentration gradient, monovalent-selective membranes can be used. This shows indeed better results with respect to the stack voltage. Therefore, it would be beneficial to use monovalent-selective membranes in reverse electrodialysis, especially in the case of a relatively high content of multivalent ions in the dilute (i.e., in the first stages of the installation where the sodium chloride content in the dilute is still relatively low).

Applying the system on feed waters with different chemical compositions as in chapter 4 may be the first step to practice, a second step is to investigate how reverse electrodialysis behaves when applied to biological active feed waters. Fouling of ion exchange membranes is considered to be one of the most important limitations for practical use of electrodialysis processes. Despite of this, little is known about the effects of fouling on the

Summary / Samenvatting

reverse electrodialysis process. In **chapter 5**, we focused on biofouling. It appeared that biofouling is primarily causing clogging of the flow channels and spacers. This clogging results in an increase of the energy losses for pumping. Cleaning with biocides or by feed water reversal (osmotic shocks) were applied but appeared to be not able to restore the system performances. It might well be that these measures inactivate the biofilm organisms, however, it did not improve the hydrodynamic resistance and electrical resistance when the inactivated biomass is left where it was. Preventive operational steps, such as a periodically applied feed water reversal (e.g., once per hour) combined with a flow direction reversal, hampered the biofouling significantly. Under worst case conditions as applied in our experiments to accelerate biofouling, the possible operational period increased from 5 days to 20 days. In order to answer the question if this can be considered as the final solution against biofouling in practice, the method of accelerated biofouling need to be validated with data from pilot tests. A combination of redesigned stacks, pre-treatment, additional operational measures, and cleaning procedures may be the way to restrict biofouling at minimum cost.

To a new stack design for reverse electrodialysis

In chapter 3, we addressed that the screen spacers between the membranes are of major importance regarding the internal losses of reverse electrodialysis. The spacers are not only identified as undesired isolators, but from chapter 5 it became clear that they also form a place for biofilm accumulation causing pressure drop increases and a subsequent decline of the electrical performances. The objective of **chapter 6** was to give a proof of principle of the spacerless reverse electrodialysis system, firstly on electrical performance and secondly on biofouling behaviour. A spacer-free stack design is not yet available. Therefore, we invented a stack design in which membranes are separated by two thin gaskets that form

together an open non-woven structure. This resulted indeed in a remarkable decrease in ohmic resistance of about a factor 2. However, the non-ohmic resistance of the stack without spacers was significantly higher, possibly due to a higher concentration polarization than in a stack with spacers (spacers are often called turbulence promoters). This concentration polarization could be prevented by other measures, e.g. with introducing heterogeneities at the membrane surfaces and applying gas sparging. Also from the perspective of biofouling, it was experimentally proven that obtaining a stack design without spacers is a good direction for further development of reverse electrodialysis.

Discussion on challenges and prospects

Wetsus - centre for sustainable water technology in the Netherlands - started in 2005 with the project 'Blue Energy' with a focus on reverse electrodialysis. The achievements of previous chapters, but also from relating academic research within the Wetsus network, formed the starting point of **chapter 7**. In this chapter, we discussed the challenges we are facing concerning the economic and technological feasibility. The following issues were discussed: (i) the challenge to achieve low-cost membranes at huge quantities can be overcome when looking to the comparable commodity market for ion-exchange resins, (ii) the challenge of a low-cost and low-energy-consuming process design can be met with applying a simple drumfilter as pre-treatment before a spacer-free stack, and (iii) the economic feasibility of an engineered 200 kW unit learns that Blue Energy can compete with wind energy. Further steps on the developing path of reverse electrodialysis were presented. The next recommended step is to start a scaled-up pilot test on the Afsluitdijk (The Netherlands), together with accompanying studies regarding the ecological and hydrological aspects.

Summary / Samenvatting

In **chapter 8** we estimated the prospects of the new technology more accurately on global and national level. The theoretical potential for salinity-gradient power is estimated at 1,724 GW. The technical potential – the share that can be recovered with current technology – is estimated at 983 GW. The technical and economic potential of the rivers Rhine and Meuse (with their river mouth located in The Netherlands) is described in more detail. The technical potential for these rivers - as derived from the global datasets – is 2.4 GW. The economic potential is estimated to be 1.5 GW, after looking into more detail to the Dutch Delta. The promising prospects, especially for Netherlands where salinity gradients could be a significant source of energy, leads to a strong recommendation to policy makers, captains of industry, and principal scientists to proceed with research and development of reverse electrodialysis.

Samenvatting en discussie

Blauwe energie

Blauwe energie is een populaire term voor energie uit zoutgradiënten, ofwel de theoretische hoeveelheid arbeid (niet expansie) die kan worden geproduceerd door het mengen van twee zoutoplossingen met verschillende concentraties. In de thermodynamica is dit gedefinieerd door de Gibbs-vrije energie van het mengen, zie **hoofdstuk 1**. De theoretisch beschikbare hoeveelheid energie van het mengen van 1 m³ zeewater (vergelijkbaar met 0,5 mol/L NaCl) en 1 m³ rivierwater (vergelijkbaar met 0,01 mol/L NaCl), beide met een temperatuur van 293 K, is 1,4 MJ. Blue Energy is een veelbelovende hernieuwbare energiebron voor de toekomst. In dichtbevolkte deltagebieden, waar de rivieren met een laag zoutgehalte uitstromen in de zoute zee, is het potentieel enorm. Schattingen uit de literatuur voorspellen een potentie van meer dan 80% van de huidige mondiale vraag naar elektriciteit. Dit betekent een potentiële vermindering van 40% van de mondiale energie-gerelateerde uitstoot van broeikasgassen.

Selectie van omgekeerde elektrodialyse voor Blue Energy

Onderdrukte osmose en omgekeerde elektrodialyse zijn de meest bestudeerde membraan-gebaseerde processen voor energie-omzetting uit zoutgradiënten. In **hoofdstuk 2** worden beide technieken beschreven. De ene techniek is gebaseerd op het transport van watermoleculen, de andere op het transport van ionen. In onderdrukte osmose bewegen de watermoleculen door een halfdoorlatend membraan van het zoete water naar het zoute water, totdat de ionenconcentraties aan beide zijden van het membraan gelijk zijn. Hierdoor ontstaat een hoge druk in het

Summary / Samenvatting

compartiment met het zoute water. Met deze druk kan een turbine aangedreven worden om elektriciteit te produceren. In omgekeerde elektrodialyse bewegen de ionen door ion-selectieve membranen van het zoute water naar het zoete water, totdat de ionenconcentraties aan beide zijden van de membranen gelijk zijn. De anionen worden in de richting van een anode getransporteerd, de kationen in de richting van een kathode. Dit ladingstransport kan worden omgezet in elektriciteit met behulp van elektrochemische reacties aan deze elektroden. Gebaseerd op de literatuur is een eerlijke vergelijking van de technieken niet mogelijk, omdat de gerapporteerde resultaten onvergelijkbaar zijn. Om een vergelijking van beide technieken, onder dezelfde condities, mogelijk te maken is een model ontwikkeld voor de vermogensdichtheid en energieterugwinning. De resultaten van deze modelberekeningen wijzen uit dat elke techniek zijn eigen toepassingsgebied heeft. Onderdrukte osmose lijkt aantrekkelijker voor de opwekking van energie uit geconcentreerde zoutstromen (brijns) vanwege de hogere vermogensdichtheid in combinatie met een hogere mate van energieterugwinning. Omgekeerde elektrodialyse lijkt aantrekkelijker voor de opwekking van energie uit zeewater en rivierwater. Met het enorme energiepotentieel van riviermondingen in gedachten, is daarom gekozen om omgekeerde elektrodialyse nader te onderzoeken in dit proefschrift.

Ruim 80% van de energie kan worden teruggewonnen

In de praktijk moeten de voedingsstromen worden opgepompt en worden behandeld voordat ze de omgekeerde elektrodialyse stacks ingaan. Deze energie-consumerende en kapitaal-intensieve inspanningen moeten worden terugverdiend met de productie van duurzame elektriciteit. Een belangrijke vraag is daarom hoeveel van de energie uit zoutgradiënten kan worden omgezet in duurzame elektriciteit. Uit de evaluatie in hoofdstuk 2 hebben we echter vastgesteld dat in het verleden eigenlijk nauwelijks

aandacht werd besteed aan de energetische efficiëntie. Beschreven experimenten zijn gericht op het vermogen of vermogensdichtheid, maar de energieterugwinning is nooit rechtstreeks gemeten. In **hoofdstuk 3** wordt aangetoond dat er geen fundamenteel obstakel bestaat om te komen tot >80% energieterugwinning. Dit is experimenteel behaald, waarbij alleen rekening is gehouden met de energetische verliezen voor ion-transport. Voor de haalbaarheid is het een noodzakelijke - maar niet voldoende - voorwaarde dat deze interne verliezen worden beperkt. De interne verliezen kunnen worden geminimaliseerd door een verkleining van de afstand tussen de membranen, met name die van de compartimenten gevuld met rivierwater met lage geleiding. Er werd vastgesteld dat een verkleining van 0,5 mm tot 0,2 mm inderdaad een verbetering geeft, hoewel niet in de verwachte mate. Uit een evaluatie van de interne verliezen wordt verondersteld dat - naast de dikte van de compartimenten - ook de geometrie van de spacer van invloed is op de interne weerstand.

Eerste stappen naar toepassing: chemische samenstelling en vervuiling

Tot nu toe is in het onderzoek naar omgekeerde elektrodialyse nauwelijks rekening gehouden met de aanwezigheid van andere ionen dan natrium en chloride. In de meeste praktische gevallen zullen echter ook andere ionen aanwezig zijn in beide oplossingen. In **hoofdstuk 4** onderzochten we de invloed van multivalente ionen op de stackspanning en het ion-transport in de stack. We hebben ook onderzocht of monovalent-selectieve membranen kunnen worden gebruikt voor het verbeteren van de prestaties van omgekeerde elektrodialyse. In aanwezigheid van multivalente ionen is de interne weerstand van de stack niet alleen hoger, het geeft bovendien – met name de aanwezigheid van multivalente ionen in de verdunde oplossing – een verlaging van het stackvoltage. Dit kan worden verklaard door een waargenomen transport van deze ionen uit de verdunde elektrolyt-

Summary / Samenvatting

oplossing naar de geconcentreerde elektrolyt-oplossing. Om dit transport tegen de concentratiegradiënt te voorkomen of te belemmeren zouden monovalent-selectieve membranen kunnen worden gebruikt. Dit blijkt inderdaad betere resultaten te geven met betrekking tot het stackvoltage. Daarom kan het voordelig zijn om monovalent-selectieve membranen in omgekeerde elektrodialyse toe te passen, met name in het geval van een relatief hoog gehalte aan multivalente ionen in de verdunde oplossing (dat wil zeggen: in de eerste ‘stage’ van de installatie waar het natrium chloride gehalte van de verdunde oplossing nog relatief laag is).

Toepassing van het systeem op voedingswaters met verschillende chemische samenstellingen, zoals in hoofdstuk 4, kan gezien worden als de eerste stap naar de praktijk. Een tweede stap is te onderzoeken hoe omgekeerde elektrodialyse zich gedraagt in toepassing op biologisch-actieve voedingswaters. Biologische aangroei op ionenwisselende membranen (biofouling) wordt beschouwd als een van de belangrijkste hindernissen voor het praktische gebruik van elektrodialyse processen. In weerwil van het belang is er echter weinig bekend over de effecten van biologische aangroei op het omgekeerde elektrodialyse proces. In **hoofdstuk 5** richtten we ons daarom op biofouling. Biofouling veroorzaakt voornamelijk verstopping van de voedingskanalen en spacers. Deze verstopping resulteert in een stijging van de pompenergieverliezen. Reiniging met biociden of omkering van de waterstromen (osmotische schokken) werden toegepast, maar bleken niet in staat om het systeem te herstellen. Weliswaar is het mogelijk dat deze maatregelen de biofilm-organismen inactiveren, maar ze verbeteren niet de hydrodynamische weerstand en elektrische weerstand zolang de geïnactiveerde biomassa niet verwijderd wordt. Preventieve stappen, zoals een periodiek toegepaste omkering van de voedingsstromen (bijvoorbeeld een keer per uur) in combinatie met een omkering van de stroomrichting, verhindert de biofouling aanzienlijk. Onder de slechtst denkbare omstandigheden, zoals

214

toegepast in onze experimenten om de biofouling te versnellen, verlengden deze maatregelen de mogelijke operationele periode van 5 dagen tot 20 dagen. Ter beantwoording van de vraag of dit kan worden beschouwd als de definitieve oplossing tegen biofouling in de praktijk zou de toegepaste methode van versnelde biofouling moeten worden gevalideerd met gegevens van pilot-installaties. Biofouling kan in ieder geval wel bestreden worden tegen minimale kosten door toepassing van een combinatie van herontworpen stacks, voorbehandeling, aanvullende operationele maatregelen en reinigingsmethoden.

Naar een nieuw stack-ontwerp voor omgekeerde elektrodialyse

In hoofdstuk 3 hebben we geconcludeerd dat de spacers tussen de membranen van groot belang zijn met betrekking tot de interne verliezen van omgekeerde elektrodialyse. De spacers zijn niet alleen geïdentificeerd als ongewenste isolatoren, maar uit hoofdstuk 5 is duidelijk geworden dat ze ook een plek zijn voor biofilm-accumulatie waardoor de drukval toeneemt en - daaropvolgend - de elektrische prestatie afneemt. Het doel van **hoofdstuk 6** is om een bewijs te geven van het principe van een omgekeerde elektrodialyse zonder spacers, in de eerste plaats lettend op de elektrische prestaties en in de tweede plaats met betrekking tot het vervuilingsgedrag. Een spacerloos ontwerp van de stack is nog niet beschikbaar. Daarom hebben we bedacht een stack te ontwerpen waarin de membranen worden gescheiden door twee dunne pakkingen die samen een open niet-geweaven structuur vormen. Dit resulteerde in een opmerkelijke verlaging van de ohmse weerstand met ongeveer een factor 2. De niet-ohmse weerstand van de stack zonder spacers was daarentegen significant hoger, mogelijk als gevolg van een hogere concentratiepolarisatie dan in de stack met spacers (spacers worden ook wel turbulentie promotores genoemd). Deze concentratiepolarisatie kan voorkomen worden door andere maatregelen te nemen, bijvoorbeeld door

Summary / Samenvatting

heterogeniteit aan te brengen in membraanoppervlakten en door luchtspoelingen toe te passen. Ook vanuit het perspectief van biofouling, werd experimenteel aangetoond dat het verkrijgen van een stack-ontwerp zonder spacers een goede richting is voor de verdere ontwikkeling van omgekeerde elektrodialyse.

Discussie over de uitdagingen en vooruitzichten

Wetsus - Centre for Sustainable Water Technology in Nederland - begon in 2005 met het project 'Blue Energy' met een focus op omgekeerde elektrodialyse. De resultaten van de vorige hoofdstukken, maar ook academisch onderzoek in breder Wetsus-verband, vormden het uitgangspunt van **hoofdstuk 7**. In dit hoofdstuk hebben we de uitdagingen besproken waarmee wij worden geconfronteerd met betrekking tot de economische en technologische haalbaarheid. De volgende onderwerpen werden besproken: (i) de uitdaging om goedkope membranen in grote hoeveelheden te verkrijgen kan als overkomelijk worden beschouwd als we kijken naar de vergelijkbare bulkmarkt voor ionenwisselaars, (ii) de uitdaging om een goedkoop en een energieuwig proces te ontwerpen is genomen met de toepassing van een eenvoudige drumfilter als voorbehandeling voor een spacer-vrije stack, en (iii) de economische haalbaarheid van een 200 kW eenheid leert dat Blauwe Energie kan concurreren met windenergie. Verdere stappen op het pad van de ontwikkeling van omgekeerde elektrodialyse werden gepresenteerd. Voor de volgende stap wordt aanbevolen om te beginnen met een opgeschaalde pilot op de Afsluitedijk (Nederland), parallel aan begeleidende studies met betrekking tot de ecologische en de hydrologische aspecten.

In **hoofdstuk 8** schatten wij de vooruitzichten van de nieuwe technologie nauwkeuriger in, op mondial en nationaal niveau. De theoretische potentie van vermogen uit zoutgradiënten wordt geschat op 1724 GW. De technische potentie - het deel dat kan worden gewonnen met de huidige

technologie - wordt geraamd op 983 GW. Het technische en economische potentieel van de rivieren Rijn en Maas (met de riviermonding in Nederland) is in meer detail beschreven. Het technische potentieel voor deze rivieren - zoals afgeleid uit de globale datasets - is 2,4 GW. Het economische potentieel wordt geschat op 1,5 GW, nadat in meer detail gekeken is naar de Nederlandse Delta. De veelbelovende vooruitzichten - vooral voor Nederland, waar het zoutgradiënten een belangrijke bron van energie kunnen worden - leiden tot een sterke aanbeveling aan beleidsmakers, captains of industry en vooraanstaande wetenschappers om verder te gaan met onderzoek en ontwikkeling van omgekeerde elektrodialyse.

Summary / Samenvatting

Post Scriptum

Verantwoording

“Ons water drinken wij voor geld; ons hout komt *tot ons* voor een prijs”, klaagt het volk Israël bij monde van de profeet Jeremia (Klaagliederen 5:4). Terugkijkend op mijn loopbaan tot nog toe, is dat toch wel de rode draad: gedreven door gebrek aan schoon drinkwater, gedreven door gebrek aan alternatieve energiebronnen. Niet alleen omdat deze crises ons en ons nageslacht raken, maar ook in het diepe besef dat wij aan de oorsprong ervan staan. Natuurlijk is dat niet alles wat ik heb te zeggen in deze verantwoording. Ik heb – juist ook in dit prachtige promotieproject – genoten van het proces van wetenschappelijk onderzoek en technologische ontwikkeling en van het samenwerken met inspirerende mensen. Het is dan ook tijd geworden om een dankwoord te schrijven.

Dankwoord / Acknowledgements

Allereerst bedank ik mijn promotor Cees Buisman. Cees, vanaf het eerste tot het laatste moment bij Wetsus heb je mij weten te inspireren. Jouw tomeloze ambitie en energie gaven dat ik mijn werk altijd met plezier en trots heb gedaan. Ik heb het altijd zeer prettig gevonden dat ik jouw onvoorwaardelijke vertrouwen genoot.

Mijn co-promotor Bert Hamelers bedank ik ook voor de fijne samenwerking. Een samenwerking die heeft moeten groeien (zie ook het curriculum vitae), maar die uiteindelijk bekroond is met een prijs. Bert, het is een voorrecht om met excellente mensen te werken. Ik zag en zie erg tegen je op, des te mooier is het om bevestiging van je te krijgen op de dingen die ik gedaan heb. Je innovatieve denkkracht zal nog tot vele nieuwe en verassende technologieën leiden. Bedankt ook voor je persoonlijke coaching.

Post Scriptum

Ik had nooit aan mijn promotieproject begonnen als REDstack niet was opgericht. Vanaf het begin was duidelijk dat ik - afkomstig uit het bedrijfsleven - mijn onderzoekswerk wilde koppelen aan commerciële relevantie. Ik bedank de directie van REDstack - in het bijzonder Pieter Hack - voor alle fasen en leermomenten die we hebben meegemaakt. Ook aan mijn collega's bij REDstack ben ik veel dank verschuldigd. Ik denk in het bijzonder aan Kristan Goeting, Jan Valk en Gerard Schouten.

Mijn tijd bij Wetsus was lang zo leuk niet geweest als ik niet onderdeel was geweest van de 'RED-army' (of het 'Blue Energy team'). Joost Veerman: ere wie ere toekomt. Dat je meer google-hits op je naam hebt, dat is gewoon terecht. Piotr Dlugolecki, thanks for all the fun (especially in Honolulu) and for your amazing results. Michel Saakes, dank voor je inbreng en niet in het minst voor de professionalisering van de meetopstellingen. Verder bedank ik Sybrand Metz, Gertjan Euverink en Kitty Nijmeijer voor de prettige samenwerking. Gerrit Oudakker, bedankt voor de onvergetelijke momenten, al voordat ik bij Wetsus begon. Ook themamanager Maarten van Riet (Alliander) en alle andere participanten: hartelijk dank voor de goede contacten.

Studenten zijn de kurk waarop ik drijf. In mijn gedachten zie ik ze een voor een voorbijkomen. Het was wennen om studenten te begeleiden, maar gaandeweg leerde ik het. Voor een optimaal inhoudelijk resultaat kun je je maar het beste richten op de persoonlijke ontwikkeling van de student (en dus aansluiten bij zijn of haar ambities en interesses). Ik bedank Shirley Zhou, Chris Roubos, Freerk Mellema, Feiko Reinalda, Bertus Nobach, Wytze Kingma, Thomas Werkhoven, Daniel Beerlings, Maurice Bosman, Joanna Kuleszo en Joran de Groot. Watse Hoekstra, ongelofelijk hoe jij als elektrotechnisch student je hebt geprofileerd: naast het maken van regelsystemen werd ook de ontwikkeling van RED je domein. Piet Leijstra, jij bent ongetwijfeld recordhouder met drie achtereenvolgende

220

stageperioden. Bedankt voor al je constructies en praktische oplossingen ('ajeto'). Simon Grasman, je hebt als mijn laatste afstudeerde een enorme bijdrage geleverd in het vervuilingsonderzoek. Je beschikt over een goed analytisch vermogen en in handigheid moet ik je als mijn meerdere erkennen. Je bent een waardige opvolger bij REDstack, ik heb er alle vertrouwen in.

Verder bedank ik alle collega's met wie ik heb mogen samenwerken, in het bijzonder binnen het Energie/waterstofthema van Wetsus en de Bio-energy groep van de vakgroep Milieutechnologie van WUR. Kirsten, bedankt voor de prettige intervisie die we hebben gehad. Alle overige onderzoekers en stafleden van WUR en Wetsus bedankt voor de secretariële, technische en inhoudelijke ondersteuning en het vertrouwen. Ik voel me schuldig dat ik jullie nu niet bij name kan noemen, maar als ik hieraan begin dan ga ik hoe dan ook mensen te kort doen!

Ik bedank Hans Vrouwenvelder voor de vele carpool-uren die we gemaakt hebben van Lelystad naar Leeuwarden. Naast persoonlijke reflecties, leverde dit vaak ook voor het werk wat op: manuscripten werden over en weer gereviewed, onderzoeksopzetten doorgesproken, etc.

Tot slot denk ik aan mijn familie, mijn gezin en in het bijzonder aan jou, Elza. Je hebt me het voordeel van je twijfel gegeven om deze stap te kunnen maken. Het heeft goed uitgepakt, je gunde mij dit geluk. Ik besef heel goed wat het jou gekost heeft. Ik hoop en bid dat ik - als de omstandigheden daarom vragen -mij net zo onbaatzuchtig kan opstellen naar jou en de kinderen toe. Ik dank God voor de kracht en gezondheid die ik gekregen heb om dit werk te voltooien.

Hoevelaken, 31 augustus 2009

Jan Post

Curriculum Vitae

Jan Post was just fooling around in his consulting firm's laboratory one day when inspiration struck. A civil engineer with DHV in Amersfoort (The Netherlands), he suddenly envisioned how energy could be derived from the mixing of salt water and freshwater. Post approached Bert Hamelers, an environmental engineer at Wageningen University, who took Post on as a Ph.D. student.



"I still remember that moments I was in our lab and had a bad Internet connection," Post recalls. Unable to work on the computer, but required to remain in the laboratory for the safety of a colleague, Post wondered, "What can I do in the lab today?" He started playing with a desalination unit, switching it on and off and thinking about osmosis. "I was struggling with the question: why does it take so much energy to desalinate water?" Post says. He claims it was not so difficult to imagine the opposite: maybe adding seawater to freshwater to make it more salty would generate energy. The discovery so fascinated him that he could not leave it alone. "Jan came around at the right time," Hamelers says. He had been discussing the potential of salt water and freshwater mixing as an energy source with Cees Buisman, scientific director of Wetsus, a research institute in Leeuwarden. A partnership between Wetsus and the university was in the works, but they were looking for a skilled student with a degree in chemical engineering. When Post made his offer, "I wondered: should I start with a civil engineer?" Hamelers admits. The project required knowledge of physical chemistry that typically is not part of the curriculum for civil engineers. But Post was a perfect fit because he was so motivated, and his civil engineering background brought a fresh and useful perspective, Hamelers says.

In: Pelley, J., Top Paper in Environmental Technology: Saltwater power, Environmental Science & Technology 43 (2009), p. 2194.

Picture: Reinout Burgers, Carrière+



Netherlands Research School for the
Socio-Economic and Natural Sciences of the Environment

CERTIFICATE

The Netherlands Research School for the
Socio-Economic and Natural Sciences of the Environment
(SENSE), declares that

Jan Willem Post

Born on: *22 January 1976* at: *Delft, The Netherlands*

has successfully fulfilled all requirements of the
Educational Programme of SENSE.

Place: *Wageningen* Date: *3 November 2009*

the Chairman of the
SENSE board

the SENSE Director
of Education

Prof. dr. R. Leemans

Dr. A. van Dommelen



The SENSE Research School declares that Mr. Jan Willem Post has successfully fulfilled all requirements of the Educational PhD Programme of SENSE with a work load of 36 ECTS, including the following activities:

SENSE PhD courses:

- Environmental Research in Context
- Research Context Activity: Preparing a teaching package for secondary schools on “Salinity-gradient energy”
- Sustainable Bio-energy and Innovation

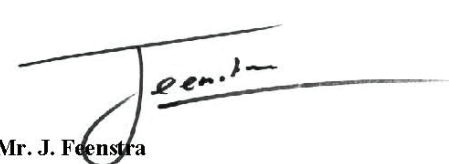
Other Phd and MSc courses:

- Techniques for Writing and Presenting Scientific Papers
- Intensive Course in Electromembrane Processes: Their principle and practical applications, L'Aquila, Italy
- Site Specific Training: Course on several OLI Software Simulation Tools
- Renewable Energy: Sources, Technology and Applications
- Personal development: inventing and writing of 6 patent applications on reverse electrodialysis (WO2007094659, WO2008108633, NL1036242, NL1035190, NL1036233, NL2002989)
- Personal development: writing and defending of 2 grant proposals (Innovatiesubsidie Samenwerkingsprojecten IS063003, InnoWator IWA07002)

Oral Presentations:

- SENSE Summer Symposium, 23 June 2005, Ede, The Netherlands
- ICOM: Int. Congress on Membranes, 14 July 2008, Honolulu, Hawai, US
- SENSE symposium, 20 February 2009, Wageningen, The Netherlands

Mr. J. Fennstra
SENSE Coordinator PhD Education and Research

A handwritten signature in black ink, appearing to read "J. Fennstra". The signature is fluid and cursive, with a large, stylized initial "J".